iram
Institut de
Radioastronomie
Millimétrique

Annual Report 2016

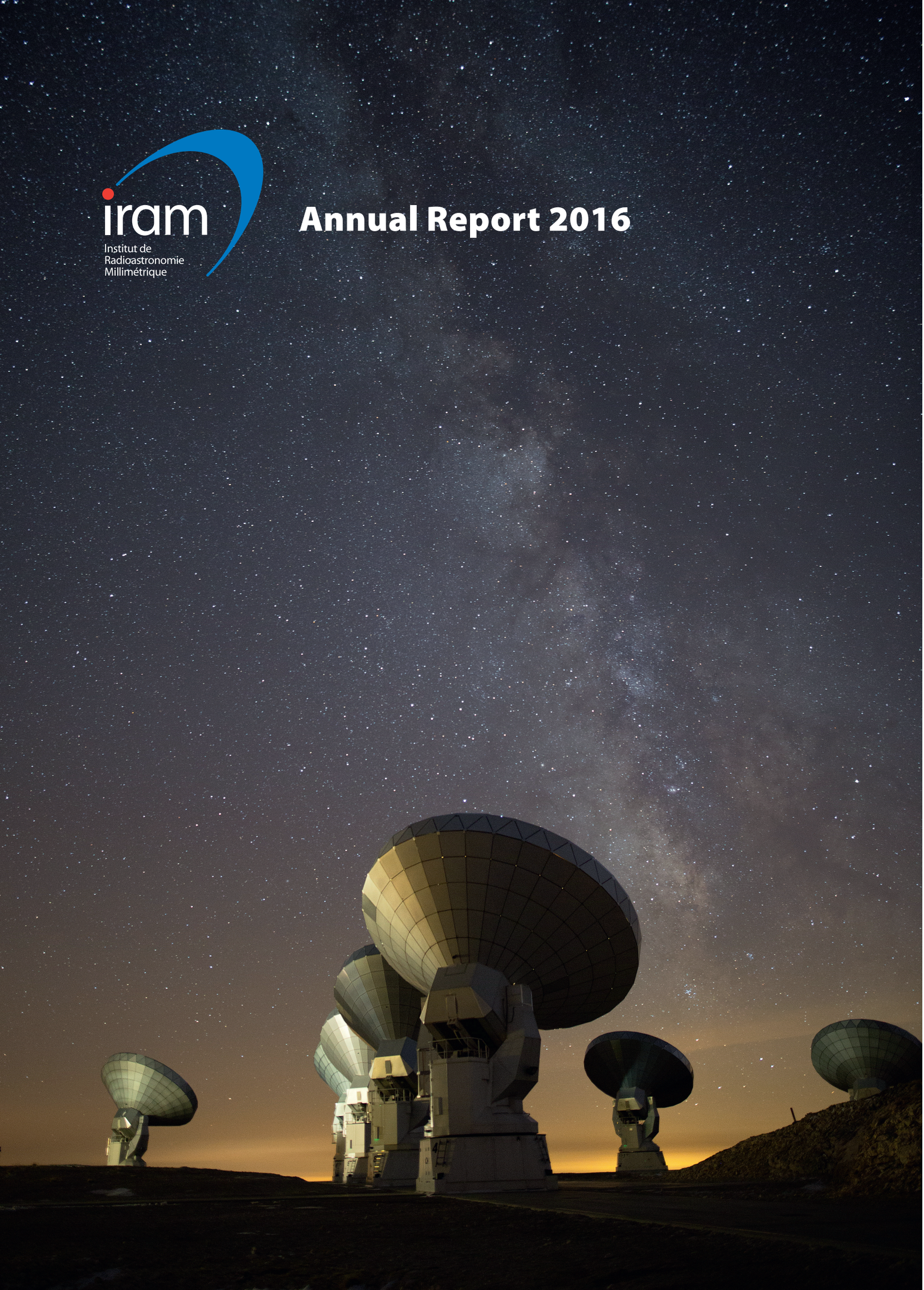

IRAM Annual Report 2016

Published by IRAM © 2017
Director of publication Karl-Friedrich Schuster
Edited by Cathy Berjaud, Roberto Neri, Karin Zacher

With contributions from:
Sébastien Blanchet, Isabelle Delaunay, Eduard Driessen, Bertrand Gautier, Olivier Gentaz, Frédéric Gueth, Carsten Kramer, Bastien Lefranc, Santiago Navarro, Roberto Neri, Juan Peñalver, Francesco Pierfederici, Karl-Friedrich Schuster

Contents

Introduction 4

Highlights of research with the IRAM telescopes 6

The observatories

The 30-meter Telescope 17

NOEMA Interferometer 23

Grenoble headquarters

Frontend Group 32

Superconducting Devices Group 35

Backend Group 36

Mechanical Group 38

Computer Group 40

Science Software 41

IRAM ARC Node 43

Administration 44

IRAM staff list 47

Telescope schedules 49

Publications 63

Committees 76

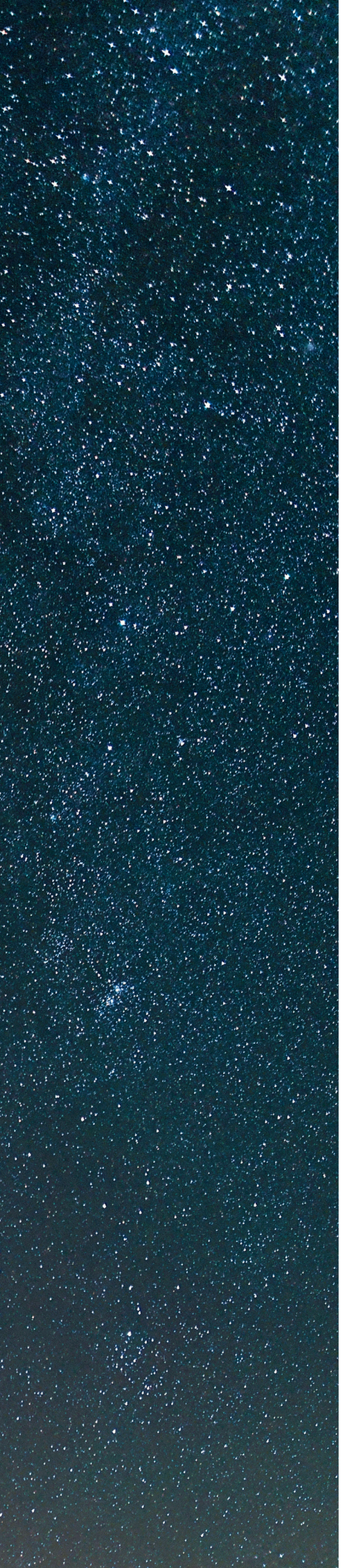

Introduction

Dear IRAM Users and Supporters,

IRAM is by definition committed to operate and to constantly improve our observatories and we would like to share with you some salient information on how this task has progressed in 2016.

First of course, there is the status of our flagship project NOEMA, which has progressed in a multitude of areas. Most importantly, NOEMA received its 8th antenna in spring 2016. The antenna was constructed and commissioned in record time and showed that both, progress in timing and quality could be made as compared to antenna 7. Routine science operation with 8 antennas started very rapidly and showed its full potential in greatly improving sensitivity and imaging quality.

At the same time nearly all receivers were upgraded to the new NOEMA frequency plan providing a quantum jump in instantaneous and tuning bandwidth, and at the same time yet lower noise.

Work on the PolyFiX backend, which will introduce groundbreaking technological concepts and instrumental performances, has steadily progressed, and mass production of the electronic components has been launched towards the end of the year. The schedule is tight, as mostly coding and testing of firmware have been quite time consuming.

With all these steps, the completion of NOEMA Phase I is expected close to schedule, and clearly within budget. I am also very happy to announce that the partners have found means to mitigate the initial funding gap for NOEMA Phase I and have given full power to IRAM to finish Phase I as foreseen.

IRAM has also made first steps into the next level of receiver and backend upgrades. The sampler chips for a second PolyFiX type correlator have been ordered from the supplier and a first analysis of receiver design alternatives has been made.

Since 2016, IRAM, together with its partners, works intensely on the preparation for NOEMA Phase II. Important civil construction activity has been carried out over the summer to create a bypass track including several track stubs for improved antenna reshuffling. This bypass construction served also as a

preparation for the future baseline extension in NOEMA Phase II. Technical and administrative preparations for the civil construction work on the track extension to 1.7 km have been done and a first round of offers has been received.

Unfortunately in November, we experienced an important technical incident after a bad weather period; this enforced a stop of the cable car operation. IRAM has initiated an in depth investigation of the circumstances and repair work is expected to last for at least 10 months. We have however made sure that workarounds for transport will allow to progress with only little slips in the schedule of NOEMA Phase I.

At the 30-meter Telescope things have not stayed at rest either.

NIKA2 has seen intense commissioning activities and many tricky problems have been tackled and solved. It should be noted that the NIKA2 instrument is a frontrunner of its kind and only little in-depth help can be obtained from other competing projects. We are now looking forward to opening the instrument in the upcoming year for the user community. At the same time, very strong GTO large programs were set up by the instrument consortium, and I have no doubt that these programs will deliver excellent science in the near future.

New spectroscopy calibration software has been developed over the last 2 years and is now installed at the telescope. This software will drastically improve atmospheric calibration, which is particularly important for the very large bandwidths EMIR is providing to the users.

During the autumn, we have started to make internal assessments on the technical and operational status of the IRAM 30-meter Telescope in order to prepare a concept for refurbishments and future improvements.

I would like to thank our partners for their excellent support and my colleagues for their work and their engagement on highest level for the progress of IRAM.

With best regards

Karl-Friedrich Schuster
Director

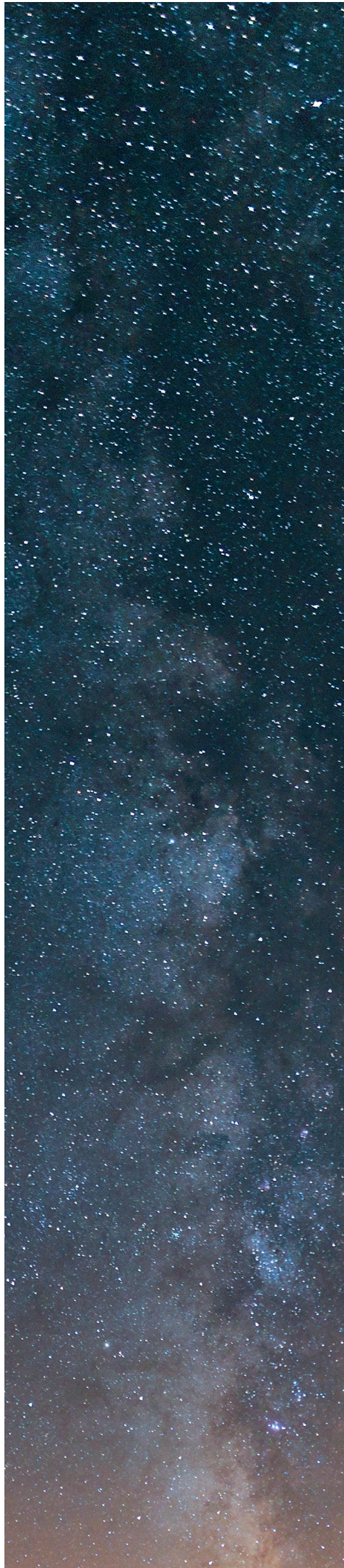

Highlights of research with the IRAM telescopes

RESOLVING THE ULTRAVIOLET-IRRADIATED SKIN OF ORION

The Orion Nebula is the closest massive star forming region. Massive stars in the famous Trapezium cluster emit up to 200,000 times the solar luminosity. Unlike our Sun, their harsh ultraviolet radiation field illuminates, erodes, and ionizes the environment at large distances. This produces HII regions of hot ionized gas. Because massive stars have short lifetimes, HII regions are still surrounded by their cold parental molecular cloud where new stars actually form.

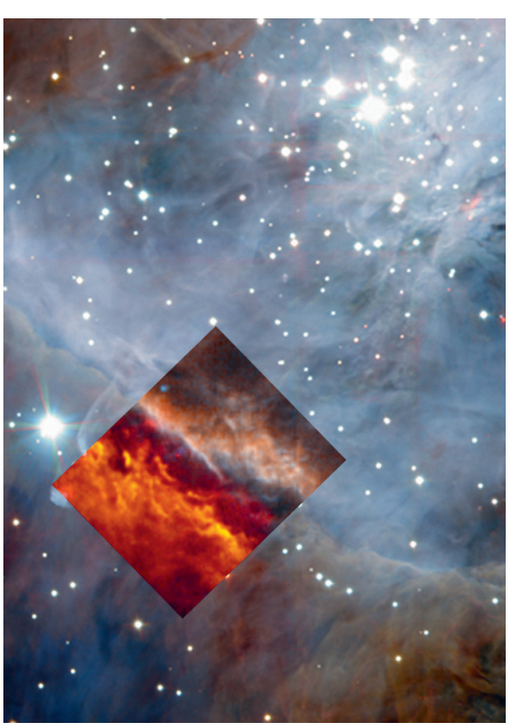

The Orion nebula observed with ESO/VLT. The inset shows the Orion Bar as traced by the combination of ALMA and IRAM 30-meter data. The Trapezium cluster lies at the top of the ESO/VLT image. Credit: ESO/ALMA/Goicoechea. Work by Goicoechea et al. 2016, Nature, 537, 207.

The expansion of an HII region into a molecular cloud is a complicated process by which the external layers of the cloud are irradiated, the gas is heated and compressed, and molecules are photo-dissociated. Understanding the radiative feedback of massive stars is of great importance to astrophysics, as it happens throughout the Universe and, in part, regulates the process of star formation in galaxies.

Combining the information from the ALMA interferometer and the IRAM 30-meter radio Telescope, an international team led by Javier Goicoechea (CSIC, Madrid) obtained the most detailed images of the Orion Bar, the transition zone between the Orion molecular cloud and the HII region around the Trapezium stellar cluster. Images of unprecedented quality and spatial resolution were made in CO and HCO^+ emission that allowed the team to study at physical scales of a few hundred astronomical units (AU), the distribution of the molecular gas and the processes that take place in this fascinating region.

The combined IRAM 30-meter and ALMA images reveal that the irradiated edge of the molecular cloud, the skin of Orion, is composed of small structures: filaments and globules, more or less organized in periodic patterns. They show that the expansion of the HII region and the strong UV radiation field impinging the cloud increase the pressure and compress the outermost cloud layers, leading to the

formation of the observed structures. At the same time, flows of gas seem to steam from the cloud surface, an obvious manifestation of the photo-evaporation of the molecular cloud. This study proves that dynamical effects are important for the evolution of molecular clouds in the vicinity of massive stars.

FIRST DETECTIONS OF THE PREBIOTIC MOLECULE P-O IN STAR FORMING REGIONS

In the past few years, new generation of telescopes have allowed the detection in the interstellar medium molecules that play an important role in prebiotic chemistry. As these molecules are believed to be the building blocks of the first living organisms, their study might help to shed light about the origin of life in the Universe.

One of the key elements for the development of life is phosphorus (P). Chemical compounds containing phosphorus, such as phospholipids and phosphates, are essential for the structure and energy transfer in cells. Especially important is the chemical bond between phosphorus and oxygen, P-O, which is crucial for the formation of the backbone of the deoxyribonucleic acid (DNA), the macromolecule that contains the genetic information of living organisms.

Recently, a group led by Víctor M. Rivilla (OAA, INAF) started a project to search for P-O in star forming regions using the IRAM 30-meter Telescope. The researchers discovered for the first time the presence of this prebiotic molecule in two well-known regions of our galaxy: W51 e1/e2 and W3(OH). The identification of this molecule is important, as it suggests that one of the basic pieces of the DNA is already available in the gas that will eventually be accreted onto the planets where life may originate. The results of this work also indicate that the

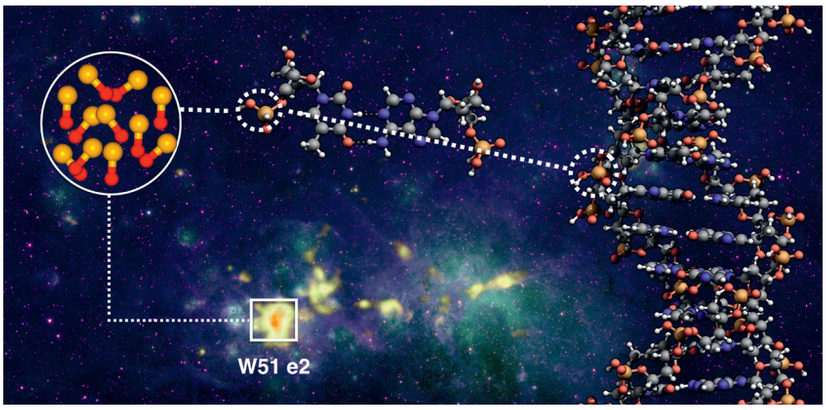

First detections of P-O towards star-forming regions. The P-O compound is one of the backbone elements of nucleic acids, the building blocks of the DNA helix. Work by Rivilla et al. 2016, ApJ, 826, 161.

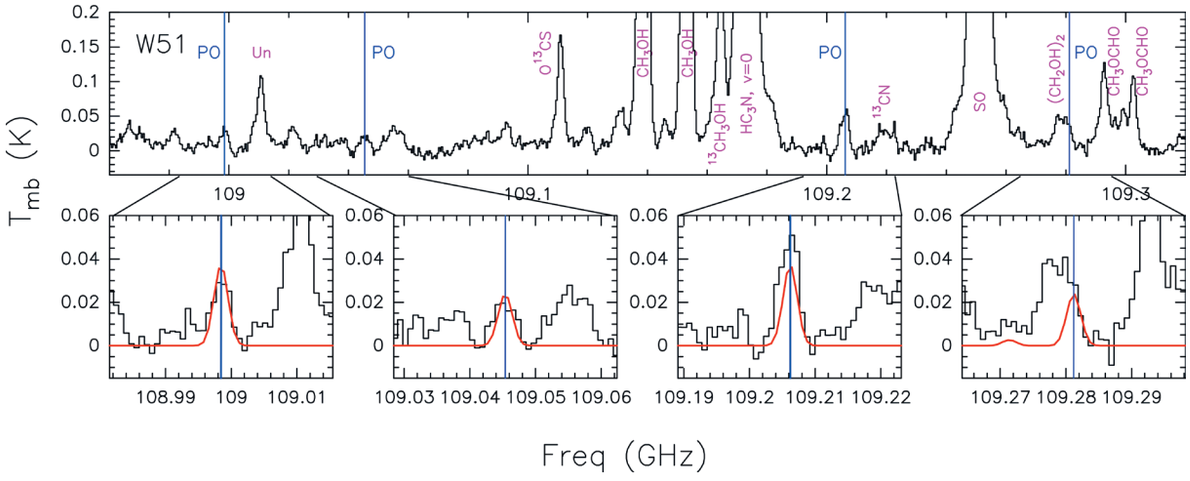

Spectral profile observed at 109 GHz towards W51. The PO transitions are indicated with blue vertical lines. The lower panels show zoom-in views of the PO transitions. The red line is the LTE fit with an excitation temperature of 35 K and an assumed source size of 20". Work by Rivilla et al. 2016, ApJ, 826, 161.

abundance of phosphorus in star forming regions is more than ten times higher than previously thought.

These first detections of the P-O chemical bond towards star forming regions might have profound implications for the prebiotic chemistry. The authors believe that they can now start to study the chemistry of phosphorus in the interstellar medium. They expect such investigations to provide further important clues about how the chemical complexity can grow to form more complex molecules of biological interest.

THE STRUCTURE AND FRAGMENTATION OF THE HIGHLY FILAMENTARY IRDC G035.39–00.33

Although a basic mechanism for the specific case of the isolated low-mass star formation has been investigated over several decades, a more generalized model, one that incorporates a consistent description for the formation of high-mass (>8 $M_{\odot}$) stars, is still lacking. An important step in developing a holistic understanding of the star formation process is identifying and categorizing the initial phases of high-mass star formation.

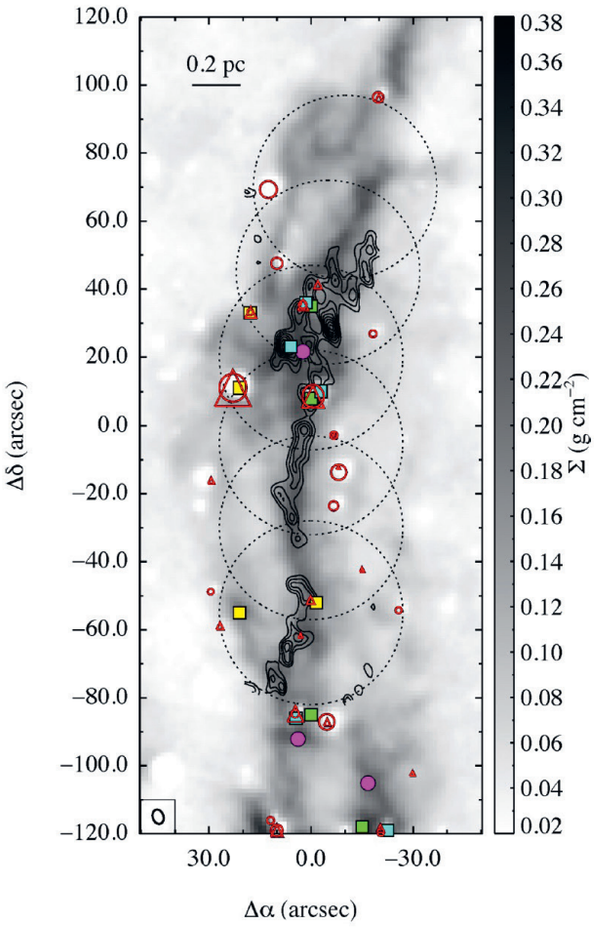

The combined mid- and near-infrared extinction-derived mass surface density map (greyscale) of Kainulainen & Tan (2013) overlaid with (~4", 0.05 pc) NOEMA 3.2 mm continuum contours. Large dotted circles indicate the 6-field mosaic. Work by Henshaw et al. 2016, MNRAS, 463, 146.

Infrared dark clouds (IRDCs) were quickly identified as having the potential to aid our understanding of the star formation process. Although the broad range in characteristics suggests that not all IRDCs will form high-mass stars, identifying massive and relatively quiescent molecular clouds is a crucially important step in understanding the initial conditions for high-mass star formation.

Jonathan Henshaw (LJM University, Liverpool) and collaborators used high angular resolution 3.2 mm NOEMA dust continuum observations with the aim of studying the structure and fragmentation of the filamentary infrared dark cloud (IRDC) G035.39–00.33. The interferometric data show the continuum emission is segmented into a series of 13 quasi-regularly spaced (~0.2 pc) regions that follow the major axis of the IRDC. The comparison between the dust continuum and the N_2H^+ observations suggests that some of the identified regions may reflect a superposition of structures associated with different velocity components. Some regions, which appear to share the same velocity, can also exhibit structured continuum emission, which is evident in their radial flux density profiles.

Henshaw's study also found significant discrepancy between the spatial distribution of the regions and that predicted by theoretical work. Their result emphasizes the importance of considering the underlying physical structure, and potentially, dynamically important magnetic fields, in any fragmentation analysis. Future higher angular resolution dust continuum observations will assist in determining whether or not the structures identified in this work have fragmented further.

AN EVOLUTIONARY STUDY OF THE INTERNAL STRUCTURES OF NGC7538 S AND IRS1

The ubiquitous multiplicity of high-mass star forming regions (HMSFRs) leads to abundant dense gas cores and associated (proto-)stellar outflows, shocks, and disk-like structures. Understanding how dense gas structures and cores form and evolve in such clustered environments, and how such massive stellar clusters come into the existence, requires high angular resolution millimeter and submillimeter interferometric observations.

To probe the processes associated with HMSFRs, such as hierarchical fragmentation and chemical evolution, Siyi Feng (MPIA/MPIfR) and collaborators started a comprehensive high-angular resolution study (~1000 AU) in the two HMSFRs, NGC7538 S and IRS1. The observations were made with NOEMA and covered abundant molecular lines, including tracers of gas column density, hot molecular cores, shocks, and complex organic molecules.

NGC7538 S was resolved into at least three dense gas condensations (MM1, MM2, and MM3). Despite the comparable continuum intensity of these condensations, their differing molecular line emission was found to be suggestive of an overall chemical evolutionary trend from the northeast to the southwest. Line emission from MM1 was found to be consistent with a chemically evolved hot molecular core (HMC), whereas MM3 was found to remain a prestellar candidate that is only exhibiting emission of lower-excitation lines. The condensation MM2, located between MM1 and MM3, is showing an intermediate chemical evolutionary status. Since these three condensations are embedded within the same parent gas core, their differing chemical properties are most likely due to different warm-up histories, rather than different dynamic timescales.

Feng's chemical model fits well the chemical variations for >60% of the observed molecular species across the condensations in NGC7538 S but it fits poorly the abundances of COMs. According to the authors, the intrinsically weak nature of these lines, the limitations of the chemical network in dealing with complex chemistries and the complexity of the source structures are likely causing these discrepancies.

Despite remaining spatially unresolved, NGC 7538 IRS1 shows a high abundance of complex organic molecules (COMs) like NH_2CHO, CH_3OH, $HCOOCH_3$ and CH_3OCH_3, suggesting that it is a more chemically evolved HMC than MM1. The results on NGC7538 S and IRS1 suggest that different chemical evolutionary stages can coexist in the same natal gas core.

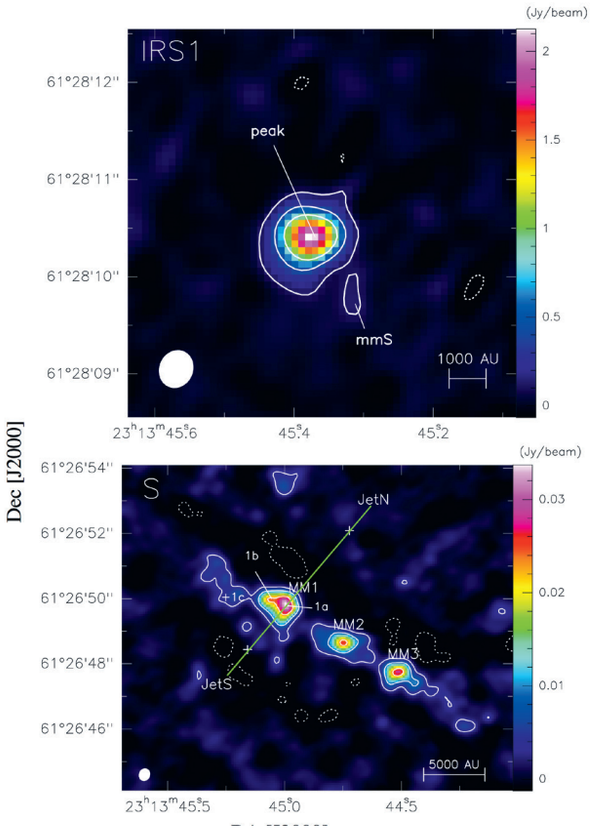

Continuum emission maps of NGC 7538 S and IRS1 obtained with NOEMA at 1.4 mm. The synthesized beam is shown at the bottom left of each panel. Work by Feng et al. 2016, A&A, 593, A46.

A VIEW ON THE CO AND METHANOL SNOW LINES IN YOUNG STARS

The earliest phases of star formation are deeply embedded in dusty molecular clouds. An understanding of the chemichal structure and evolution of the molecular envelope surrounding young protostars is key to predicting the composition of the material that eventually forms planets. In this

respect, variations in the accretion rates can drive significant density and temperature gradients in the envelopes and disks around these stars. These variations may give rise to chemical stratifications, characterized by a progressive freeze-out of molecular species beyond the so-called snow lines. Investigating these regions is therefore important to get the full picture of the early protostellar collapse and the subsequent evolution of young protostars.

In the frame of CALYPSO, an IRAM Large Program, Sibylle Anderl (IPAG, Grenoble) and collaborators used the NOEMA Interferometer to observe the sublimation regions of $C^{18}O$, N_2H^+, and CH_3OH towards four low-luminosity protostars: IRAS4A, L1448C, L1157 and IRAS4B. Their results provide direct evidence for an anti-correlation of the emission regions observed in $C^{18}O$ and N_2H^+ i.e. N_2H^+ is found to originate from a ring-like structure around the centrally, relatively compact emission of $C^{18}O$. Using a binding energy of 1200 K for CO and of 1000 K for N_2, the researchers build models that reproduce the observations towards all four sources with reasonable accuracy. Their modeling suggests the CO freeze-out temperatures are reached at distances of a few hundred AU. According to the researchers, CO abundances are derived that are about an order of magnitude lower than the abundances observed in the gas phase on large scales in molecular clouds before depletion sets in. Despite the possibility that CO abundances are lower because of uncertainties in the temperature profiles in the immediate vicinity of the protostar, such abundances are comparable to values found in protoplanetary disks, which may indicate an evolutionary scenario where the low CO abundances are already established in the protostellar phase.

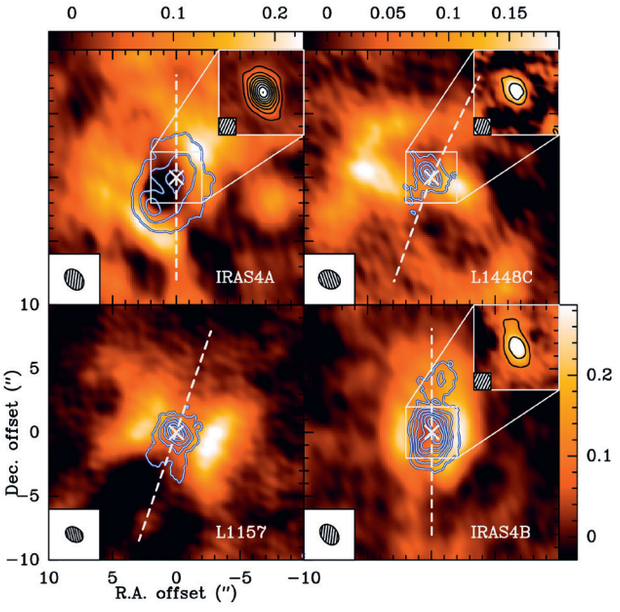

Maps of the velocity integrated $C^{18}O$ (contours) and N_2H^+ (color background) emission testifying to their anti-correlated spatial distribution. The inlays in the upper right corners show the CH_3OH emission. Work by Anderl et al. 2016, A&A, 591, A3.

THE LOW LUMINOSITY OUTBURST IN HBC 722

Sun-like pre-main sequence stars are often surrounded by circumstellar disks from which material is accreted by the growing protostar. The accretion of infalling material generally occurs at a low rate but occasionally it can be interrupted by brief, sometimes very intense episodes of enhanced accretion. When the mass accretion rate through the circumstellar disk of a young star increases by orders of magnitude from typically 10^{-7} to 10^{-4} $M_\odot.yr^{-1}$, FU Orionis-type (FUors) outbursts can occur. During the outburst, the disk outshines the central star by factors of 100–1000, and a powerful wind emerges, which may have a significant impact on the surrounding interstellar medium.

To investigate the role and impact of the circumstellar environment, and the physical changes and processes associated with FUor events, Ágnes Kóspál and collaborators observed HBC 722, a young eruptive pre-main sequence star that is undergoing a major outburst phase since 2010. According to the results of their study, NOEMA did not detect HBC 722 in the millimeter continuum but combined NOEMA and IRAM 30-meter Telescope observations in the ^{13}CO (1-0) line revealed the presence of a flattened elongated molecular gas structure with a diameter of 1700 AU and a mass of 0.3 $M_\odot$ centered on HBC 722. The proximity of this reservoir of molecular gas suggests it is a possible source of replenishment of

material to sustain the accretion rate over time. In addition, the study revealed the presence of seven sources in the vicinity of HBC 722, presumably embedded protostars or starless cores that might have formed together with HBC 722.

According to Kóspál, HBC 722 is showcasing that accretion-related outbursts can occur in young stellar objects even with very low-mass disks in the late Class II phase. Their observations are consistent with the predictions for a system where thermal instability is triggered at an intermediate radius within the disk area and where a rapid ionization front propagating toward the star is causing a short-lived brightness peak similar to the one observed in 2010. The results also strengthen the theory that eruptive phenomena may appear throughout star formation from the embedded phase to the Class II phase, and that possibly all pre-main sequence stars undergo phases of temporarily increased accretion.

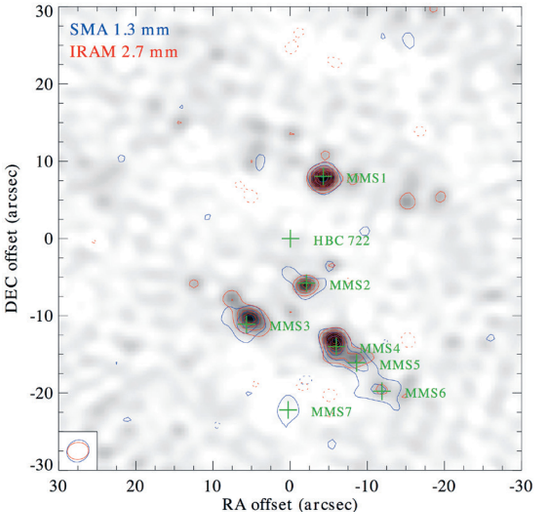

Millimeter continuum emission map of the area around HBC 722. The greyscale image and the red contours are NOEMA 2.7 mm observations, while the blue contours are SMA 1.3 mm data. Work by Kóspál et al. 2016, A&A, 596, A52.

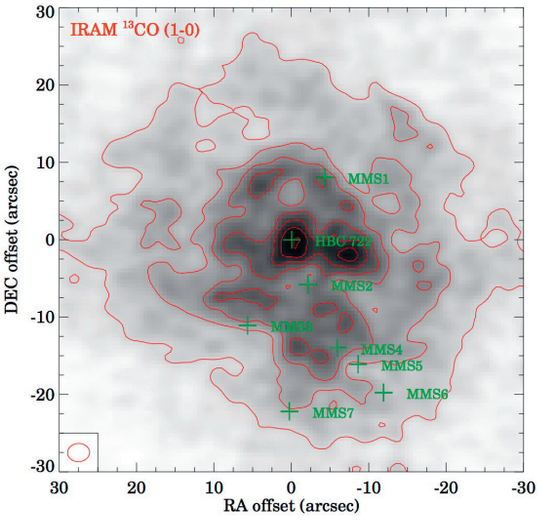

Total intensity map of the ^{13}CO (1-0) emission around HBC 722.

AN EXPANDING MOLECULAR BUBBLE SURROUNDING TYCHO'S SUPERNOVA REMNANT

As standard candles for measuring distances to distant galaxies, Type Ia supernovae play a crucial role in studying the expansion of the Universe. Despite decades of study, the nature of these systems remains a puzzle. Two competing models for their formation are considered: the single-degenerate scenario, in which a white dwarf accreting matter from a nearby normal star grows too massive to support itself and explodes as supernova, and the double-degenerate scenario, in which two white dwarfs orbit one another and eventually merge to produce a supernova explosion. It remains to be decided which of the two scenarios is the correct one, if any.

To address this question, an international team of astronomers from China, UK, and Canada led by Ping Zhou (Nanjing University) observed the remnant of Tycho's supernova (SN 1572) with the IRAM 30-meter Telescope. To the surprise of the researchers, the ^{12}CO observations revealed the existence of a massive (~220 $M_{\odot}$), slowly expanding (~4.5 km.s^{-1}) molecular gas bubble surrounding the supernova remnant. The observations suggest the molecular material is highly clumped in both velocity and space, and only slighted impacted by the blast wave of the supernova remnant. Type Ia supernovae are usually expected to appear in

a low density interstellar medium, and therefore the interaction of the supernova remnant with the surrounding molecular clouds is an unexpected phenomenon.

This unprecedented discovery of an expanding molecular bubble in a Type Ia supernova constitutes supportive evidence for the single-degenerate scenario, since a double white dwarf system is not likely to generate winds powerful enough to create such molecular bubble. According to the researchers, the most plausible origin of the expanding bubble is the fast outflow driven from the vicinity of the progenitor system as it accreted matter from a non-degenerate companion star. If the wind stopped shortly before the SN explosion, the estimated wind velocity of ~140 km.s^{-1} and duration of ~4.10^{5} yr at a typical mass-loss rate of ~10^{-6} $M_{\odot}$.yr^{-1} would be consistent with those expected for the single-degenerate scenario.

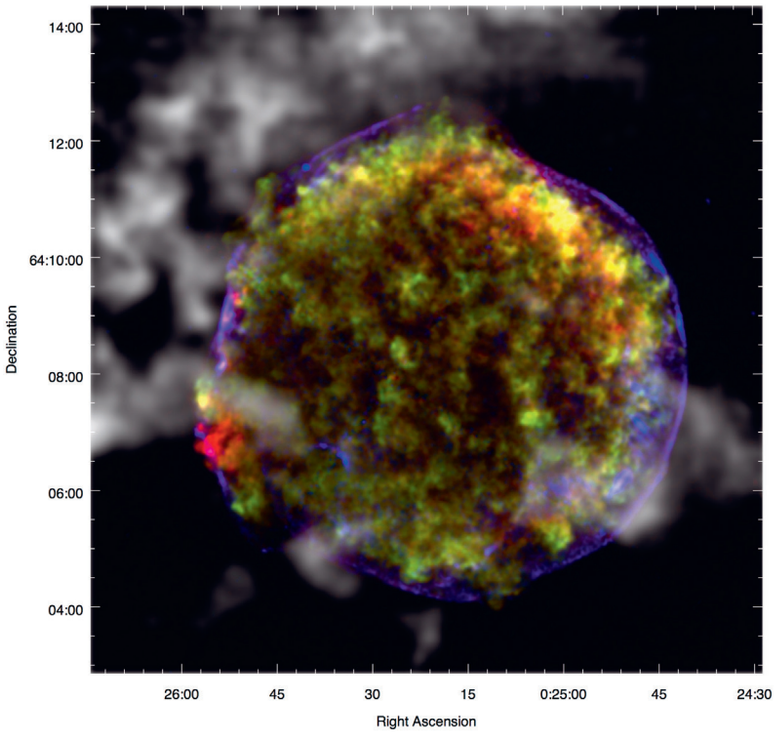

Tycho's supernova remnant (SN 1572) surrounded by a molecular gas bubble (grey) traced by the ^{12}CO emission and superposed on a composite X-ray emission (color) observed with the Chandra X-ray Observatory. Work by Zhou et al. 2016, ApJ, 826, 34. Image credit: NASA/CXC/Rutgers/J. Warren & J. Hughes et al.

THE EMPIRE SURVEY – TRACING STAR FORMATION ACROSS THE DISK OF M51

The past years have seen a major transition in studies of the ISM in normal, star forming disk galaxies. Focus has shifted from mapping the distribution of the bulk molecular medium using low-J CO lines to systematically studying the actual dense, star forming gas. This gives access to the gas volume density distribution as a function of environment, a quantity that is of fundamental interest for theories of star formation. According to models the dense gas fraction is almost all that matters to determine the star formation rate.

With these goals in mind, Frank Bigiel (MPIA) and collaborators used the sensitivity of the IRAM 30-meter Telescope to construct EMPIRE (EMIR Multiline Probe of the ISM Regulating Galaxy Evolution), the first wide-area multiline mapping survey targeting the most common tracers of dense gas across the disks of star forming galaxies. The key goals are to measure dense gas fraction variations from ratios like HCN/CO and relate these to local interstellar medium (ISM) conditions, and to evaluate the dense gas fraction as a driver for the star formation efficiency of the bulk molecular medium.

Among the first results from the EMPIRE survey, are the maps of HCN (1-0), HCO^+ (1-0), and HNC (1-0) across the disk of M51. As expected, the dense gas is found to correlate with tracers of recent star formation but compared to previous works that were targeting galaxies as a whole, these results confirm a tighter scaling between the amount of dense gas, traced by the HCN line, and the recent star formation rate, traced by the infrared emission.

The authors, however, show that the underlying physics is more complex: both the dense gas fraction and the star formation efficiency of dense gas appear to depend on local conditions in the disk of M51. This agrees with previous research work and is consistent with the ISM pressure playing an important role in setting the density of the ISM and the ability of dense gas to form stars.

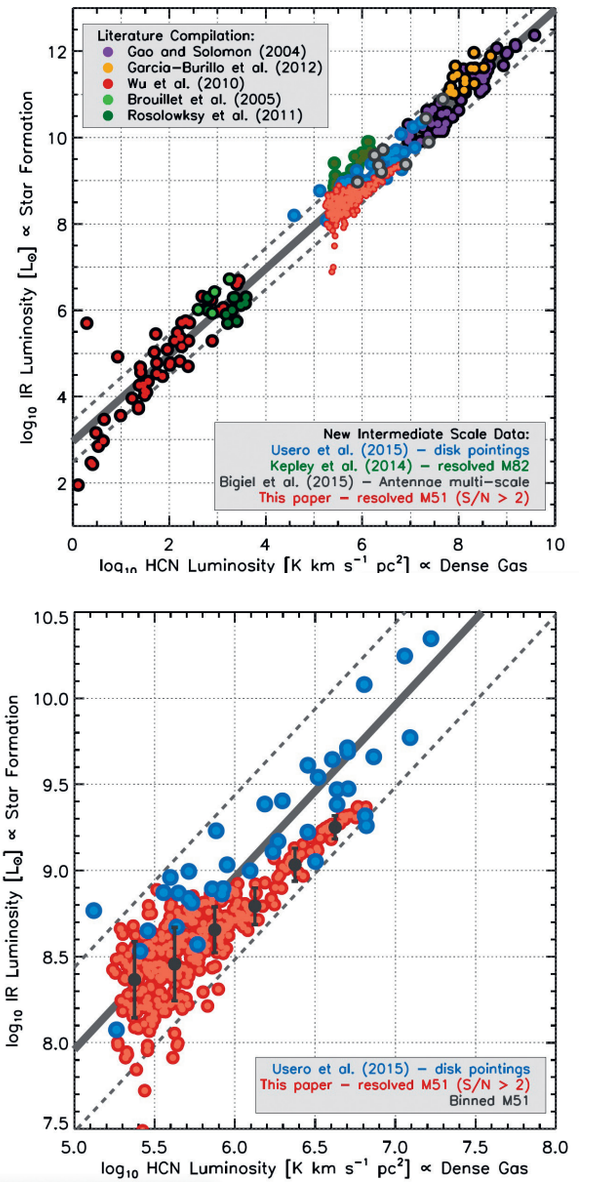

Top right: Infrared (IR) luminosity as a function of HCN luminosity for structures from galactic cores and Local Group clouds to whole starburst galaxies. Along with other recent results, Bigiel's new M51 data extend the observed correlation into the luminosity gap corresponding to large parts of galaxies.

Right: zoom-in on data for the full-galaxy map of M51. The IR luminosity correlates well with HCN luminosity for individual regions, but not all regions show the same IR-to-HCN ratio. Work by Bigiel et al. 2016, ApJ, 822, L6.

VLBI IMAGING OF THE JET BASE IN CYGNUS A

The launching mechanism of relativistic extragalactic jets is a much debated and crucial issue for understanding these fascinating objects. There is currently a broad consensus on the fundamental role that strong magnetic fields anchored in the accretion disk play in the launching process. The understanding and modeling of the observed properties of magnetically driven jets, however, is still a major challenge for theorists. General relativistic magneto-hydrodynamic simulations have shown that highly collimated, relativistic jets can be efficiently powered by the black hole's rotational energy extracted through the magnetic fields, a scenario that is supported by recent observational studies of blazars. Alternatively, the rotation of the accretion disk has been proposed as a viable power source for magnetic jet launching.

To discriminate between the two launching mechanisms, a team led by Biagina Boccardi (MPIfR, Bonn) performed 86 GHz Global Millimeter VLBI array (GMVA) observations of the jet base of Cygnus A and determined its transverse size at the onset of the bipolar flow. The jet base appears to be extended over 227 ± 98 Schwarzschild radii, a result, which is supported by earlier observations at 5 GHz and which suggests the emission region is significantly larger than the innermost stable orbit and that it is produced by a mildly relativistic, parabolically

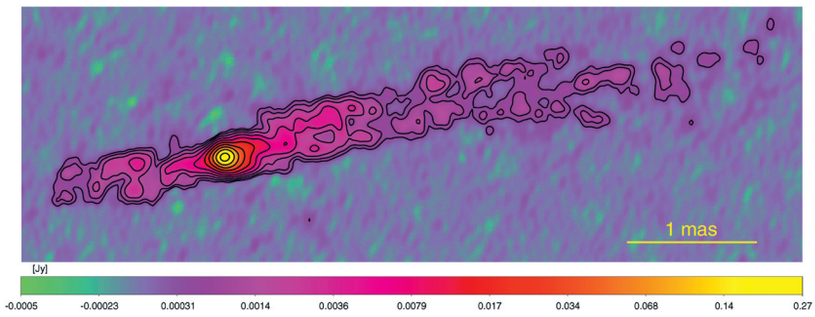

Stacked image of Cygnus A at 86 GHz. Each single epoch was restored with a circular beam of 0.1 mas. The GMVA observations included NOEMA and the IRAM 30-meter Telescope. Work by Boccardi et al. 2016, A&A, 588, L9.

expanding disk wind. The authors, however, cannot exclude the existence of a central and faster jet, possibly driven by the black hole and invisible to observations because of Doppler de-boosting. However, the existence of such fast jet, powered either from the rotation of the inner regions of the accretion disk or by the spinning black hole, is suggested by the kinematic properties and by the observed limb brightening of the flow. Indeed, the comparison of the width profiles at 86 GHz with earlier observations at 43 GHz suggests that free-free opacity and/or synchrotron opacity are still strong at lower frequency but not at 86 GHz. The authors conclude that observing at high radio frequencies is therefore fundamental for unveiling the physical properties of jets at their onset.

SUNYAEV-ZEL'DOVICH OBSERVATIONS OF MACS J1423.8+2404 WITH NIKA

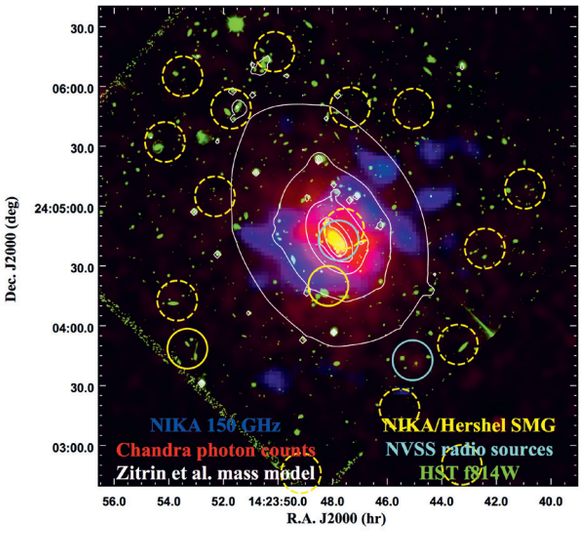

Composite multiwavelength image of MACS J1423.8+2404: NIKA 150 GHz (blue) shows the tSZ signal, Chandra photon counts (red) trace the electron density, HST F814W (green) shows the galaxies in the field. The image also shows the surface mass distribution model (white) and the (sub)millimeter candidate source locations (yellow) obtained with NIKA at 260 GHz (solid line), and identified using the Herschel satellite (dashed-line). Work by Adam et al. 2016, A&A, 586, A122.

In the standard scenario of structure formation, clusters of galaxies form through the hierarchical merging of smaller groups and the accretion of surrounding material. Though the main lines of cluster formation are well understood, many aspects of the underlying physical processes are not, and lead to scatter and biases in the observable mass scaling relations, thereby limiting the use of clusters as cosmological probes. To overcome this problem, astronomers rely nowadays on measurements of the thermal Sunyaev-Zel'dovich effect (tSZ), the inverse Compton interaction of cosmic microwave background photons with energetic electrons in the intra-cluster medium, an observable with a relatively small dependence on the dynamical conditions of the cluster and the physics of the electron gas.

To investigate the tSZ effect towards a cluster of galaxies, a team of researchers led by Rémi Adam (LPSC, Laboratoire Lagrange) used NIKA at the IRAM 30-meter Telescope to observe MACS J1423.8+2404, a massive cluster at z = 0.545. The main goals of the NIKA observations were to examine the morphology of the tSZ signal at 150 and 260 GHz and to compare it to other datasets. The electron pressure and density of the intra-cluster medium were determined by combining NIKA, Planck, XMM-Newton, and Chandra data, focusing on the impact of the radio and sub-millimeter sources on the reconstructed pressure profile. The researchers were able to set strong constraints on the electron pressure distribution after accurately removing the contribution of point sources. The comparison with X-ray only data shows good agreement for the pressure, temperature, and entropy profiles, which all indicate that MACS J1423.8+2404 is a dynamically relaxed cool core system. The comparison with Herschel satellite data allowed in addition the investigation of the spectral energy distribution of the sub-millimeter point source contaminants.

The present observations illustrate the possibility of measuring the properties of the intra-cluster medium with a relatively small integration time, even at high redshift and without X-ray spectroscopy. These observations act as a pathfinder for the surveys that will become possible in the long term with NIKA2, the second-generation camera which is currently under testing at the IRAM 30-meter Telescope.

A GALAXY CLUSTER WITH A VIOLENTLY STARBURSTING CORE AT Z = 2.5

Clusters of galaxies represent the most massive dark matter halos in the universe. Studying the formation and evolution of galaxy clusters and their member galaxies is fundamental to the understanding of both galaxy formation and cosmology. Studies of galaxy clusters and numerical simulations suggest that massive clusters and their member galaxies have experienced a rapid formation phase at z > 2. Observations of galaxy structures in this rapid formation phase are therefore critical to map the full path of galaxy cluster formation and to answer fundamental questions about the effect of dense environments on galaxy formation and evolution. Such structures, however, have been so far difficult to detect due to their rareness and distance.

In an attempt to look at this question, Tao Wang (CEA Saclay/Nanjing University) and collaborators report the discovery of CL J1001+0220, a remarkable concentration of massive galaxies at z~2.5 in the central COSMOS region, and presumably the most distant X-ray galaxy cluster known to date. This overdensity was detected at sub-millimeter waves with SCUBA-2 and ALMA and motivated a series of follow-up observations with NOEMA, VLT and JVLA to explore the properties of the member galaxies.

These observations spectroscopically confirmed 17 members including 7 red galaxies in the cluster core. The redshift was determined by NOEMA to be z = 2.506 with a velocity dispersion of 530 ± 120 km.s^{-1}. The region exhibits a high star formation density in the 80 kpc core with a combined SFR of ~3400 $M_{\odot}$.yr^{-1} and a gas depletion time of ~200 Myr, suggesting that the cluster is in a rapid build-up of a dense core. The high star formation rate is driven by both a high abundance of star forming galaxies and a higher starburst fraction (~25%, compared to 3%-5% in the field). The presence of both a collapsed, cluster-sized halo and a predominant population of massive SFGs suggest that this structure could represent an important transition phase between protoclusters and mature clusters. It provides evidence that the main phase of mostly passive evolution of massive galaxy takes place after galaxies accrete onto the cluster.

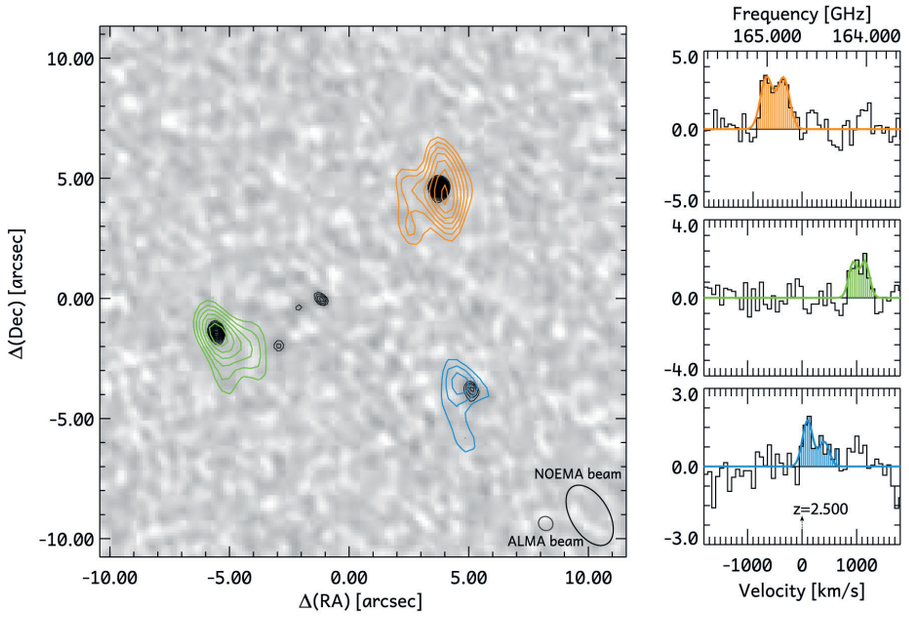

NOEMA and ALMA observations of the cluster core. ALMA 870 µm continuum map of the cluster core overlaid with ^{12}CO (5-4) emission line detections from NOEMA. In total, five sources in the cluster are detected with ALMA, three of which are also detected in ^{12}CO (5-4) with NOEMA (right panel). The NOEMA and ALMA beams are denoted by the small and large ellipses, respectively. Work by Wang et al. 2016, ApJ, 828, 56.

H_2O LINES AS PROMISING DIAGNOSTICS OF THE ISM IN HIGH-REDSHIFT STARBURSTS

After H_2 and CO, H_2O is one of the most abundant molecules in the interstellar medium (ISM) and probably one of the most powerful diagnostics of the physical conditions of the ISM in starbursting galaxies such as the sub-millimeter galaxy (SMG) population. Strongly gravitationally lensed SMGs offer an extraordinary potential to detect the presence of water and eventually gain a representative picture of the gas distribution in SMGs of the early Universe. By picking the brightest, lensed SMGs from the Herschel-ATLAS survey and using the sensitivity of the NOEMA Interferometer, Chentao Yang (PMO, IAS-Orsay) and collaborators have built the largest sample of high-redshift H_2O detections to date.

The researchers report to have detected 21 out of 23 H_2O transitions and 4 H_2O^+ lines in 17 lensed SMGs at redshifts between 2 and 4. Among the lines are 16 transitions of para-H_2O (2_{02}–1_{11}) or (2_{11}–2_{02}), and 5 of ortho-H_2O (3_{21}–3_{12}), with velocity integrated fluxes ranging from 2 to 15 Jy.km.s^{-1}. The similarities in linewidth and flux between CO and H_2O are sufficiently strong to suggest that both molecules are probing the same regions. Yang and collaborators also find strong correlations between the luminosity of the H_2O lines and the total infrared luminosity, $L_{H_2O} \sim L_{IR}^{1.1-1.2}$. These results suggest that, like for local starbursting galaxies, the sub-millimeter emission of water in the early universe is dominated by the radiative pumping via the far-infrared dust emission. The authors derive warm dust temperatures of 45-75 K and H_2O column densities $N(H_2O)/\Delta V \geq 0.3 \times 10^{15}$ cm^{-2} km^{-1}s. The researchers also detected H_2O^+ lines and found a very tight correlation between the luminosities of the H_2O and H_2O^+ lines. The line flux ratio indicates that intense cosmic rays generated by strong star formation are possibly driving the oxygen chemistry in the gas-phase ISM.

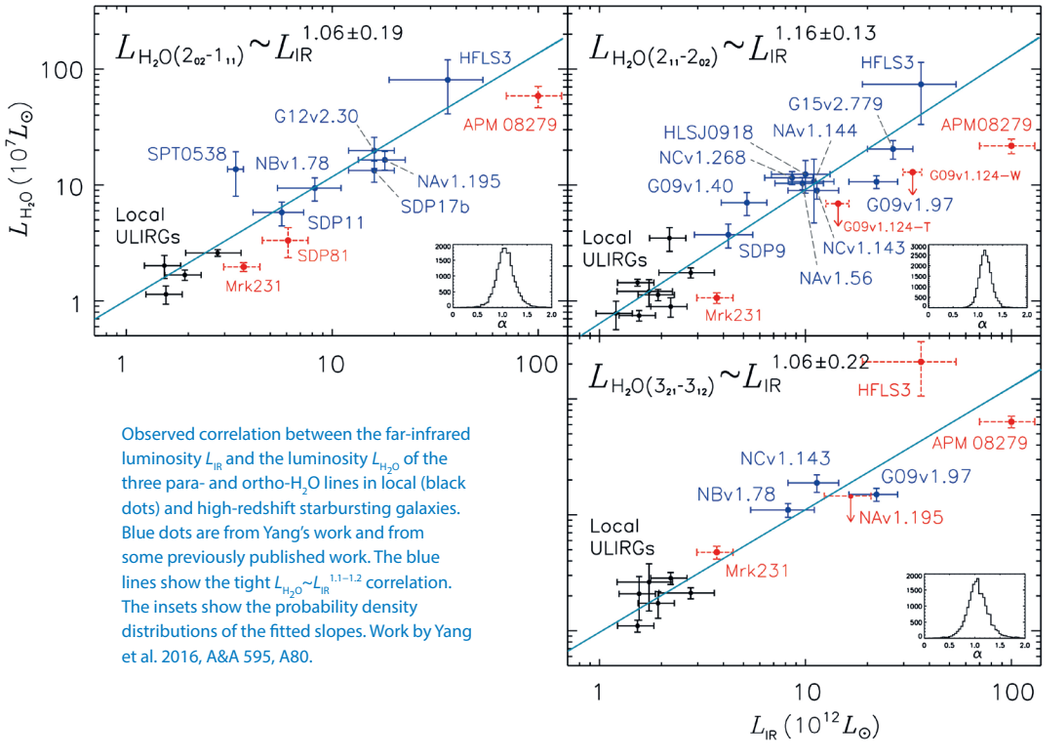

Observed correlation between the far-infrared luminosity L_{IR} and the luminosity L_{H_2O} of the three para- and ortho-H_2O lines in local (black dots) and high-redshift starbursting galaxies. Blue dots are from Yang's work and from some previously published work. The blue lines show the tight $L_{H_2O} \sim L_{IR}^{1.1-1.2}$ correlation. The insets show the probability density distributions of the fitted slopes. Work by Yang et al. 2016, A&A 595, A80.

The 30-meter Telescope

Early afternoon view of the observatory with a sea of clouds rolling underneath. Credit: DiVertiCimes/IRAM.

The 30-meter Telescope and especially its Eight Mixer Receiver, EMIR, with its large bandwidths and frequency agility, were in high demand by the astronomical community throughout the year, while the intense phase of testing and commissioning of the New IRAM KID Array, NIKA2, continued with vigour. NIKA2 was installed in October 2015. The NIKA2 consortium, led by Alessandro Monfardini (Institut Néel), and the IRAM staff have been heavily involved in the commissioning of NIKA2 during the whole of 2016.

New IRAM KID Array (NIKA2)

NIKA2 operates simultaneously at 2.0 mm and 1.15 mm with a field-of-view of 6.5 arcmin. It is comprised of three arrays of superconducting Kinetic Inductance Detectors (KID). The 2.0 mm array has 616 pixels, which are polarisation insensitive. The two 1.15 mm arrays each have 1140 pixels, which allow for polarimetry. NIKA2 has a closed cycle cooling circuit allowing it to be continuously operated over periods of several weeks or even months, as this year showed. Cooling-down the cryostat to its operational temperature of about 150 mK takes about 5 days in total. The first stage of 4-5 K is reached by two pulse tubes, while the final temperature is reached by a closed-cycle ^{3}He/^{4}He dilution fridge.

During several cool-downs, the receiver group at IRAM Granada has closely shadowed their colleagues in the NIKA2 consortium. The cool-down and the much shorter warming-up cycles can be remotely controlled and followed by the teams in Grenoble and in Granada. Operation also showed that the new water cooling system of the two cryostats in the telescope pedestal works well, even under elevated outside temperatures in the summer months.
A lesson learned is that the pressures, especially in the ^{3}He circuit, need to be closely watched, and that a spare of this precious gas needs to be in storage. Wrong positioning of the pulse tubes can create unwanted noise contributions, which are to be avoided. In September, the 2.0 mm array, the dichroic, which splits the two wavelengths, and several lenses inside the cryostat, were replaced. In addition, a homogeneous set of electronic readout boards was successfully installed.

Commissioning observations have consisted of several EMIR pointing sessions adapted for the different Nasmyth offsets of NIKA2. During commissioning, primary calibrators Mars and Uranus were regularly observed, in addition to secondary calibrators like MWC349, CRL2688, NGC7027 and W3OH. To extend the number of calibrators, the three brightest asteroids Ceres, Pallas and Vesta were regularly observed, as their fluxes, though time variable, are accurately known. Beam maps were done to investigate not only the shape of

the main beam, but also the structure of the error beams, sidelobes, and the structure caused by the quadrupod secondary support legs to low levels of intensity. Focussed and de-focussed beam maps were done in the direction of the optical axis, and in the perpendicular directions. The resulting maps, and the variation of the best focus over each of the three arrays were compared with predictions from ZEMAX simulations. Some weak sources were observed, and integrated over few hours, further improving knowledge on the NIKA2 sensitivities at 1.15 mm and 2.0 mm, under different weather conditions. Regular skydips were compared with the skydips of the 225 GHz radiometer and used to establish the relation between total power detected with NIKA2 and sky opacities to correct individual scans for atmospheric transmission. During commissioning, the timing and the procedures used to tune the KID elements were improved to reduce operational overheads. With the installation of a new set of electronic boards, the NIKA2 time synchronization was improved. The IRAM raw data format, IMBfits, does now include a subset of the NIKA2 level-0 raw data, including telescope information. At present, raw data are further digested by an IDL pipeline created and constantly improved by the NIKA2 consortium. First steps were done to read the IMBfits data into MOPSIC software package with the aim to develop the future data reduction software for NIKA2. Preliminary commissioning results have been published already in May.

An IRAM internal 2-day workshop was organized in November to discuss the status of the 30-meter Telescope and future plans. The aim was to evaluate its current operational and science performance, and discuss possible improvements to achieve an overall improved telescope. In December, a shorter and smaller follow-up meeting was held on the Antenna Mount Drive (AMD) telescope control software. A second 2-day workshop is planned for spring 2017, to focus on the operation system, telescope control software, and data management.

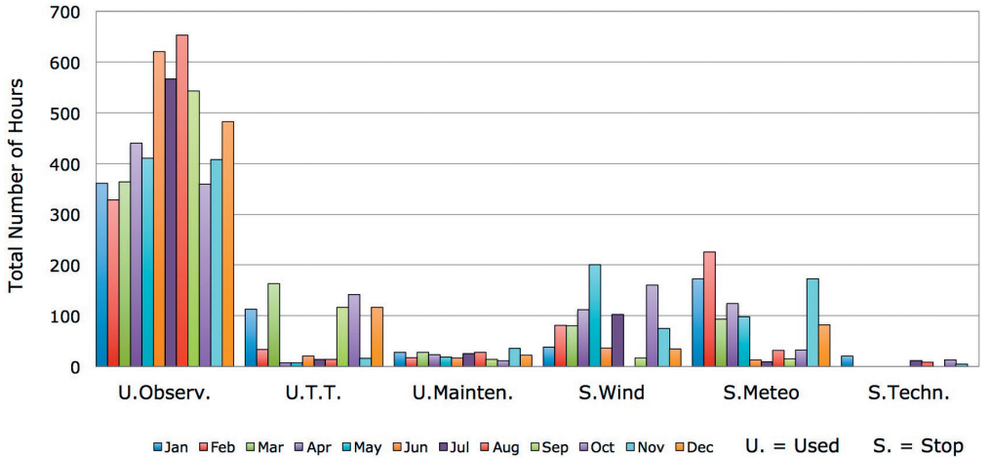

Monthly time distribution of observing time, technical projects (T.T.), maintenance, time lost due to high wind speeds, other adverse meteorological conditions, and technical issues.

ASTRONOMICAL PROJECTS

During the year, a total of 171 projects were observed at the 30-meter Telescope. This number includes one Large Program, 5 Director's time projects, and 13 VLBI projects. About 13% of these proposals were scheduled in heterodyne pool weeks. The fraction of remotely observed projects has increased over recent years, as this observing mode has matured thanks also to the increased bandwidth and greatly improved stability of the internet connection to the telescope. About 26% of the scheduling units were observed remotely. Galactic topics were addressed by about 75% of the scheduled projects, while the remainder was devoted to nearby galaxies and more distant objects. The vast majority of the scheduled projects used the multiband, dual-polarization heterodyne receiver EMIR. The remaining time was dedicated to observations with the 1.15 mm 3x3 pixel array receiver HERA (4% of the projects). NIKA2 was being commissioned with no science projects scheduled.

During the scheduling year, 127 astronomers visited the telescope to support projects, of whom, 21 came to support the observing pools. In addition, the NIKA2 consortium provided strong support to the NIKA2 commissioning by sending observers to the telescope. As in previous years, two groups of together 6 Master2 students from the Astrophysics program of the Universite Grenoble Alpes and from the Paris Master Astrophysics Program (Paris M2 AAIS), and their tutors, visited the telescope to observe short projects as part of their training courses.

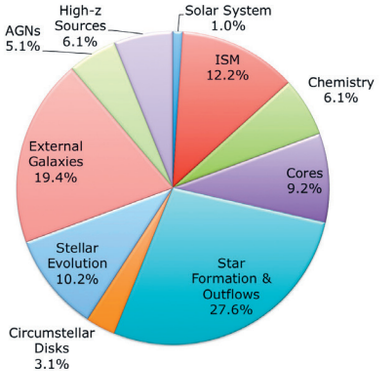

Time distribution of scientific categories observed in 2016.

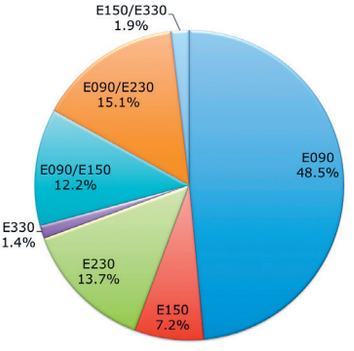

Usage of EMIR bands in 2016.

OBSERVATORY OPERATION

Despite of the strong demands for technical time, which was mostly due to the commissioning of NIKA2, the total time spent on observations was high: 64% of the total time were used for observing science projects. As in previous years, a quarter of the total time was lost because of adverse meteorological conditions, including high wind velocities. The time lost due to unforeseen technical issues was 2.5 days (0.7% of the total time).

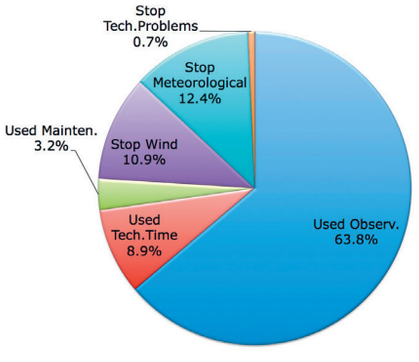

Usage of the total time at the 30-meter Telescope.

The main activities carried out by the telescope group are related with the daily operation of the observatory: the maintenance of the systems and equipment of the observatory and helping with the daily problems concerning the observation and operation, repair or replacement of failing equipment. Among the activities related to the support of NIKA2 are the installation of a new ventilation system in the receiver cabin to improve the air flow for cooling the electronic boards of NIKA2, and the installation of a new cooling machine for the air conditioning system on the roof of the receiver cabin and the servo room to increase the cooling capacity for NIKA2. In the context of improving the telescope control, software was developed to stop the antenna immediately in case of unexpected behaviour of the motors. The tool is monitoring the motor currents and works directly on the servo system, bypassing the Antenna Mount Drive software (AMD).

Among many other activities, work was undertaken to improve the electrical grounding of the observatory. New metal rods have been burrowed that had been welded with a special technique to

prevent corrosion reactions on the rods. Further on, a new false floor was installed in the observers control room.

To address the short and long term evolution of mechanical losses in the telescope gearboxes, periodical vibration measurements have been continued in collaboration with the Predycsa company. In the context of protecting the 76-81 Hz band against interferences from car radars, the Spanish Ministry SETSI inquired IRAM about the astronomical interest in this frequency range. IRAM Granada participated in a meeting with SETSI on May, 6th. Finally, a new electrical contract for the electricity supply was signed with the Sevillana-Endesa company.

SAFETY

Every two years, a training course on fire extinguishing is organized for all staff members at the 30-meter Telescope with the Granada fire brigade. The course was held at the observatory on June 16. End of November, eight staff members participated in a training course on driving in adverse circumstances, also offered by the Granada fire brigade. The goal was to improve driving skills under possible difficulties which can occur on the access road to the observatory.

A fire at the observatory is always a potential risk that deserves special training for the operators. This training includes the use of autonomous breathing equipment. Six sets are available at the observatory. The operators repeat an internal training exercise twice per year. For fire protection, 90 fire sensors are distributed in the observatory and connected to a central in the control room. In addition, the observatory has 70 fire extinguishers, 7 fire hoses with 30 m^3 of water directly available. Two automatic fire extinguishing systems are installed in the computer room and servo room. All these equipments are periodically revised by an external company. New ropes have been installed for emergency evacuations from the servo room, the antenna, and from the lifting platform to the prime focus. IRAM staff who works in the observatory unaccompanied, is asked to carry a dead man's switch. Every second year, a first aid training course is held with the public emergency health service. A first aid kit is maintained at the observatory and a videoconference system is now available to communicate with the emergency health service. The IRAM Grenoble safety engineer visited IRAM Granada to discuss safety issues and attend the fire extinguishing training course.

FRONTENDS

In 2016, most of the effort was dedicated to the improvement of the existing equipment and to allow an easy and fast change between the different observing modes. Other tasks like the protection of the equipment from water leaks in the cabin and the constant fight against radio frequency interferences were ongoing.

NIKA2

Several hardware modifications were made, both on the external electronics as well as inside the cryostat. Three crates are available for the readout electronics, one for each KID array, and all of them populated with the latest model of the NIKEL acquisition board. The ventilation on the area around the electronics has been improved to get a better evacuation of the heat dissipated by the NIKA2 electronics. The preparation of the documentation and the transfer of know-how is still an ongoing task. Documents on the operation of the cryostat cool down and maintenance procedures, list of spares and others are in a very advanced stage. After the failure of one of the gas circulation pumps, part of the $^3He/^4He$ gas mixture was lost. A spare ^3He bottle has been ordered and now forms part of the general list of spares.

EMIR

Interferences have been found on all EMIR bands where a Gunn oscillator is used in the LO subsystem. This includes all the lower frequency bands but not the 0.8 mm band (E330), which uses a YIG oscillator. Installation of a waveguide band-pass filter at the output of the local oscillator box has proven to efficiently eliminate this type of interference. Bands E090 and E150 are already equipped with waveguide filters, band E230 will follow soon.

Another source of interference was found to be associated with the E090 mixer bias circuit. The problem was finally solved by exchanging the bias box. Interferences from auxiliary equipment have also been detected. Several ethernet network switches were at the origin of strong interferences in the IF band.

A new dichroic filter has been installed in September to replace the E090/E230 band combiner. The new filter has a much lower loss at the highest frequency end of the E230 band. This is especially important for the simultaneous observation of different transitions of the same molecule. In particular, this will allow efficient simultaneous observations of the 1-0 and 3-2 transitions of HCN, HNC and HCO+. After the installation of the new optics block on the E090 band, the alignment was found to be off by up to 4". The misalignment was finally corrected but it turned out to be a very tricky issue due to the interrelation between the different EMIR bands.

A precise knowledge of the single sideband (SSB) rejection is needed for a good calibration of the data, especially when the rejection is below the nominal 13 dB level. A SSB measurement system has been designed and built. It should allow the remote measurement of the rejection at any particular frequency and band of the EMIR receiver. The system simultaneously controls the signal generation, the EMIR calibration optics and the data acquisition and will provide a fast estimation of the SSB rejection.

The holography transmitter has been repaired and prepared for a near field holography test in fall 2016. The test was finally cancelled because of adverse weather conditions.

Very Large Baseline Interferometry (VLBI)

The 30-meter Telescope participated in two observing campaigns of the Global Millimeter VLBI Array (GMVA) at 3 mm. Good quality fringes were obtained during the first campaign May 19 to 25. For the second campaign running from September 24 to October 3 no fringes were obtained on strong sources. This is still being investigated by the Bonn correlator team. However, during a short dedicated test campaign on December 16, fringes were again detected at 3 mm, between the 30-meter and the antennas at Yebes, Onsala and Metsahovi.

In preparation of 1.3 mm Event Horizon Telescope, EHT, campaigns, which are planned for 2017, more Mark 6 recorder units were installed and tested, in addition to two units of Roach (R2DBE) backends from Haystack. The arrival of the new DBBC3 backend from Bonn was prepared. The goal is to record 2x4 GHz in dual polarisation with DBBC3 and two times 2x2 GHz in dual polarisation with R2DBE. The total data rate will then increase from currently 2 Gbit/s to 4x16 Gbit/s.

In preparation of a VLBI test at 0.8 mm between NOEMA and the 30-meter Telescope, the EMIR Band 4 was equipped with a new local oscillator harmonic mixer necessary to cover the 4-5 GHz range of the VLBI reference system, and a quarter-wave plate was testwise installed. A local phase noise test was successfully conducted by injecting a line into the EMIR receiver.

The VLBI observing mode at the telescope is changing as more time is being requested. And, contrary to the past, VLBI observations now don't use the complete 24 hours per day slot, requiring frequent changes in the observing mode. In order to facilitate the fast and reliable switching between VLBI and non-VLBI observations, a remotely controllable unit has been designed and built to allow the insertion of the quarter wave polarizing plates and the signal generator in the receiver beam, which is needed during VLBI observations and phase noise tests. In addition, a high quality, remotely controlled RF switch was installed for the local oscillators.

COMPUTERS & SOFTWARE

The year 2016 has seen several upgrades and improvements in the area of networks, internet connectivity, and computer infrastructure. These efforts are leading to lower operational costs, better resource utilisation, better science support, and overall enhanced security.

A reliable, redundant network link between the Granada offices and the observatory at Pico Veleta was put in place. The internal network at the observatory has been segmented into operational and general purpose sub-networks. Redundant network equipment was installed and tested. The net effect was protection from hardware failures and misuse of the infrastructure which is critical for science operations. The same strategy was applied to the offices in Granada and to the link between the two sites.

As for science support, significant work has been performed in support of NIKA2 operations and data processing during the commissioning of NIKA2 and in preparation for science runs. This has involved improvements to the TAPAS online metadata archive and observation logbook, and significant disk space provisioning for long-term data storage as well as short to medium term science processing. Some software development took place for EMIR and VLBI observation support as well. Noteworthy, work has continued to introduce special features for NIKA2 in the New Control System, NCS, and in the observers user interface to NCS, paKo.

In terms of general computer infrastructure, a move towards service virtualisation was started with the purchase and commissioning of a new powerful server and installation of the needed software infrastructure. Virtualisation is an industry standard technique to achieve better computer hardware utilization and shorter service downtime resulting in improved reliability and lower operational costs.

MISCELLANEOUS

As in previous years, IRAM offered guided tours through the observatory and public talks to a broader public during the summer months. Eight events were organized by the astronomers group, in collaboration with the Instituto de Astrofísica de Andalucía (IAA) and the Universidad de Granada.

NOEMA Interferometer

The NOEMA array standing out against the sky in late April. Credit: A. Rambaud/IRAM

The highlight this year was the opening of the NOEMA eight-element interferometer to the astronomical community. First fringes were observed with antenna 8 towards the high-mass star-forming region Orion KL on April 19, and by early spring, three weeks after antenna delivery for scientific commissioning, NOEMA was performing regular science observations with all 8 antennas. In parallel, the observatory was on track to meet the next milestones: the delivery of antennas 9 and 10, and the commissioning of PolyFiX, a broadband correlator with 8 GHz frequency coverage in each sideband and in the two polarizations. Both upgrades were progressing well by the end of the year, and are scheduled to achieve completion in 2017.

The operation of the NOEMA Interferometer has been as exciting as in previous years. The combination of operational efficiency and system reliability for scientific observations led to a strong scientific productivity. The observatory completed the commissioning and science verification operations of antennas 7 and 8 and worked on the construction of the next two antennas. New bypass-tracks to facilitate antenna relocation for maintenance and array reconfiguration purposes were constructed, and a major renovation program to prepare for the arrival of PolyFiX was pursued. The NOEMA observatory also continued with the upgrade of computer systems and network infrastructure, and performed the yearly antenna maintenance activities. No interferometer downtime has been reported for observatory work related to the construction of the next NOEMA antennas. The antennas, receivers and the correlators, all performed well throughout the year.

All interferometer observations were performed exclusively in service observing mode, as usual. Observing conditions at the beginning of the year were reasonably good in terms of atmospheric transparency and stability during short periods until March. Band 1 (3 mm) and typically fair Band 2 (2 mm) observing conditions were met in the summer months, during the second part of the night until around noon. Observing conditions improved in September becoming excellent in October. NOEMA saw outstanding atmospheric conditions at the end of year.

The 7-antenna A-configuration was scheduled from January 24 until the second half of March, followed by the B-configuration until April 10, when the interferometer was moved to the intermediate C-configuration and the commissioning of antenna 8 started. The antenna maintenance period started on May 2, when antenna 2 entered the hangar. Due to major groundwork along the northern track that involved the extensive use of explosives for the construction of the service tracks, a special, somewhat extended configuration was scheduled from the end of May until early July, followed by a special 8-antenna D-configuration until the end of September. The interferometer was then moved into the 8-antenna C-configuration until mid December. To maximize the exploitation of the exceptional weather conditions at the site, the interferometer was

moved to the extended 8-antenna A-configuration on December 12, two months earlier than usual. Due to the heavy work activities, and unlike previous years, observations in the extended configurations during summer have not been possible this year.

The percentage of array-correlation-time invested on science observing programs was 30% of the total time, or equivalently, 113 days and nights. An additional 40% have to be accounted for array reconfigurations, array improvements and maintenance work, software developments, commissioning and science verification operations, and installing new equipment; the remaining 30% were lost because of precipitation, wind and poor atmospheric phase stability.

The IRAM observing program committee met twice during the year, around four weeks after the deadlines for the submission of proposals, and reviewed 219 regular proposals, including 25 proposals for observations in the Global Millimeter VLBI Array (GMVA, 3 mm) and 9 proposals for observations in the frame of the Event Horizon Telescope project (EHT, 1 mm). The large number of requests for VLBI observations is attributed to the fact that ALMA started offering VLBI observations with Cycle 4. The program committee recommended 144 (+16%) of the regular proposals, and recommended the approval of 16 (+266%) VLBI projects in the frame of the GMVA sessions and 6 proposals in the frame of the EHT project. Over the year, 5 proposals were received for Director's Discretionary Time (DDT). In total 243 individual sub-projects were accepted, plus 4 DDT proposals comprising 6 additional sub-projects. Counting the backlog of projects from 2015, science goals from 114 proposals were scheduled in 2016 at the NOEMA Interferometer, including science from 3 Large Programs, 4 DDT proposals and 5 VLBI GMVA proposals. This corresponds to 223 individual sub-projects that received time on the interferometer. All proposals were submitted and evaluated through PMS, the web-based Proposal Management System. Due to the large investment in technical time necessary in the current extension phase of the NOEMA project, no new Large Program was accepted for the interferometer under the Calls for Proposals. All the proposals for which time was granted in the course of the year are listed at the end of this annual report.

The NOEMA observatory continued to provide unique and exciting scientific results. As in 2015, the observing time requested to carry out galactic research was well below the level of time requested for extragalactic science. The lower interest (about 20% of the requested time) is largely to be ascribed to the inability of the narrow-band correlator to handle the signals of more than six antennas. As in previous years, a fairly large amount of observing time was invested in the most compact configuration of the interferometer, between spring and autumn, in the detection of line-emission from molecular and atomic transitions in galaxies at high redshift. The scientific section of the annual report presents some of the most relevant results obtained with the interferometer.

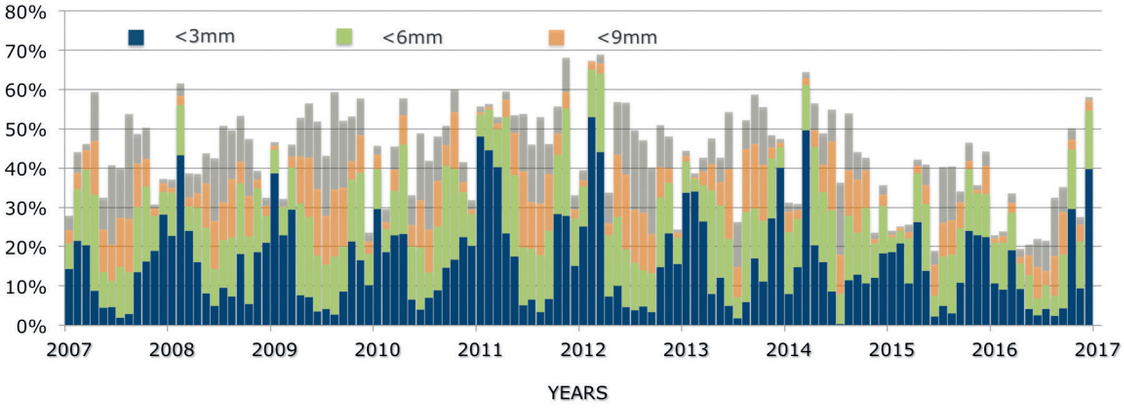

NOEMA observing time and atmospheric water vapor statistics over the last ten years. The overall correlation time accounts for 30% of the total time in 2016. Band 3 (200 – 268 GHz) programs and observations in the most extended (AB) configurations are for the most part carried out in the winter months when the atmospheric stability and transparency are highest.

ONGOING WORK AND ACTIVITIES

The integration of antenna 8 into the NOEMA array was the most significant event and among the most exciting and intense activities of the NOEMA Commissioning and Science Operations team (NCSO) in 2016. The start of the NCSO phase of antenna 8 began on April 10, with the delivery of the antenna to the commissioning team. The goal of the NCSO team was to take the new antenna from the stage reached at the end of construction to an instrument that meets the science requirements, and to deliver quantitative information on the antenna performance in terms of sensitivity, image quality and accuracy. The vast majority of the NCSO investigations were aimed at finding those characteristics that are not within the specifications. To achieve this objective, the NCSO team devised specific test procedures, carried out measurements, and processed data to identify and solve problems in close collaboration with the computing, engineering and construction teams. The NCSO activities included single-antenna verifications such as pointing and tracking, surface accuracy measurements, interferometric efficiency, and verification of the overall interferometer performance. First images from the commissioning and science verification operations of antenna 8 revealed the power of the new interferometer and helped to identify first areas where work had to be done to improve operational reliability. After a successful commissioning period lasting less than three weeks, antenna 8 started regular science operations on April 28.

Coupled to the arrival of antenna 8, work was necessary to adapt and prepare the real-time software of the IF processor and wideband correlator. While the wideband correlator was designed to process the signals of up to eight antennas with fixed spectral resolution (2 MHz), the narrowband correlator is limited to processing the signals of up to six antennas but with variable spectral resolution (down to 39 kHz). More on a technical side, a major refurbishment program took place in the autumn to prepare the observatory and the correlator room for the installation of the new correlator (PolyFiX).

Work on the construction of antenna 9 proceeded according to schedule. The construction of the antenna 10, the last antenna in the frame of NOEMA Phase 1 project, started at the end of July. The stop of the cable car services at the end of November was not expected to influence the construction schedule of antenna 9 – it might however delay the delivery of antenna 10. By the end of the year, studies were in progress to assess means and opportunities for keeping at a minimum delays in the antenna construction schedules.

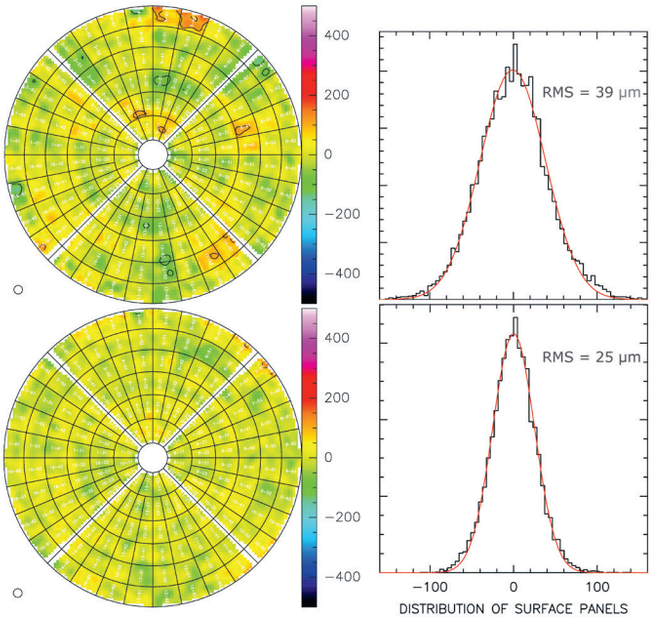

Surface panel distributions of antenna 8 relative to the ideal paraboloidal surface *(left)* and associated surface RMS *(right)*.
Top: holographic results of the antenna surface after delivery to astronomical commissioning.
Bottom: improved antenna surface after one iteration of panel adjustments.

In the frame of the NOEMA project, we also report the installation and commissioning of new receivers on antennas 3, 4, and 5. The new receivers are dual sideband mixers designed to operate in orthogonal linear polarization. They cover a nominal bandpass of 8 GHz in each sideband and in the two polarizations, and operate in three spectral windows (Band 1: 72-116 GHz, Band 2: 127-179 GHz, Band 3: 200-276 GHz). On the long term, a fourth spectral window (Band 4: 275-373 GHz) is planned to be installed on all antennas, but only 5 antennas were equipped with such receiver by the end of the year. The full receiver bandpass (32 GHz) will not be available for science observations until the arrival of the new correlator (PolyFiX). The performance of the receivers was evaluated over a limited part of the bandpass (4 GHz) through a series of technical verifications with the current wideband correlator. To improve the operational reliability of the new receiving systems for astronomical observations, work continued to optimize the receiver performance for fixed frequencies on a grid of 500 MHz steps. By the

Members of the IRAM Program Committee viewing into the depths of the hangar where NOEMA antenna 9 is being assembled. Credit: K. Kohno (Univ. Tokyo).

end of the year seven of the eight NOEMA antennas were equipped with new receivers, and all were found to show excellent performance across the bandwidth covered by the current correlator system. The current schedule foresees the completion of the receiver renovation project by early spring 2017.

Work was underway in 2016 to develop a new multi-channel water vapor radiometer with improved sensitivity to atmospheric phase fluctuations. It is thus expected to provide much improved interferometric efficiencies on long baselines and at high frequencies. The radiometer was also designed to facilitate its maintenance. According to planning, the prototype radiometer should be completed and tested in 2017, and by summer 2018, it should be installed in all NOEMA antennas.

While much of the focus at the NOEMA observatory has been on the construction of antenna 9 and 10, time and efforts have also been put into the regular maintenance program of the eight antennas. As in previous years, a huge investment in coordination and integration of the technical departments and external suppliers was required to achieve the necessary level of efficiency in both planning and execution, and a sustainable balance between science production, construction activities and maintenance work. To ensure that antenna maintenance work matches the schedule of the different activities, part of the maintenance was executed outside the hangar. The surface quality of each antenna was verified at the end of the maintenance period by means of holographic measurements. When necessary, surface panels were readjusted, verified and iteratively improved by holographic means. All in all, the primary surfaces of all antennas were adjusted to a median surface RMS of 32 µm at 45° elevation and exhibit excellent stability. In the same line of work, an effort has been started to investigate the presence of an elevation dependent large-scale surface deformation, characteristic of a gravity-induced astigmatism. The aim of these investigations is to further improve the surface quality of the NOEMA antennas to achieve best interferometer performance at the highest observing frequencies.

LONG BASELINE PROJECT

One of the main projects currently being undertaken at the NOEMA observatory is the east-west baseline extension of the interferometer. The goal is to extend the baseline from currently 760 m to about 1670 m, thereby providing NOEMA with high contrast imaging capabilities down to a spatial resolution of 0.1" at 345 GHz. To this end, a number of project tasks and objectives have been laid out in 2016. Among them, environmental impact studies have led to protected plant species being relocated to outside the track extension areas. Further, to determine the technical specifications for the new

antenna stations, a study was conducted to assess the altimetry accuracy of the existing stations. A project manager assistant was also appointed to oversee the consultation procedures with companies, launch a call for tender, assess offers received, and select the company to commission with the track construction work. The first heavy works of NOEMA Phase II for the extension of the east-west track were carried out during summer. The delivery of the track extension for astronomical commissioning and first scientific operations are not anticipated before the end of 2018.

The IRAM Baseline Extension Working Group inspecting the site in the proximity of the future NOEMA stations. In the background, the Pic de Bure.

VLBI

IRAM joined the Event Horizon Telescope (EHT) consortium, whose aim is to map the inner regions of nearby supermassive black holes in unprecedented detail, and participated in the proposal rating process. While first observations in the frame of the EHT project at 1 mm wavelength are foreseen in April 2017, NOEMA is not expected to participate before 2018. In the context of extending NOEMA capabilities to broadband VLBI, it was decided to wait for the arrival of the PolyFiX correlator.

In the spring GMVA session, NOEMA's observing efficiency was 82%. In autumn, the combination of adverse weather conditions and a software problem led to an efficiency of 42%.

USER SUPPORT

The NOEMA Science Operations Group (SOG) is part of the Astronomy and Science Support Group, a group of astronomers and software engineers with a wide range of expertise and technical knowledge in millimeter wave astronomy and associated techniques. The SOG is staffed with astronomers that regularly act as astronomers on duty to optimize the scientific return of the instrument, directly on the site or remotely from Grenoble. The SOG also provides technical support and expertise on the interferometer to investigators and visiting astronomers for questions related to instrumental performance, observing procedures, data reduction and calibration, pipeline-processing, and archiving of NOEMA data. The SOG interacts with the scientific software development group for developments related to the long-term future of the interferometer, performs the technical reviewing of the science proposals, collaborates with technical groups to ensure that operational requirements are being met, and keeps documentation up to date. Providing the best science data is at the core of the SOG's mission. As in previous years, the SOG managed to meet the objectives and to overcome organizational and technical development challenges in the NOEMA project. The requirements for the evolution of the tools needed to efficiently integrate the PolyFiX correlator into NOEMA end-to-end operations were identified and included in the development activities of the SOG.

The IRAM headquarters hosts a regular stream of visiting astronomers from around the world who stay at the institute for periods between a few days and a few months. While some of the visiting astronomers come to calibrate and analyze data from the NOEMA Interferometer, others are part of the IRAM Visiting Astronomers Program (VAP).

The VAP aims at training research scientists and postgraduate students in interferometry concepts, instrumentation and data reduction, and at strengthening science collaborations. In the frame of the VAP, IRAM welcomed a researcher from the University of São Paolo/Brazil on a ten-month stay and an INAF researcher from SNS/Italy to prepare and support work for the commissioning of the new antenna. Advice and assistance was also given to 47 investigators from Europe and overseas, visiting IRAM Grenoble for a total of 182 days to reduce and analyze data from the interferometer. Further assistance was provided to experienced astronomers from CEA/Saclay, DPAS/Dalhousie, MPIA/Heidelberg, MPIfR/Bonn for a total of 23 days to calibrate and analyze 4 NOEMA projects remotely from their home institutes. In total 41 science projects received support and advice. The overall level of user support remained constant over the last years. As in 2015, IRAM astronomers collaborated on more than 40 projects in which they were directly involved.

As the European RadioNet3 project came to an end in 2015, no financial support has been available this year to facilitate access to the NOEMA Interferometer for European astronomers.

DATA ARCHIVE

Data headers of observations carried out with the NOEMA and the former Plateau de Bure interferometer are conjointly archived at the Données astronomiques de Strasbourg (CDS), and are available for viewing via the CDS search tools. In 2016, the archive contained coordinates, on-source integration time, frequencies, observing modes, array configurations, and project identification codes among other data, for observations carried out in the period from January 1990 to September 2015. The archive is updated at the CDS every 6 months (May and October) and with a delay of 12 months from the end of a scheduling semester in which a project was observed in order to keep some pieces of information confidential until that time.

Access to the science data is initially limited to the principal investigators of the observing programs and to their delegates. While the proprietary period of Large Programs lasts 18 months after the end of the last scheduling semester in which the program was observed, the proprietary period of science data from standard NOEMA observing programs is set, since December 01, to end 36 months after the end of the last scheduling semester.

MILLIMETER INTERFEROMETRY SCHOOL

Participants at the 9th IRAM millimeter interferometry school, October 10-14, 2016.

The 9th IRAM Millimeter Interferometry School took place from October 10 to 14, at the IRAM headquarters in Grenoble. The school focused on both theoretical and observational aspects of millimeter interferometry. The IRAM scientific staff presented the lectures. The program of the school was structured to provide the participants with a broad base knowledge of the NOEMA Interferometer and its future upgrades. One morning session was dedicated to the use of ALMA. Participants had the opportunity to present posters on their own work, discuss results obtained with NOEMA and the IRAM 30-meter Telescope, share knowledge, and learn from each other's experience. The school was limited to a total of 57 researchers from Europe and overseas: France (15), Germany (16), The Netherlands (5), United Kingdom (6), China (2), Czech Republic (2), Italy (2), Spain (2), USA (2), Canada (1), Denmark (1), Portugal (1), Switzerland (1) and Vietnam (1). The lectures of this school and the proceedings from previous Interferometry Schools are available on the IRAM web.

ANTENNA MAINTENANCE

Due to the high occupancy level of the hangar for the assembly of antennas 9 and 10, the antenna maintenance plan tested on antenna 1 during summer 2015 was adjusted to minimize the time spent on the maintenance activities in the hangar. The planning was set up with one week of maintenance in the hangar per antenna, and 60% of the activities being done outside in a second phase. Following this organization, half of the hangar has been dedicated to the maintenance teams from the beginning of May, after the delivery of antenna 8, till the mid of July at the beginning of the construction of antenna 10, the other half being used for the assembly of antenna 9. The very mild weather of the summer period significantly helped to reach the goal of a directed maintenance program outside the hangar. However, the generalization of this methodology for future maintenance periods seems difficult, as efficient work organization and a quality maintenance program are largely incompatible with the climatic constraints of the site.

Technician verifying the subreflector mechanics in the frame of the regular antenna maintenance activities.

SITE DEVELOPMENT AND MAINTENANCE

Service tracks

Antenna relocation for maintenance purposes and array reconfiguration was becoming increasingly more difficult with the larger number of NOEMA antennas. To alleviate this problem and ensure minimum disruption of the interferometer when moving the antennas along the north-south and east-west tracks, three new bypass tracks were built during the summer.

The completion of this project, which was heavy in terms of logistics, required the supply of more than 1500 tons of materials and equipment to the site. These materials, as well as the dismantled equipment and its reassembly once on site, were carried up to the observatory as of April, thanks to the winch of the cable car. Around 300 trips spread over the whole spring and summer period, were necessary. Particular care was given to the sealing ring of station N13b at the end of the northern bypass track. Its construction allowed the testing and the improvement of the methodology required for the correct positioning of the centering ring. This approach proved to be essential to ensure the quality of the oncoming stations on the track extensions planned for NOEMA Phase II.

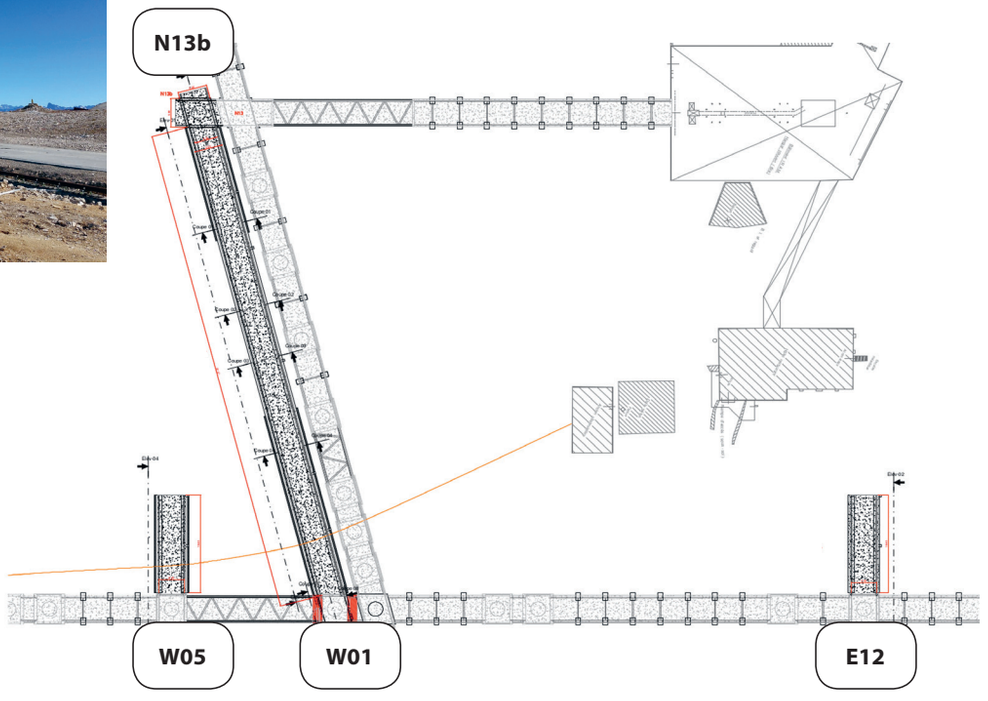

Top: NOEMA antennas performing science observations during the construction of the northern bypass track.

Right: the 104-meter long bypass track, parallel to the north-south track, connects station W01 to N13b. The two 20-meter long dead-end tracks, perpendicular to the east-west track, and respectively running from stations W05 and E12 northwards, are used to bypass antennas on the east-west track.

Correlator room

The correlator room underwent a technical upgrade to prepare for the arrival of new computer servers and PolyFiX, the new NOEMA correlator. The electric power distribution was completely redesigned to provide redundant and uninterruptible power supplies and to ensure a functional and physical separation of the various equipments. Similarly, the technical floors were fully refurbished and the cable routing paths were systematized and standardized to facilitate the implementation of additional cables in the future. Since the thermal specifications of the maser reference clock are incompatible with the new equipment installed in the correlator room, it has been moved to an adjacent location to ensure the best thermal stability.

IRAM staff taking advantage of the northern bypass track to relocate two antennas for an array configuration change.

Building maintenance

The most significant activity this year was the renewal of the waterproofing of the power generator room roofing, which had many leaks due to aging. The outer parts of the roof were stripped off completely, tarred membranes were replaced, and all parts re-sealed. In addition, the emergency staircase of the first floor of the observatory's residence building is planned to be relocated. The new staircase will be positioned parallel to the wall of the east facade, and will allow a much easier snow clearing of the ground floor emergency exit. The foundations were built in the autumn, and the staircase itself is scheduled for spring 2017.

CABLE CAR

Operation

The operation of the cable car by the SEETi company facilitated the transport of people, goods necessary for the everyday operation of the observatory, and materials for the construction of the service tracks. The cable car operation was stopped on November 21, following a technical incident. The operation has not been resumed by the end of the year.

	Transport of persons (cabin)					Transport of loads (lifting beams)				
2016	# of days	# people carried up	# people carried down	Weight up in tons	Weight down in tons	# of days	# loads carried up	# loads carried down	Weight up in tons	Weight down in tons
January	16	154	160	14,1	13,9	16	130	56	90,3	15,9
February	17	156	137	11,4	10,7	17	123	55	142,2	26,4
March	16	178	144	14,9	12,4	16	391	48	344,1	14,9
April	19	189	194	14,2	17,6	19	883	74	588,7	21,6
May	18	174	138	15,3	12,2	18	328	68	297,8	19,7
June	18	256	240	22,4	21,4	18	377	122	231,1	60,2
July	18	281	301	20,1	21,5	18	336	121	290,4	65,5
August	18	251	234	19,0	16,4	18	195	148	229,8	65,5
September	19	384	369	28,7	27,7	19	219	212	197,5	79,6
October	13	153	139	12,3	10,8	13	158	273	97,0	54,3
November	10	124	119	10,3	9,3	10	88	110	43,2	50,1
Total	**182**	**2 300**	**2 175**	**182,7**	**173,9**	**182**	**3 228**	**1 287**	**2 552,1**	**473,8**

Overview table of the monthly traffic of people and loads with the cable car in 2016.

Dismantling of the old cable car

The mandatory dismantling of the blondin started in 2015 with the removal of the wire and supporting cables. It continued this year, with the complete disassembly and dismantling of the pylons. The pylons foundations have been removed and some topsoil brought in to level the ground to the initial natural state. The whole equipment at the upper and lower cable car stations was dismantled, including pulleys, counterweights and the electronic control system. With the removal of the equipment, new storage space became available in both stations. Some of the space in the upper station might also be used in the future for IRAM external projects, such as the one currently conducted by the Institut Matériaux Microélectronique Nanosciences de Provence (IM2NP) in the premises of POM2 (Petite Opération Millimétrique 2) observatory.

OTHERS

Scientific visitors

At the NOEMA observatory, like in previous years, IRAM welcomed the visits of botanists and zoologists from various institutes and organizations in France and Europe working in the fields of ptarmigan counting (ONCFS), research on bats (ONF, Natura 2000), malacological prospecting (CEN PACA, ARIANTA association), botanical monitoring of the snowbeds (CBNA, LECA) and of the Helvetic Androsace (CBNA), and the study and counting of the nocturnal Lepidoptera (Natura2000). The scientific interest for flora and wildlife reflects the quality and importance of the site.

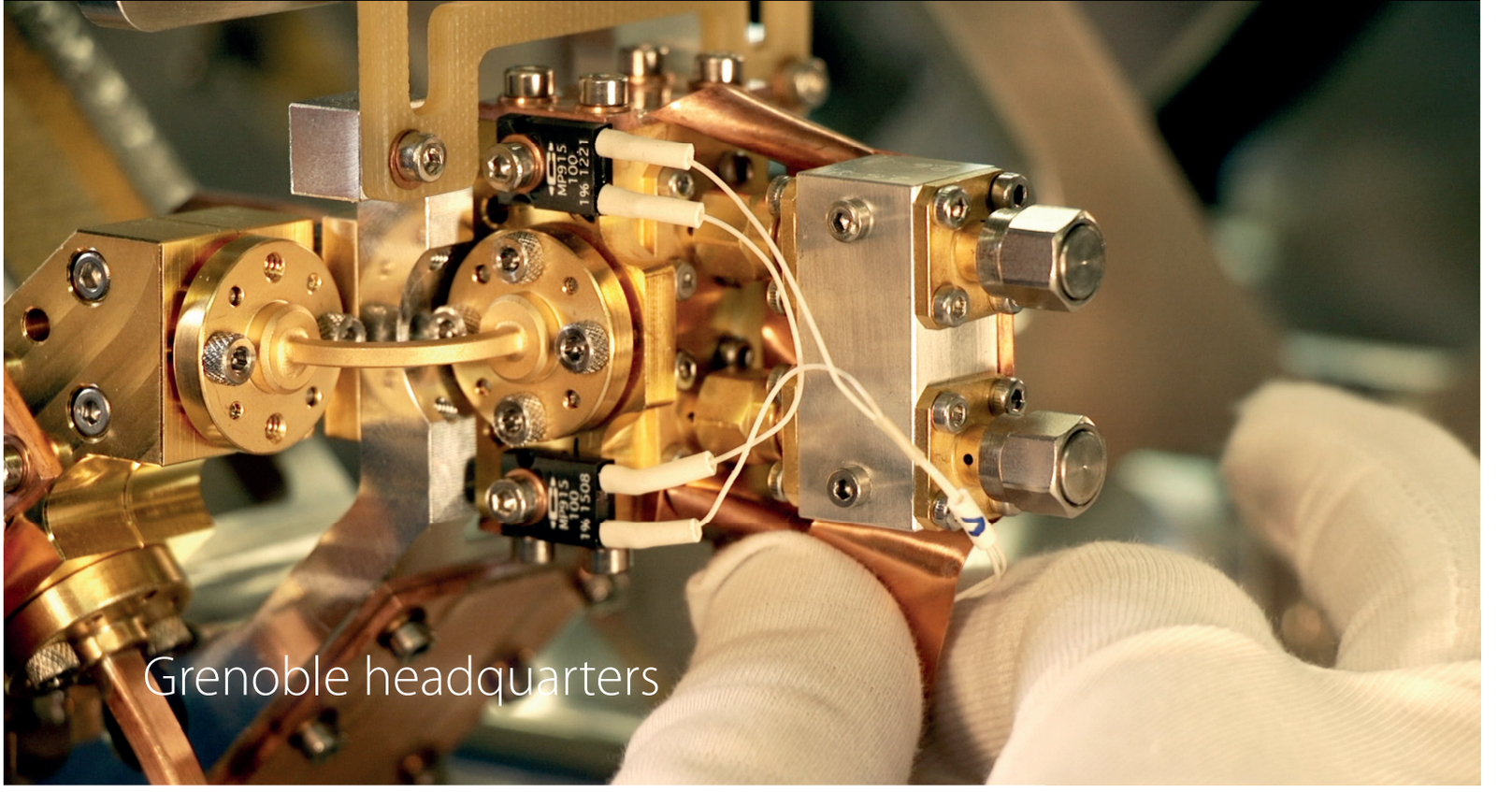

Frontend Group

In addition to the new developments summarized below, the IRAM Frontend group is responsible for the maintenance and repair of the receivers installed on both NOEMA and the 30-meter Telescope. This represents a continuous effort that is critical to support smooth operations of the IRAM observatories. In 2016, several operations such as replacing the 1st local oscillator (LO1) reference boxes or exchanging mixers took place.

EMIR

The EMIR receiver on the 30-meter Telescope underwent two important upgrades. Filters were installed in the LO path on the E0, E1, E2 bands, in order to suppress ghost lines that were visible in some observations and created by the local oscillator signals. A new dichroic for E0/E2 operations was installed in September. As a consequence, the noise introduced in the dual-band observations was significantly reduced, down to ~8-25K.

NOEMA RECEIVERS

After the installation of the first new receiver on the NOEMA Antenna 7 in December 2014, and its successful commissioning early 2015, the IRAM Frontend Group has started the series production of these new-generation receiver systems. All antennas were successfully equipped following a very tight time schedule: after each installation in an antenna, the old receiver was transported to Grenoble and dismounted, so that various elements, in particular the cryostat itself, the cryogenerator system, and part of the optics, can be retrofit and used in the next assembled receiver. The full process went smoothly, resulting in the production and installation of 8 receivers in an 18-month period. Having all antennas equipped with new receivers marks a paramount milestone for the NOEMA project, and was a major deliverable from the Frontend Group.

The NOEMA receivers are the result of several years of design and prototyping. All major elements, like 2SB mixers, optics, IF amplifier chains, optical-fiber laser racks, control electronics, calibration loads, local oscillators, were the focus of critical design reviews and optimization efforts, as described in the 2014 IRAM Annual Report.

NOEMA receivers installation schedule								
A7	A1	A2	A8	A3	A4	A5	A9	A6
Dec. 14	Nov. 15	Dec. 15	Apr. 16	Jun. 16	Aug. 16	Oct. 16	Feb. 17	May 17

The performances of the NOEMA receivers are unsurpassed worldwide in the millimeter domain. They are equipped with four bands, covering the 72-371 GHz frequency range. The new generation sideband-separation (2SB) mixers deliver 2x8 GHz IF and the full dual-polarization system thus delivers a total of 32 GHz per antenna to the correlator.

The commissioning of the receivers showed excellent on-site performances, well within the specifications. Pending the deployment of the PolyFiX correlator, the upper 8-12 GHz IF band has however not yet been commissioned.

In collaboration with the Science Operations Group, a significant effort was devoted to the development of new, automatized procedures to tune and characterize the receivers at the observatory. In addition, the tuning procedure of the receivers for science projects was improved, by using a much finer, fixed tuning grid, which allows optimized tunings to be used for the vast majority of the observations.

Top: NOEMA receiver assembly stages. The photos show the complex optical modules, mixers, and amplifiers positioning *(left and center)* and the full system closed in a cryostat *(right)* with four astronomical windows (Band 1 to 4), and two additional windows dedicated to calibration.

After testing, the complete 2SB receiving system, including the control electronics, is installed in the NOEMA antennas (*bottom:* during lift-off in one antenna).

NOEMA WATER VAPOR RADIOMETERS

Water vapor radiometers (WVRs) are an essential element in the phase calibration process of the array. For the NOEMA project, a new WVR system has been designed, to equip the new antennas as well as replace the old generation WVRs currently used on antennas 1-6. While still observing the 22 GHz water line, it provides 14 channels (instead of 3), with sensitivity and stability significantly improved. The radiometer includes an 18-26 GHz RF frontend followed by a 4-12 GHz IF filter-bank, which combines band–pass filters and a 16-channels splitter (14 detectors + 2 monitoring channels). Most of the design and first prototyping of the new system was done in 2016, with efforts principally focused on the filter bank.

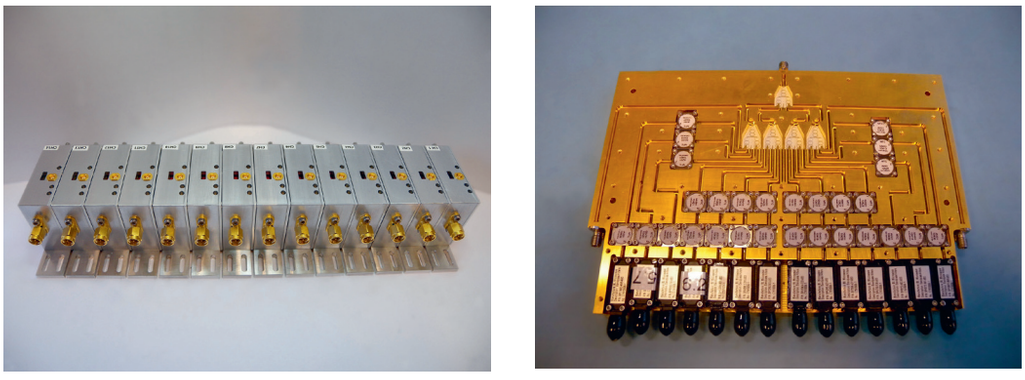

The 14 detectors and the filter bank of the NOEMA 18-26 GHz water vapor radiometers.

DUAL-BAND RECEIVER FOR THE MAX-PLANCK-INSTITUTE FOR SOLAR SYSTEM RESEARCH

During the last years, IRAM has designed and assembled a complete dual-band (2 mm + 1.3 mm) receiver for the Max-Planck-Institute for Solar System Research (MPS) in Göttingen, Germany. This receiver is intended to be used as radiometer for atmospheric sounding and be installed at the Zugspitze scientific station in the German Alps. The receiver is based on NOEMA developments. In particular, it is equipped with the Band 2 and Band 3 2SB mixers. The assembling of this receiver was completed and the system was fully characterized. A full end-to-end validation including the actual calibration unit, to be delivered by the MPS, must still be performed before the final acceptance.

7-PIXELS MODULE FOR FUTURE MULTI-BEAM RECEIVER

In the framework of the AETHER program of the EU-funded RadioNet collaboration, IRAM has designed a linear module of seven 2SB SIS mixers operating in the 1.3 mm band. It is intended to be one of the elements of a future 7x7 pixels array for the 30-meter Telescope on Pico Veleta. Two designs were studied in order to optimize the cost, construction complexity and mechanical precision.

Superconducting Devices Group

On a technological level, the activities of the Superconducting Devices Group (SDG) have focused around three main themes: fabrication of SIS junction devices, KID production and development, and development of other microwave components and new technologies.

SIS DEVICES

SIS devices are still the main workhorse of the SDG and the IRAM instruments. With the production of 14 SIS wafers, both the production for the three frequency bands of NOEMA and that of SIS junctions for broadband receivers in the 330-420 GHz band at the Smithsonian Astrophysical Observatory (SAO) have been completed. The production run for the SAO has revealed that IRAM junctions have a remarkably high quality factor Q of 28. This emphasizes once more the state of the art of the IRAM production facilities.

The finalization of the SIS device production has allowed investing in process development and redundancy. The SIS process has successfully been transferred to a new deposition machine to anticipate an eventual breakdown of the 30-year old machine that is currently used. The possibility of bringing the final wafer-lapping stage of the SIS production process in house has been investigated in view of the complete independence from external partners in this crucial technology for our observatories. This development will continue at full speed in 2017.

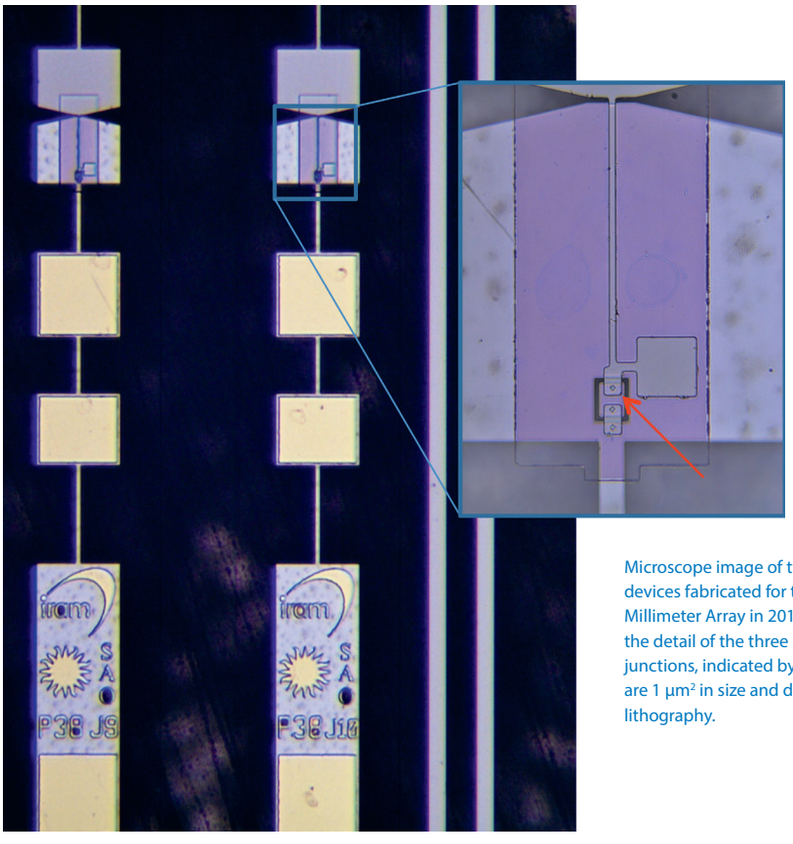

Microscope image of two of the SIS devices fabricated for the Smithsonian Millimeter Array in 2016. The inset shows the detail of the three SIS junctions. The junctions, indicated by the red arrow, are 1 μm^2 in size and defined by e-beam lithography.

KID DEVICES

With the completion of the NIKA2 installation in summer, the need for direct fabrication of aluminum KID arrays has decreased. Instead, the SDG has focused on several developments in the technology. Inhomogeneity of the aluminum film thickness is still the major challenge for large arrays closely packed in readout frequency. Several avenues for tackling this challenge, both in array design and in better material control, have been and are still being investigated. Additionnally, investigations on the ultimate detection performance of individual pixels are being performed, aimed at attaining the limit of the already very good sensitivity of the NIKA2 camera. A PhD student arrived in October to help make progress on these subjects.

OTHER DEVICES AND PROCESS DEVELOPMENT

The activities to produce normal-metal microwave elements for use in the detector integration (IF couplers, resistors) have continued at the request of the Frontend Group. Moreover, investigations on beam-lead technology, started in 2015, have continued and first devices equipped with this technology are to be expected in 2017.

Finally, many critical processes in the SDG depend on an ageing machine park, in which simple repairs are not always possible anymore. Discussions have been started with various suppliers to assess the situation in detail and come up with a long term investment plan that allows IRAM to secure its position as worldwide leader in superconducting detector technology in the future.

Backend Group

2016 was an extremely busy and productive year for the backend group. The main goal was the development of the analog IF processor and PolyFiX, the new NOEMA correlator.

ANALOG IF PROCESSOR

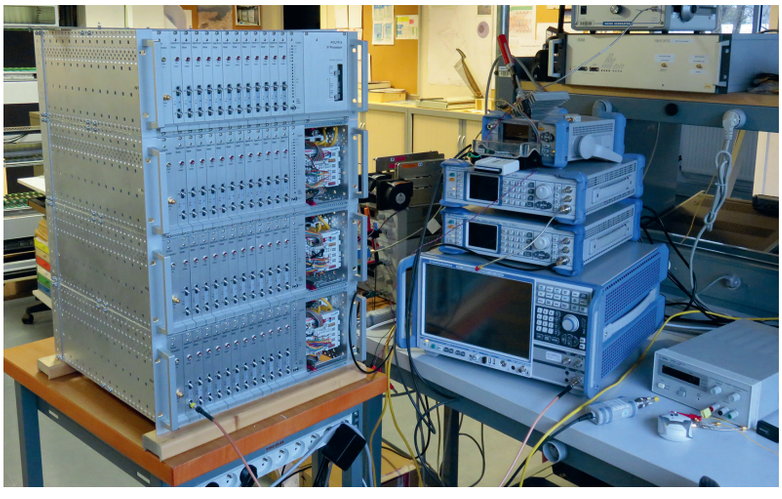

View of the NOEMA IF processor test setup.

Prior to the integration into the correlator system, the PolyFiX IF processor has gone through an extensive qualification phase. The performance range has been characterized for each of the 96 RF paths that will serve the 12 NOEMA antennas, 4 basebands and 2 polarizations. By the end of the year, the IF processor was found to operate reliably and within specifications.

DIGITAL CORRELATOR

The PolyFiX correlator hardware and gateware developments have continued throughout 2016.

Digitizer card

After tests on the first digitizer card version, substantial hardware modifications have been made in the second version to the power supply and the FPGA configuration scheme. The design of this version, intended for production in series, had already started by the end of the year.

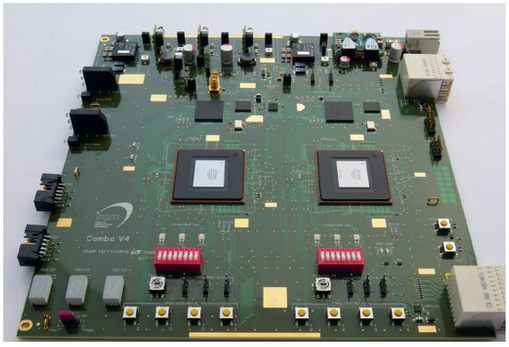

View of the correlator board (Combo V4) showing the 2 FPGAs that support baseline processing of 256 MHz bandwidths each.

Correlator card

The complex gateware development for the FPGAs of the correlator card continued throughout the year. Meanwhile, several hardware iterations have enabled the final version into series production.

Readout Card

Once integrations of the spectra and cross-spectra are performed, the contents of the integrators are collected and formatted by an FPGA in the READOUT card and transferred to a dedicated Linux computer via a high-speed fiber optic serial data link. The connection to the host computer is controlled by a data link (DDL) from Cerntech Ltd. that supports data rates up to 2 Gbps to transmit the 1.327.104 spectral channels generated every 31.25 ms. The readout board also ensures the generation and distribution of the system clocks. To minimize electrical path differences, it is located at the center of the correlator rack. After three design changes in the hardware versions, 9 of these cards, including one spare, have been produced, thus covering the need for the complete PolyFiX system.

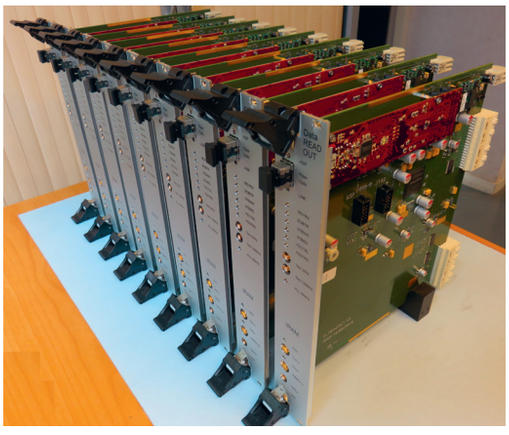

First batch of tested rack-mountable readout cards ready for installation.

Correlator unit prototype

By the mid of the year, a new version of the PolyFiX midplane board has been designed. This board supports the 384 high-speed serial links (3 and 6 Gbps) required to transmit data from the 12 digitizer cards to the 8 correlator cards. A series of 9 midplane has been realized for the PolyFix full system.

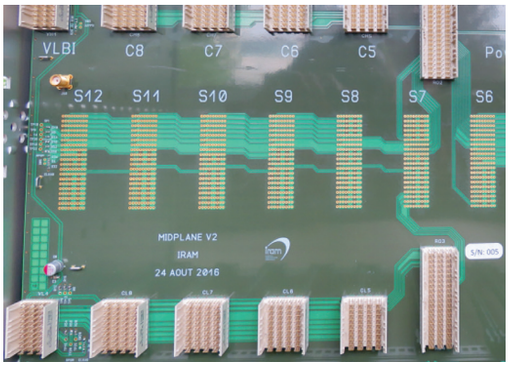

Close view of a PolyFiX midplane board showing high-speed connectors for the 3 and 6 Gbps serial links.

System Housing

The whole PolyFiX system will be housed in 4 cabinets. Each cabinet will be populated with a central IF processor and two correlator units to process an 8 GHz bandwidth as a whole.
Most of the mechanical parts have been purchased and assembled by the end of the year.

View of the 4 cabinets partially populated with future racks.

Mechanical Group

DRAWING OFFICE

The Mechanical Group's drawing office worked on numerous mechanical designs, in close collaboration with the other IRAM groups and also for other external laboratories. The group focused on the following projects:

Coupler for Band 3 mixer array

Following the results and success of the first prototype coupler, the group designed a new mechanical subassembly, in close collaboration with the engineers of the IRAM Frontend Group and with a a focus on reducing the time needed for production and quality control and lower production costs. The prototype coupler, which was put into production by the mid of the year, was delivered to the Frontend Group to pass the functional and performance verification tests. By the end of the year, first tests were suggesting the manufacturing process fulfilled technical requirements.

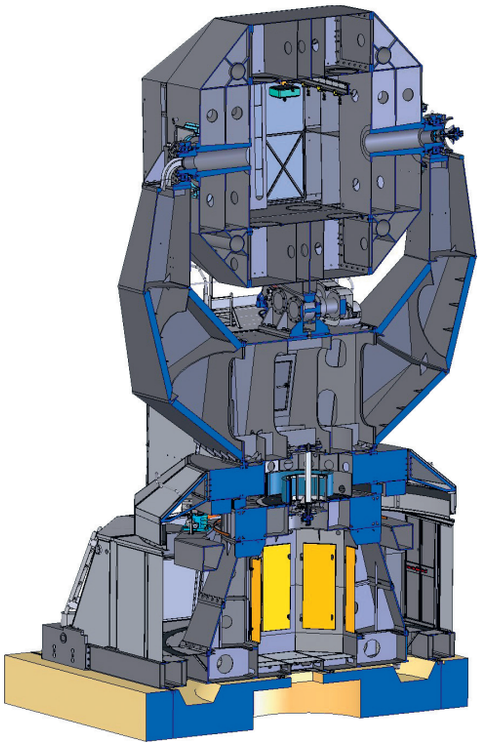

Cutaway drawing of a NOEMA antenna showing the inside of the mount and receiver cabin.

NIKA2

In the frame of the NIKA2 project, the drawing office worked on the design of mechanical and optical components, like mechanical supports for optical elements, lenses and mirrors.

NOEMA design

The drawing office completed all technical drawings of the NOEMA antennas. This project represents 4 years of study joining up two IRAM technicians and several external suppliers, more than 800 detailed 2D drawings for the antenna mount, more than 250 detailed 2D drawings for the reflector and more than 500 item references.

MECHANICAL WORKSHOP

The production of receiver components for the NOEMA antennas having been completed in 2015, the workload of the mechanical workshop was redirected to the prototyping and manufacturing of high precision components. The production of prototypes and small series with increased precision is one of the requirements to meet or exceed future technological challenges. Increased accuracy has several potential benefits as components must no longer be mounted and dismounted, the manufacturing of high precision components can be conducted in-house and lead times and production costs are reduced.

The mechanical workshop realized a first breakthrough with the successful drilling of sub-millimeter sized etched areas using a computer numerical controlled (CNC) high precision horizontal lathe machine. As part of the 2 mm band-pass filter project, the workshop developed and refined a method for the etching of regular 0.4 mm-sized grooves with a groove-to-groove spacing of 0.15 mm. The main difficulty in the milling process was the use of cutters with an important length-to-diameter ratio whose vibrations are susceptible damaging the grooves pitch.

The workshop took on a graduate intern to work on the high-precision components manufacturing project and help him gaining professional experience. By using computer-aided manufacturing (CAM) to facilitate and automate the production process, the production of the first prototype waveguide block took about three weeks, including the preparation of tooling and various stages of prototype adjustment and machining. The mechanical workshop has worked on 28 large projects in the scope of the NOEMA project, 10 of which were for the construction of a prototype 22 GHz water vapor radiometer.

In addition, the workshop was supplying components in more than 50 different side projects producing: OMTs, horns, optical components, including the design and fabrication of components for NIKA2, the new continuum dual-band camera for the IRAM 30-meter Telescope.

Cutter with 0.2 mm width and 1.0 mm length for the high-precision milling of grooves of the 2 mm band-pass filter block.

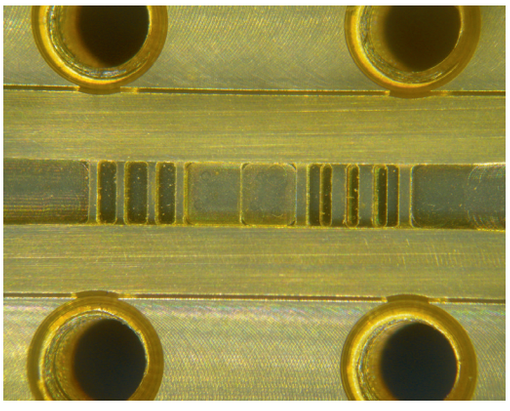

Close view on the 135-184 GHz band-pass filter for the NOEMA Band 2 local oscillator. It consists of the combination of one high-pass filter given by the waveguide cutoff and a low-pass filter whose rejection frequency is fixed by the 0.22 ± 0.01 mm large and 0.41 ± 0.01 mm deep slots.

NOEMA PROJECT – CONSTRUCTION OF ANTENNAS

Feedback received from the construction of antenna 7 was taken into consideration to accelerate the construction of antennas 8, 9 and 10. The objective is to produce one new antenna every year. Reaching this goal was particularly challenging, yet the mechanical group succeeded in delivering antenna 8 in April, according to the initial schedule. The construction planning of antenna 9 suggests the group will meet the objectives and deliver the antenna for astronomical commissioning at the end of March 2017. The construction of antenna 10, which started in June, was also advancing according to schedule by the end of the year.

Computer Group

INFRASTRUCTURE UPGRADES

The Computer Group has acquired two EMC Isilon storage systems to host the NOEMA astronomical archive. The first cluster has been installed in the NOEMA computer room at the observatory, and the second in the headquarters datacenter. Each cluster has 3 nodes (240 TB), but can grow up to 144 nodes (15 PB). Each node has its own processors, memories and 10G Ethernet interfaces to build a true scale-out platform, whose performances rise linearly with data storage capacity. To avoid bottlenecks, the nodes communicate together through a low latency dedicated 40G InfiniBand network. Moreover, unlike traditional systems, Isilon does not use RAID6 groups but Reed Solomon codes for faster data rebuilding when a disk fails. Finally this machine will allow IRAM to store as much data as needed in the future.

EMC Isilon cluster at IRAM headquarters.

The network core has been upgraded to 10G Ethernet in Grenoble and at the NOEMA observatory. The network backbone runs now with Ethernet switches from Extreme Networks (Summit X670-G2-48X). These Top-of-Rack switches have 48 SFP+ ports of 10G and four QSFP+ ports of 40G, so there are enough connection plugs for all the IRAM servers. At the same time, the Grenoble router has been upgraded to a Dell PowerEdge R430 with four 10 GB Ethernet, running Scientific Linux 6.7.

Finally, all the remaining servers in the headquarter datacenter have been virtualized and all the Windows computers have been upgraded to Windows 10, as scheduled.

NOEMA

Since 2012, antenna 5 has a hybrid control system with NOEMA-class motors associated with a legacy VME control rack. The dilemma was that on the one hand, the tracking performance was reduced in the presence of strong wind, but on the other hand, it would take weeks to install a genuine NOEMA antenna control bay. Fortunately an elegant solution has been found to get out of this complex situation. Firstly, a faster VME single-board-computer (Abaco XVB602) has been installed to keep access to the legacy VME bus while dedicating one of its dual Ethernet controler to the EtherCAT bus to drive the motors in real-time. Secondly, a VME software interface has been added to the NOEMA Antenna Control Software (NACS) Hardware Abstraction Layer (HAL). This way, it has become possible to run NACS on antenna 5 with neither hardware modification nor new software development. This solution has been commissioned in August, and has improved significantly the tracking performance at minimal costs.

Science Software

The main goal of the science software activities at IRAM is to support the preparation, the acquisition and the reduction of data both at the 30-meter Telescope and NOEMA. This includes the delivery of 1) software to the community for proposing and setting-up observations, 2) software to the IRAM staff for use in the online acquisition system, and 3) offline software from the GILDAS package to end users for the final reduction of their data. The GILDAS software is also freely available to and used by other radio telescopes, like APEX, Herschel/HIFI, SOFIA/upGREAT, and YEBES/40m. Specific efforts are also done to image and deconvolve ALMA data inside GILDAS.

On the single-dish side, much work was invested to ensure a smooth integration of MRTCAL, the calibration software for spectroscopic data which will progressively replace MIRA, in the online data flow of the 30-meter Telescope. In addition to devising solutions to remaining technical issues, work included coordination with the telescope staff. After a period of knowledge transfer from the development team to the operations staff, discussions took place to tailor software behavior. For instance, the Online Data Processing is set up to refuse by default calibrating data when the matching calibration scan is too far in time. The aim is to ensure that users invest telescope time regularly to properly calibrate the science data. This also included the definition of the online output that the software will automatically deliver, that are the real-time plots to help the observers verify the acquired data, and the daily reports to provide the staff with a regular overview. A list of systematic calibration tests was also devised to check the continuity and improvement of the calibration accuracy. Discussion of the schedule and of the exact scenario of the swap from MIRA to MRTCAL led to the decision to perform this transition in February 2017. Finally, the development team invested time on writing the end-user documentation that introduces main calibration concepts and illustrates main use cases. At the same time, work continued to support CLASS, the GILDAS software for the reduction and analysis of spectroscopic data. Efforts were also directed to the support of an improved calibration. The support of the concept of associated arrays introduced in 2015 was improved to allow CLASS to consistently deal with frequency varying parameters like system temperature and angular resolution. This step is required by the large increase of instantaneous bandwidth delivered by the current and future generations of spectroscopic receivers. Other developments were aimed at improving the imaging capabilities of the 30-meter Telescope. The internal code to produce position-position-frequency cubes was refurbished to ensure that datasets larger than the available RAM memory can be processed by slicing the data in intervals of frequency. Finally, support was provided for third-party telescopes. For instance, at the request of the SOFIA/up-GREAT team the internal buffer of the User Section has no more internal limited size. Another example is the possibility to change the intensity scale from Jy/Beam to Kelvin and vice-versa in order to better support the importing of interferometric data for further analysis or the exporting of single-dish data for the use as short-spacings to complement interferometric wide-field observations.

The commissioning of NIKA2, the dual color continuum camera, continued in 2016 at the 30-meter Telescope. Software activities were aimed at supporting the commissioning activities. In particular, the data format that was defined in 2015 was fine-tuned and functionalities to check the internal data consistency like the synchronisation between instrument and telescope, and gain stability, were developed or improved. A quick-look pipeline was also set up to monitor the online data acquisition.

On the interferometric side, 2016 was a key year in the NOEMA project with the delivery of antenna 8 in April and the finalization of the replacement of the old generation of receivers for the existing antennas. Both of these actions required time-consuming changes in the software to prepare the observations acquire and reduce the data. However, the main activity was directed towards the preparation of the arrival of PolyFiX, the new NOEMA correlator. Indeed, with the advent of this correlator, the full power of the NOEMA array will result in an increase of the data rate by a factor of 30. After the adoption of a common nomenclature for the new frontend/backend system to ensure good communication between developers, actual developments started in four areas: 1) development of the test software required to deal with the correlator in the back-end laboratory and the online software that will apply the real time calibrations, 2) the submission of science proposals for NOEMA, 3) the data format

and calibration engines, and 4) the adaptation of the monitoring and calibration pipelines. The association of wide bandwidth capabilities (16 GHz in each polarization) with the requirement to simultaneously acquire continuum and spectroscopic data at two different spectral resolutions (2 MHz over the full band and 62.5 kHz over a quarter of the band) makes PolyFiX an extremely versatile spectrometer. Work on ASTRO was necessary to help users easily and finely set up the correlator. This was done with the goal to ease the setup for newcomers while providing power users the full flexibility of the machine. This work will culminate with the delivery of the proposal submission interface early 2017. At the same time, the power of PolyFiX challenges the standard calibration engines of the CLIC software. First, the data format had to be fully overhauled to deal with the improved flexibility. Second, the atmospheric calibration and the calibration of the RF bandpass were revised. The monitoring and calibration pipelines available before the advent of PolyFiX have reached a state that almost delivers optimal calibration products. However, a dedicated audit showed that the large data-rate increase with PolyFiX required a thorough code optimization of reading/writing of the data. This work was started in 2016. Finally, the science software team made a specific benchmark effort to specify the requirements for the new online acquisition computers at the NOEMA observatory.

While the tuning of the calibration algorithms is extremely instrument specific, imaging and deconvolution of interferometric data is mostly independent of the acquisition instrument. Hence, the advent of ALMA broadband spectra with 8 GHz per polarization at high spectral resolution triggered a series of changes in MAPPING, the GILDAS imaging and deconvolution software. In particular, we continued to refurbish the software with a major revision of bookkeeping items related to the wide-field imaging capabilities. New functionalities such as the possibility to self-calibrate in phase the data or the way MAPPING deals with the variation of the dirty beam with the frequency, were fine-tuned. This work, made in collaboration with the Observatoire de Bordeaux, lays out the groundwork to the unprecedented wide bandwidth, high spectral resolution of the NOEMA Interferometer when PolyFiX will become available.

All these software developments are based on the common GILDAS services, a set of common low-level libraries, collectively named GILDAS kernel, which take care of the scripting and plotting capabilities of GILDAS. Many points, like the resurrection of the output plots in the Scalable Vector Graphics to facilitate the communication between GILDAS and the web-base proposal management system, were addressed in 2016. On a point that is more anecdotal but extremely valued by end-users, GILDAS now supports a much larger number of predefined colors to plot curves.

Finally, the Science Software Group organized a user meeting in April to present the projects that were developed in the past 5 years and the projects that are planned for delivery in the next few years. This also was a great opportunity to discuss face to face with the IRAM community and gather as much feedback as possible.

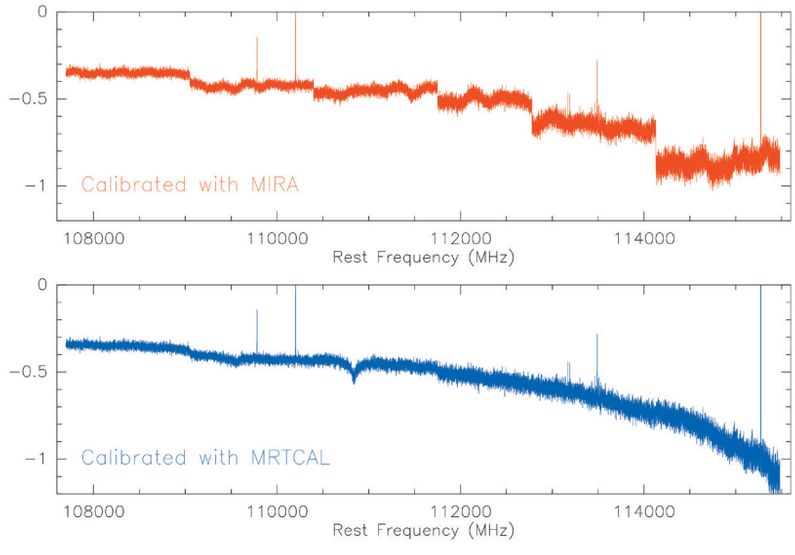

Illustration of the calibration improvement at the IRAM 30-meter Telescope. The top panel shows the old software solution and the bottom panel the new solution that will be used at the telescope after mid-February 2017. MRTCAL fixes the staircase pattern that was a calibration artifact.

IRAM ARC Node

Credit: C. Malin/ESO

IRAM is a node of the European ALMA Regional Center (ARC), the structure responsible for the ALMA science operations in Europe. The nodes are specifically in charge of supporting users, in particular for the data reduction.

IRAM's involvement in the ARC is part of a long-term, global involvement in the ALMA design, construction, and user support. One of the main goals of the IRAM ARC node is to provide to the astronomical community a common support for the IRAM and ALMA facilities, hence maximizing the scientific synergies between the observatories.

ALMA USER SUPPORT

The ARC node staff act as "Contact Scientists" for the accepted ALMA projects, providing help and expertise to check and validate the Scheduling Blocks that are created from the initial proposals.

The IRAM ARC node supports projects from the French, German, and Spanish communities. After a complicated year in 2015 due to manpower shortage, the ARC node welcomed an additional member. IRAM was able to support all Cycle 4 projects from its community in August/September 2 (Phase 2 for accepted programs).

A major service provided by the IRAM ARC node is face-to-face support for data reduction: users can obtain direct help for the data reduction, in a way similar to the support provided for the NOEMA projects. Travel funding is available for users affiliated to the IRAM funding agencies. In 2015, more than 20 projects were supported during face-to-face visits in Grenoble.

TELESCOPE CALIBRATION SOFTWARE

IRAM is responsible for the development and maintenance of one of the key software for the real-time operations of ALMA, the Telescope Calibration (TelCal) software. TelCal is performing all real-time calibrations necessary to operate the array. The involvement of IRAM is gradually decreasing, with a scheduled end of contract at the end of 2017.

Administration

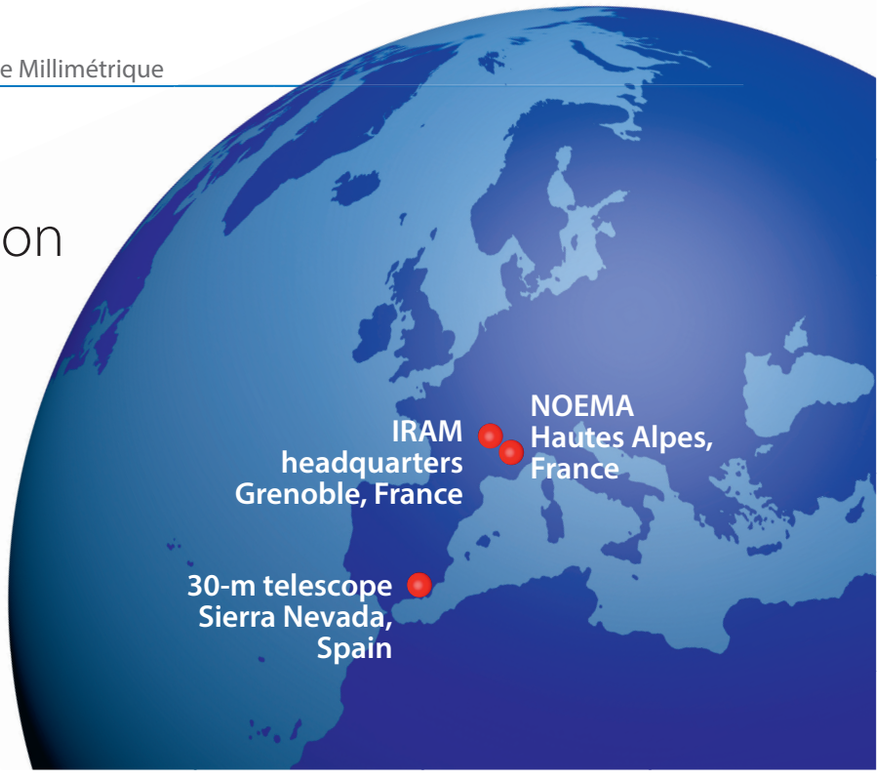

ADMINISTRATIVE ACTIONS

Dematerialization and globalization: those have been the keywords for the administration in 2016. Already effective for the accountancy, the globalization of administrative resources between France and Spain is evolving in two other administrative domains: legal issues and human resources. To this effect, the administration has created a common database and a dematerialized, real-time, traceable information system which guarantees the same service and management quality at all IRAM sites. The objective has been to disengage employees from tasks with low added value, which are now automated, and to position them mainly on the analysis and treatment of information. This is for the IRAM administration, an organizational but also a human commitment. In fact, this sophistication and complexification of work marks a qualitative evolution of job positions towards more attractive and motivating professional situations. Generally, the valorization of human resources has been a challenge for IRAM in 2016. Among several measures, the administration has created a transversal position dedicated to the operational management of human resources, and launched annual appraisal interviews. IRAM wants to attract talented people and does everything to achieve this objective.

FINANCIAL RESULTS

Income in k€	Actual 2016
Contributions from associates	21 568
Other income including budgetary result	10 649
Total income	**32 217**

Expenditure in k€	Actual 2016
Operation	12 473
Investment	6 919
Total expenditure	**19 392**

SAFETY

Rescue exercise with SDIS dog units

A rescue exercise was performed in winter conditions in collaboration with the Hautes Alpes fire workers and rescue department (SDIS). Six groups operating in 13 French departments performed a one-day training in rescue and orientation on the NOEMA site. This exercise helped the rescue services of the SDIS to be more reactive and ensure a better knowledge of the on-site conditions in case of emergency.

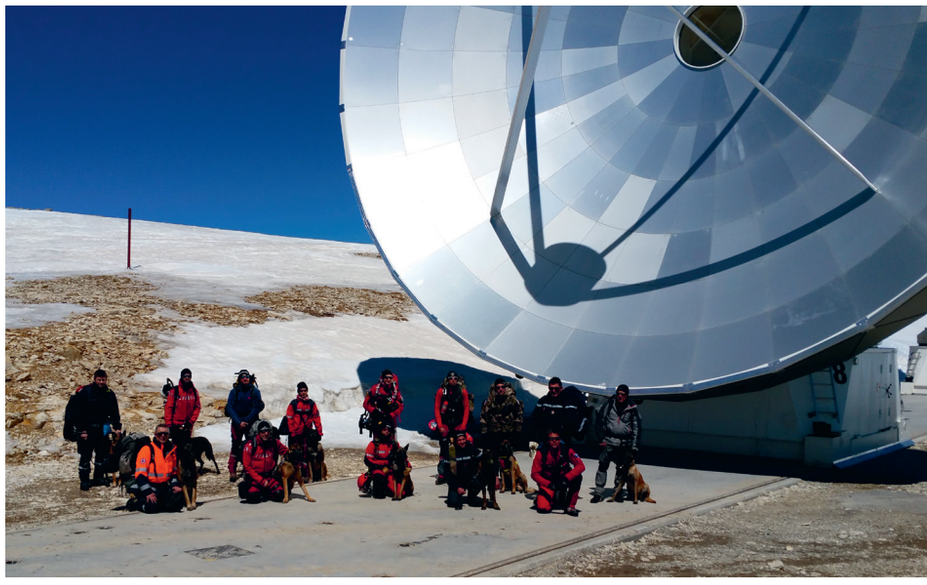

SDIS officers and fire dog handlers of the six canine rescue units attending the Jäger 2016 exercise at the NOEMA observatory.

New software Previsoft Health and Safety

In the area of safety regulation in France, the list of hazards due to risks at work has been entered in the database of the Previsoft software, along with a description and an analysis of the hazards. The aim is to find common preventive actions and solutions for the workers' health and safety. This new software automatically manages the list of chemical dangers as well as all identification sheets of any chemical product used at work. It is now possible to visualize common links between workers, their work station, their equipment and possible risks on a single document. This provides significant improvement and help for the follow-up of health and safety at work, and allows having an active preventive plan to avoid work accidents and health risks on IRAM workers.

New fire extinguishing system for the NOEMA maser

Due to temperature changes in the NOEMA correlator room, the maser equipment was relocated to an adjacent room to minimize impacts on maser performance. A new automatic system with Argonite 55 (50% Argon + 50% Nitrogen) is now used to protect the new maser room against fire. The extinguishing system reduces the percentage of oxygen by about 50% to effect the extinguish fires without damaging the electronic equipment and still preventing people from asphyxia.

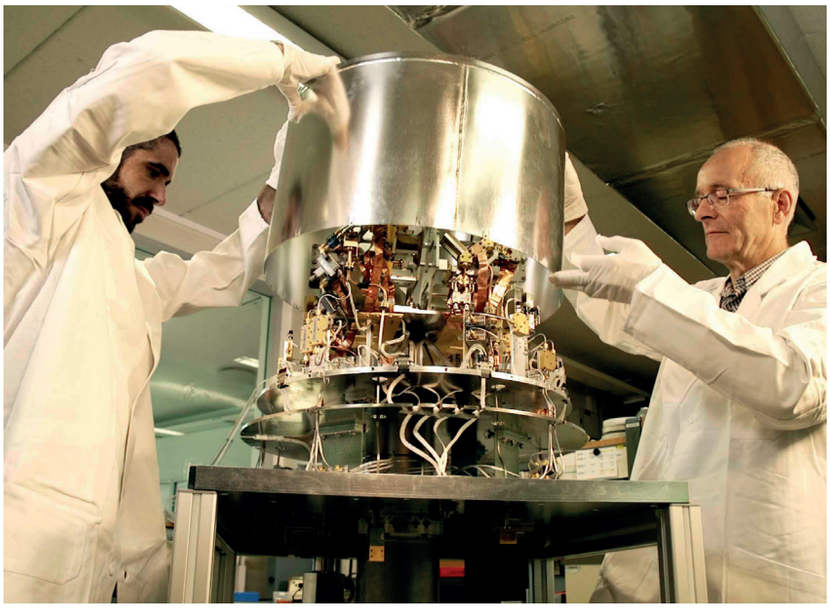

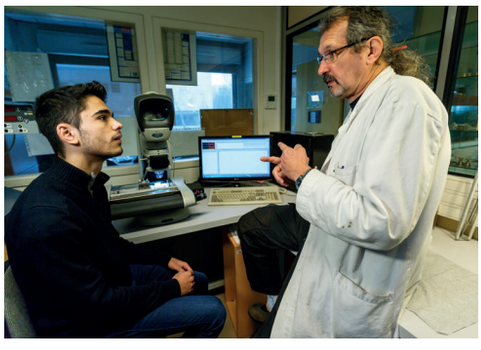

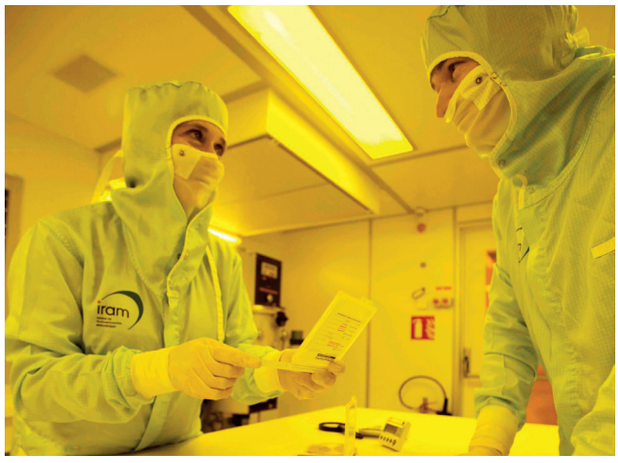
iram


iram
iram

IRAM staff list

IRAM Headquarters, Grenoble, France

DIRECTION	**SCHUSTER Karl-Friedrich**	Director
	GUETH Frédéric	Deputy Director
	DELLA BOSCA Paolo	
	ZACHER Karin	
ADMINISTRATION	**DELAUNAY Isabelle**	Head of Administration
	BACHET Claude	
	DAMPNE Maryline	
	FERREIRA Dina	
	INDIGO Brigitte	
	MAIRE Béatrice	
	MANFREDI Marilyne	
	MARCOUX Stéphane	
	PALARIC Laurent	
	SIMON Lauriane	
	SIMONE Jeannine	
ASTRONOMY & SCIENCE SUPPORT GROUP	**NERI Roberto**	Head of Astronomy & Science Support Group
	BARDEAU Sébastien	
	BEAKLINI Pedro Paulo*	
	BERJAUD Catherine	
	BOISSIER Jérémie	
	BREMER Michael	
	BROGUIERE Dominique	
	CASTRO CARRIZO Arancha	
	CHAPILLON Edwige	
	DOWNES Wilfriede	
	FERUGLIO Chiara*	
	HERRERA CONTRERAS Cinthya	
	KRIPS Melanie	
	LEFEVRE Charlène	
	LOPEZ SEPULCRE Ana	
	MONTARGES Miguel	
	PETY Jérome	
	PIETU Vincent	
	REYNIER Emmanuel	
	ROCHE Jean-Christophe	
	ROMERO Charles	
	WINTERS Jan Martin	
	ZYLKA Robert	
FRONTEND GROUP	BERTON Marylène	
	BORTOLOTTI Yves	
	CHENU Jean-Yves	
	FONTANA Anne-Laure	
	GARNIER Olivier	
	LECLERCQ Samuel	
	MAHIEU Sylvain	
	MAIER Doris	
	MATTIOCCO François	
	MOUTOTE Quentin	
	PARIOLEAU Magali	
	PERRIN Guillaume	
	PISSARD Bruno	
	REVERDY Julien	
	SERRES Patrice	
BACKEND GROUP	**GENTAZ Olivier**	Head of Backend Group
	BALDINO Maryse	
	CHAVATTE Philippe	
	GARCIA GARCIA Roberto	
	GEOFFROY Daniel	
	MAYVIAL Jean-Yves	
	SASSELLA Remi	
SUPERCONDUCTING DEVICES GROUP	**DRIESSEN Eduard**	Head of Superconducting Devices Group
	BARBIER Arnaud	
	BILLON-PIERRON Dominique	
	COIFFARD Grégoire	
	HAMELIN Catherine	
	SHU Shibo	

* Visiting Astronomer

MECHANICAL GROUP

LEFRANC Bastien	Head of Mechanical Group
COPE Florence	
COUTANSON Laurent	
DANNEEL Jean-Marc	
JUBARD Vincent	
LAZARO Gaëtan	
ORECCHIA Jean-Louis	

COMPUTER GROUP

BLANCHET Sébastien	Head of Computer Group
CHALAIN Julien	
DUMONTROTY Patrick	
REYGAZA Mickaël	

NOEMA, Plateau de Bure, France

GAUTIER Bertrand	Station Manager
AZPEITIA Jean-Jacques	
CASALI Julien	
CAYOL Alain	
CHAUDET Patrick	
CONVERS Bruno	
DAN Michel	
DI LEONE Cécile	
GROSZ Alain	
KINTZ Philippe	
LAPEYRE Laurent	
LEONARDON Sophie	
MASNADA Lilian	
MOURIER Yvan	
RAMBAUD André	
SALGADO Emmanuel	

IRAM 30-meter Telescope, Granada, Spain

KRAMER Carsten	Station Manager
PENALVER Juan	Deputy Station Manager
BILLOT Nicolas	
BRUNSWIG Walter	
DAMOUR Frédéric	
ESPANA Gloria	
FRANZIN Esther	
GALVEZ Gregorio	
GARCIA José	
GARCIA Pablo	
HERMELO Israel	
JOHN David	
LARA Maria	
LOBATO Enrique	
LOBATO Javier	
MARKA Claudia	
MELLADO Pablo	
MENDEZ Isabel	
MORENO Maria	
MUNOZ GONZALEZ Miguel	
NAVARRO Santiago	
PAUBERT Gabriel	
PEULA Victor	
PIERFEDERICI Francesco	
RUIZ Carmen	
RUIZ Ignacio	
RUIZ Manuel	
SANCHEZ Salvador	
SANTAREN Juan Luis	
SANTIAGO Joaquin	
SERRANO David	
SIEVERS Albrecht	
TORNE Pablo	
UNGERECHTS Hans	

Telescope schedules

30-METER TELESCOPE

Ident.	Title of Investigations	Investigators
206-14	The EMIR Nearby Galaxy Dense Gas Survey	Frank Bigiel, Adam Leroy, Antonio Usero, Fabian Walter, Diane Cormier, Karl-Friedrich Schuster, Santiago Garcia-Burillo, Carsten Kramer, Jérôme Pety, Karin Sandstrom, Eva Schinnerer, Annie Hughes, Amanda Kepley, Alberto D. Bolatto, Andreas Schruba, Gaëlle Dumas, Laura Zschaechner
094-15	Understanding the biochemistry below the surfaces of icy Solar System moons	Emily Drabek-Maunder, David Clements, Jane Greaves, Helen Fraser, Leah-Nani Alconcel
095-15	Molecular survey of comet C/2013 US10 (Catalina)	Nicolas Biver, Dominique Bockelee-Morvan, Jacques Crovisier, Pierre Colom, Raphael Moreno, Darek LIS, Gabriel Paubert, Jeremie Boissier, Alice Decock, Harold Weaver, Neil Dello Russo, Ronald Vervack, Hideyo Kawakita
096-15	Last gas before the frost	Stephanie Cazaux, David Teyssier, Paola Caselli
097-15	Deep search for hydrogen peroxide - a probe for interstellar water formation on grains	Guido Fuchs, Doris Herberth, Johanna Chantzos, Daniel Witsch, Harold Linnartz, Karl M. Menten, Thomas Giesen
098-15	Search for the DCO radical: a clue to the formation of the complex organic molecule precursor HCO	Aurore Bacmann, Alexandre Faure, Yasuki Endo, Enrique Garcia-Garcia
100-15	The role of environment and of cloud depth in the formation of small hydrocarbons (cont.)	Sara Cuadrado, Javier R. Goicoechea, Jose Cernicharo, Asuncion Fuente, Christine Joblin, Paolo Pilleri
103-15	A study of the c-C_3HD/c-C_3H_2 ratio in low-mass star forming regions (and comparison with the N_2D^+/N_2H^+ ratio)	Silvia Spezzano, Paola Caselli, Luca Bizzocchi, Barbara Michela Giuliano, Olli Sipila
104-15	An Unbiased Survey of Deuterium Fractionation toward Protostellar Cores in Perseus	Muneaki Imai, Yoko Oya, Nami Sakai, Ana Lopez-Sepulcre, Yoshimasa Watanabe, Satoshi Yamamoto
105-15	Detailed kinematics of the deuterated gas and ionisation fraction across a prototypical pre-stellar core	Luca Bizzocchi, Paola Caselli, Silvia Spezzano, Barbara Michela Giuliano, Valerio Lattanzi
107-15	Deuteration in early stages of high-mass star-formation	Friedrich Wyrowski, Marion Wienen, Timea Csengeri, Thushara Pillai, Tobias Albertsson, Andrea Giannetti
108-15	Deuterium Astration in the Galactic Center	Thushara Pillai, Denise Riquelme, Tobias Albertsson, Jens Kauffmann, Arnaud Belloche, Miguel Angel Requena-Torres, Rolf Gusten
109-15	[HCN]/[HNC]: A fundamental problem in Astrophysics	Asuncion Fuente, Sandra Trevino-Morales, Jose Cernicharo, Evelyne Roueff, Alvaro Sanchez-Monge, Javier R. Goicoechea, Paolo Pilleri, Maryvonne Gerin, Jerome Pety, Santiago Garcia-Burillo, Jean-Christophe Loison, Kevin M. Hickson
110-15	Probing molecular cloud properties with the newly available formaldehyde para ground state line	Hans Nguyen, Friedrich Wyrowski, Andreas Brunthaler, Karl M. Menten
111-15	Survey of the chemical nature of low-mass protostars in OMC-2/3	Ana Lopez-Sepulcre, Yoshito Shimajiri, Yoko Oya, Nami Sakai, Muneaki Imai, Yoshimasa Watanabe, Satoshi Yamamoto
112-15	CO and N_2 depletion and the age of dark cloud cores	Laurent Pagani, Charlene Lefevre, Pierre Lesaffre, Francois Dulieu
113-15	Unraveling the Nature of "CO-dark" Gas: High-sensitivity CO Observations toward the Perseus Molecular Cloud	Min-Young Lee, Snezana Stanimirovic, Claire Murray, Carl Heiles, Elijah Bernstein-Cooper, John Dickey, Harvey Liszt, Yoshito Shimajiri
114-15	Observations toward CO Dark Molecular Gas with Extinction A_v > 1.5 mag	Bo Zhao, Zhiyu Zhang, Guang-Xing Li, Ningyu Tang, Di Li, Junzhi Wang, Hui Shi, Lei Qian
115-15	On the Physical Properties of Galactic Edge Clouds	Xindi Tang, Christian Henkel, Karl M. Menten, Xingwu Zheng, Yan Sun, Yan Gong, Jarken Esimbek, Jian-Jun Zhou, Gang Wu, Ye Yuan
116-15	Cloud-cloud collision at the edge of the Galactic center region	Denise Riquelme, Jens Kauffmann, Thushara Pillai, Karl M. Menten, Miguel Angel Requena-Torres, Nanase Harada, Rebeca Aladro

Ident.	Title of Investigations	Investigators
117-15	High Velocity Gas Towards the Sgr A Complex	Pablo Garcia, Denise Riquelme, Miguel Angel Requena-Torres
118-15	Irradiated shocks and ionisation sources in the central pc of the Galaxy	Javier R. Goicoechea, Jerome Pety, Maryvonne Gerin, Jose Cernicharo, Miguel Angel Requena-Torres, Sara Cuadrado, Benjamin Godard, Franck Le Petit, Emeric Bron
120-15	Mapping the Bones of the Milky Way	Cara Battersby, Alvaro Sanchez-Monge, Alyssa Goodman, Peter Schilke, Catherine Zucker, Fanyi Meng, Thushara Pillai, Paul F. Goldsmith, Peregrine McGehee, John Bally, Sarah Ragan, Blakesley Burkhart, Hector Arce, Jaime Pineda, Nia Imara, John Carpenter, Rowan Smith, Darek LIS, James Jackson, Laura Lopez
122-15	The Anatomy of the Orion B Giant Molecular Cloud	Jerome Pety, Jan Orkisz, Viviana Guzman Veloso, Pierre Gratier, Emeric Bron, Sebastien Bardeau, Javier R. Goicoechea, Maryvonne Gerin, Franck Le Petit, Francois Levrier, Harvey Liszt, Karin Oberg, Evelyne Roueff, Albrecht Sievers, Pascal Tremblin
123-15	Short spacings to complete the ALMA Science Verification data	Belen Tercero Martinez, Jose Cernicharo, Nathalie Brouillet, A. Lopez, Didier Despois, Alain Baudry, Arancha Castro-Carrizo, Nuria Marcelino
124-15	Mapping Rosette with 32 GHz Bandwidth	Jens Kauffmann, Paul F. Goldsmith, Karl M. Menten, Friedrich Wyrowski, Satoshi Yamamoto, Yoshimasa Watanabe, Axel Weiss, Helmut Wiesemeyer, Tobias Albertsson
125-15	Kinematics and Chemistry of Dense Filamentary Structures	Michael Mattern, Jens Kauffmann, Karl M. Menten, Friedrich Wyrowski
126-15	Statistical properties of Fibers in Molecular Clouds	Alvaro Hacar, Joao Alves, Stefan Meingast, Josefa Grossschedl, Jan Forbrich, Paula Teixeira
127-15	Characterizing the Filamentary Molecular Structure of Orion A	Sumeyye Suri, Alvaro Sanchez-Monge, Peter Schilke, John Carpenter, John Bally, Doug Johnstone, Steve Mairs, Ralf Klessen, Anika Schmiedeke, Jaime Pineda, Jens Kauffmann, Paul F. Goldsmith, Thushara Pillai, Simon Glover, Rowan Smith, Fumitaka Nakamura, Marzieh Azhini, Yoshito Shimajiri
128-15	Probing the velocity structure of a system of filaments discovered by Herschel in the Northern part of Orion B	Doris Arzoumanian, Andrea Bracco, Arabindo Roy, Philippe Andre, Francois Boulanger, Vera Konyves, Yoshito Shimajiri
129-15	Probing the growth of the Taurus B211 filament by accretion	Philippe Andre, Yoshito Shimajiri, Pedro Palmeirim, Bilal Ladjelate, Vera Konyves, Alexander Men'shchikov, Patrick Hennebelle, Doris Arzoumanian, Eva Ntormousi, Arabindo Roy
130-15	Are Filaments composed of Fibers throughout their Mass Spectrum?	Jouni Kainulainen, Henrik Beuther, Alvaro Hacar
132-15	Large scale infall or local collapse forms massive clusters?	Timea Csengeri, Friedrich Wyrowski, Karl M. Menten, Sylvain Bontemps, Nicola Schneider
133-15	Is gravity the driver of non-thermal motion in star formation?	Alessio Traficante, Gary Fuller, Nicolas Billot, Ana Duarte Cabral, Sergio Molinari, Alvaro Sanchez-Monge, Jaime Pineda, Frederique Motte
134-15	First Galactic Census of the Coldest Milky Way Cores	Thushara Pillai, Silvia Leurini, Friedrich Wyrowski
135-15	Characterising the primitive material of star formation.	Pierre Gratier, Valentine Wakelam, Jean-Christophe Loison, Kevin M. Hickson, Evelyne Roueff, Romane Le Gal, Liton Majumdar, Maxime RUAUD, Thomas H. G. Vidal
136-15	An ASAI followup to explore the origin of Molecular Complexity	Bertrand Lefloch, Cecilia Ceccarelli, Rafael Bachiller, Jose Cernicharo, Claudio Codella, Mario Tafalla, Ana Lopez-Sepulcre, Charlotte Vastel
137-15	Completion of the ASAI spectral survey of the L1544 prestellar core	Charlotte Vastel, Bertrand Lefloch
139-15	Classification of very low-mass/sub-stellar Class I systems	Basmah Riaz, Daniel Harsono
140-15	Feedback of a massive star: a case study of S106	Nicola Schneider, Rolf Gusten, Sylvain Bontemps, Volker Ossenkopf-Okada, Sibylle Anderl, Robert Simon, Markus Roellig
141-15	Towards understanding formaldehyde masers	Hendrik Linz, Esteban D. Araya, Peter Hofner

Ident.	Title of Investigations	Investigators
142-15	Characterizing the turbulence and protostellar outflows in the L1251B protocluster	Anaelle Maury, Stephane Corbel
143-15	A project for Master students of Grenoble University : Radiatively Driven Implosion in M20	Bertrand Lefloch
144-15	The Cosmic-Ray Flux in Dense Cores	Nick Indriolo, Edwin A. Bergin, Sebastien Maret
145-15	Shocked molecular clumps around Cassiopeia A - A key probe of CR acceleration and asymmetric SN explosion	Li Jiangtao, Ping Zhou, Zhiyu Zhang, Yang Chen, Joel N. Bregman
146-15	The first targeted CO observation of the youngest Galactic SNR G1.9+0.3	Gao-Yuan Zhang, Ping Zhou, Yang Chen
147-15	High Density Polarization in Perseus B1-E	Sarah Sadavoy, Martin Houde, James di Francesco, Pierre Bastien, Shantanu Basu, Nicole Bailey, Dan Clemens, Talayeh Hezareh, Loic Albert
148-15	CN N=2-1 Zeeman Observations of Massive Star Forming Cores	Richard Crutcher, Edith Falgarone, Thomas Troland, Pierre Hily-Blant
149-15	The magnetic field in photodissociation regions	Marta Alves, Paolo Pilleri, Francois Boulanger, Edith Falgarone, Katia Ferriere, Thomas Troland, Richard Crutcher, Jose Cernicharo, Sandra Trevino-Morales, Javier R. Goicoechea, Asuncion Fuente
150-15	Mapping the magnetic field in IRC+10216	Alizee Duthu, Fabrice Herpin, Helmut Wiesemeyer, Gabriel Paubert, Eric Josselin, Agnes Lebre
151-15	Polarization measurements in the lines of CCH, CN and HCN towards IRC+10216	Andres Asensio Ramos, Jose Cernicharo, Marcelino Agundez, Maria Jesus Martinez Gonzalez, Javier Trujillo Bueno
152-15	Polarimetric Monitoring of SgrA*	Ivan Agudo, Clemens Thum, Carolina Casadio, Helmut Wiesemeyer, Jose L. Gomez, Albrecht Sievers, Bong Won Sohn
153-15	Identifying circumstellar disk tracers in the (almost) massive YSO AFGL490	Claudia Marka, Katharina Schreyer
154-15	Hydrocarbon molecular emission in young disks: A link between evolution of solids and chemistry?	Ke Zhang, Edwin A. Bergin, Kamber Schwarz
156-15	Searching for Molecules in edge-on disks	Stephane Guilloteau, Thomas Henning, Dmitry Semenov, Anne Dutrey, Edwige Chapillon, Vincent Pietu, Richard Teague, Valentine Wakelam
157-15	Determining the initial mass of Mira by means of the $^{17}O/^{18}O$ isotopic ratio	Rutger De Nutte, Leen Decin, Alex de Koter, Hans Olofsson, Sofia Ramstedt, Stefanie Milam, Amanda I. Karakas, R. Stancliffe, Robin Lombaert, Marie Van de Sande
158-15	ALMA and IRAM-30m observations of the proto-planetary nebula CRL2688	Paolo Pilleri, Christine Joblin, Jose Cernicharo, Arancha Castro-Carrizo, Marcelino Agundez, Carmen Sanchez Contreras, Guillermo Quintana-Lacaci, Nick Cox, Karine Demyk, Javier R. Goicoechea
159-15	Exploring the chemical richness of the Ring Nebula	Paolo Pilleri, Nick Cox, Christine Joblin, Jose Cernicharo, Arancha Castro-Carrizo, Marcelino Agundez, Luis Velilla Prieto, Karine Demyk
160-15	The molecular richness of Minkonwsky's Footprint	Javier Alcolea, Valentin Bujarrabal, Carmen Sanchez Contreras, Marcelino Agundez, Arancha Castro-Carrizo, Miguel Santander-Garcia
161-15	Radioactive ^{26}AlF in the remnant of an ancient stellar merger	Tomasz Kaminski, Karl M. Menten, Romuald Tylenda, Nimesh Patel, Jan Martin Winters
163-15	Searching for heavy molecules in IRC+10216 in the 70.8-80 GHz domain	Jose Cernicharo, Marcelino Agundez, Santiago Navarro, Claudia Marka, Michel Guelin, Carsten Kramer, Luis Velilla Prieto, Guillermo Quintana-Lacaci, Claudine Kahane
164-15	Molecular seeds of SiC dust in carbon stars	Marcelino Agundez, Luis Velilla Prieto, Jose Cernicharo, Guillermo Quintana-Lacaci, Javier Alcolea, Valentin Bujarrabal
165-15	What stuff is dust made of in O-rich CSEs ?	Javier Alcolea, Marcelino Agundez, Valentin Bujarrabal, Jose Cernicharo, Guillermo Quintana-Lacaci, Carmen Sanchez Contreras, Luis Velilla Prieto
167-15	Studies of the spectrum of emission of pulsars and millisecond pulsars at millimetre wavelengths	Pablo Torne, Ralph Eatough, Gregory Desvignes, Axel Jessner, Ramesh Karuppusamy, Michael Kramer, Gabriel Paubert
168-15	CO in extremely metal poor galaxies	Yong Shi, Junzhi Wang, Zhiyu Zhang, Yu Gao, Xiaoyang Xia, Qiusheng Gu, Caina Hao

Ident.	Title of Investigations	Investigators
169-15	The formation of stars in the outer disk of M33	Edvige Corbelli, Jonathan Braine, Carlo Giovanardi
170-15	Triggered star formation in the gravitationally perturbed galaxy NGC 4449	Oskar Karczewski, Suzanne Madden, Deidre Hunter, Frederic Galliano, Vianney Lebouteiller, Diane Cormier, Seb Oliver
172-15	Extra-planar CO in NGC 4565: Completing the Multiphase Census	Laura Zschaechner, Jerome Pety, Eva Schinnerer, S. Meidt, Fabian Walter, Ute Lisenfeld, Adam Leroy, Richard Rand, George Heald, Gianfranco Gentile, Flor Allaert, Ilse De Looze
173-15	The H_2/HI balance, dust-to-gas ratio, conversion factor, and depletion time from HERA maps of nearby galaxies	Andreas Schruba, Adam Leroy, Karin Sandstrom, Fabian Walter, Laura Zschaechner, Eva Schinnerer, Annie Hughes, Antonio Usero, Carsten Kramer
174-15	A direct measurement of the dust destruction timescale in passive galaxies	Michal J. Michalowski, Jens Hjorth, Jorge Zavala, Christa Gall, K. Rowlands
176-15	The relation between the ionised and molecular gas phases in galactic-scale outflows revealed by SAMI	Amelie Saintonge, Barbara Catinella, Luca Cortese, Scott Croom, Timothy Davis, Brent Groves, Joss Hawthorn, Geraint Lewis, Angel Lopez-Sanchez, Anne Medling, Guido Roberts-Borsani, rachel somerville, Edoardo Tescari
177-15	Star formation efficiency in mass-selected mergers: Difference between spiral-spiral and spiral-elliptical pairs?	Ute Lisenfeld, Cong Kevin Xu, Chen Cao, Yu Gao, Min Yun
178-15	Molecular Gas and its Excitation in LARS	Johannes Puschnig, Matthew Hayes, Goran Ostlin, John M. Cannon, Daniel Schaerer, Veronica Menacho Menacho, Ivan Oteo, Arjan Bik, Jens Melinder, Angela Adamo
180-15	Chemical Composition of Molecular Clouds in NGC 6822	Yuri Nishimura, Takashi Shimonishi, Yoshimasa Watanabe, Nami Sakai, Yuri Aikawa, Akiko Kawamura, Satoshi Yamamoto
181-15	Hydrogen millimeter recombination lines as a SFR indicator - resubmission	Toma Badescu, Frank Bertoldi, Alexander Karim, Yujin Yang, Benjamin Magnelli
182-15	Unveiling Bottom-Heavy Star Formation in Early-Type Galaxies	Joel N. Bregman, Edwin A. Bergin, Lars E. Kristensen, Edmund Hodges-Kluck, Li Jiangtao
183-15	The HCN conversion factor and the star-formation laws in galaxy disks	Antonio Usero, Adam Leroy, Frank Bigiel, Erik Rosolowsky, Amanda Kepley, Santiago Garcia-Burillo, Fabian Walter, Andreas Schruba, Karin Sandstrom
187-15	A Census of Dense Molecular Gas in Dual AGN	George Privon, Ezequiel Treister, Julia Comerford, Aaron S. Evans, Michael Koss, Francisco Mueller-Sanchez, Kazushi Iwasawa, Kevin Schawinski
189-15	Warm and Dense Molecular Gas in Ultra-luminous Infrared QSOs	Qinghua Tan, Yu Gao, Kotaro Kohno, Xiaoyang Xia, Shude Mao, Caina Hao, Alain Omont, Yinghe Zhao
190-15	Probing The Accretion Disk of NGC 7469 with Simultaneous 3 mm and X-Ray Monitoring	Ehud Behar, Ranieri D. Baldi, Nicolas Billot, Ari Laor, Jelle Kaastra, Missagh Mehdipour, Gabriel Paubert, Chiara Feruglio, Yuval Shoham
191-15	MAPI: Monitoring AGN with Polarimetry at the IRAM-30m	Ivan Agudo, Clemens Thum, Carolina Casadio, Jose L. Gomez, Alan Marscher, Svetlana Jorstad, Helmut Wiesemeyer
192-15	The COMA CORPS - CO survey of Coma Ram Pressure Stripped tails	Pavel Jachym, Ming Sun, Jeffrey Kenney, Luca Cortese, Francoise Combes, Masafumi Yagi, Jan Palous, Elke Roediger, S. Sivanandam
194-15	The molecular gas of low-z submm galaxies	Ivan Oteo, Ian Smail, Rob Ivison, Mark Swinbank, Zhiyu Zhang
195-15	Completing the CO Redshift Search for the Herschel Lensing Survey (HLS) Bright Sources	Eiichi Egami, Miroslava Dessauges-Zavadsky, Tim Rawle, Johan Richard, Jean-Paul Kneib, Francoise Combes, Frederic Boone, Pablo G. Perez-Gonzalez, Daniel Schaerer, Bruno Altieri
196-15	Molecular gas excitation in lensed high-z ULIRGs with submillimeter H_2O emission	Chentao Yang, Alain Omont, Alexandre Beelen, Paul van der Werf, Eduardo Gonzalez-Alfonso, Dominik A. Riechers, Rob Ivison, R. Gavazzi, Yu Gao, Pierre Cox, Melanie Krips, Daizhong Liu, Roberto Neri, Ivan Oteo, Saskia van den Broek

Ident.	Title of Investigations	Investigators
197-15	Spectroscopic redshifts of high-z proto-cluster candidates discovered with Planck and Herschel	Clement Martinache, Herve Dole, Melanie Krips, Guilaine Lagache, Alexandre Beelen, Martin Giard, Jean-Loup Puget, Sabine Konig, Emeric Le Floc'h, Ranga-Ram Chary, Ruediger Kneissl, Bruno Altieri, Alessandro Rettura, Matthieu Bethermin, Juan Macias-Perez, Chentao Yang, George Helou, Etienne Pointecouteau
198-15	Confirming Redshifts of Ultra-red, Bright Herschel Galaxies beyond z=4	Helmut Dannerbauer, Ismael Perez-Fournon, Dominik A. Riechers, Paloma Martinez-Navajas, Rui Marques-Chaves, Rob Ivison, David Clements, Seb Oliver, Julie Wardlow, Asantha Cooray
199-15	Spectroscopic Confirmation of the Nature of a U/HLIRG SPIRE Dropout.	Joshua Greenslade, Helmut Dannerbauer, Alexandre Beelen, David Clements
202-15	Disentangling outflows in massive star forming regions	Veronica Allen, Floris van der Tak, Riccardo Cesaroni, Maria Teresa Beltran, Alvaro Sanchez-Monge
203-15	The role of SiC and SiC_2 in the dust formation region of IRC+10216	Luis Velilla Prieto, Jose Cernicharo, Marcelino Agundez, Guillermo Quintana-Lacaci, Arancha Castro-Carrizo, Jose Pablo Fonfria, Michel Guélin, Christine Joblin
D06-15	Time variability monitoring of molecular emission in IRC+10216	Jose Cernicharo, Michel Guélin, David Teyssier, Marcelino Agundez, David A. Neufeld, Guillermo Quintana-Lacaci, Claudia Marka, Luis Velilla Prieto, Pedro Garcia-Lario
D07-15	RHRS1: The puzzle of a lensed source with no lens	Laure Ciesla, Emanuele Daddi, Chentao Yang, Matthieu Bethermin, Alexandre Beelen, Johan Richard, Tao Wang, David Elbaz, Mark T. Sargent, Tanio Diaz-Santos, Médéric Boquien, Sebastien Heinis, Denis Burgarella
D08-15	A deep search for ozone in the dense cloud rho Oph A	Ewine F. Van Dishoeck, Vianney Taquet, Kenji Furuya, Catherine Walsh
001-16	Methylene cyclopropene: A new carbocyclic species in space?	Izaskun Jimenez-Serra, Paola Caselli, Jose Cernicharo, Serena Viti, Nuria Marcelino, Nicolas Billot, Leonardo Testi
002-16	Is formamide present in prestellar cores? Clues to cold prebiotic chemistry	Aurore Bacmann, Alexandre Faure, Enrique Garcia-Garcia
003-16	Deep search for hydrogen peroxide - a probe for interstellar water formation on grains	Guido Fuchs, Doris Herberth, Johanna Chantzos, Daniel Witsch, Harold Linnartz, Karl M. Menten, Thomas Giesen
004-16	Mapping methanol deuteration in L183	Valerio Lattanzi, Paola Caselli, Luca Bizzocchi, Silvia Spezzano, Barbara Michela Giuliano
005-16	The chemical structure of starless cores	Silvia Spezzano, Luca Bizzocchi, Paola Caselli, Barbara Michela Giuliano, Valerio Lattanzi
006-16	A study of the c-C_3HD/c-C_3H_2 ratio in low-mass star forming regions (and comparison with the N_2D^+/N_2H^+ ratio)	Silvia Spezzano, Luca Bizzocchi, Paola Caselli, Barbara Michela Giuliano, Olli Sipila
007-16	Multiple isotopic reservoirs of nitrogen in prestellar cores	Victor de Souza Magalhaes, Pierre Hily-Blant, Fabien Daniel, Alexandre Faure
008-16	The volatile sulphur content of prestellar cores	Pierre Hily-Blant, Alexandre Faure, Fabien Daniel, Francois Lique
010-16	CO and N_2 depletion and the age of dark cloud cores	Laurent Pagani, Pierre Lesaffre, Charlene Lefevre, Francois Dulieu, Phuong Thanh Nguyen Hoang
011-16	The missing sulfur in the interstellar medium	Asuncion Fuente, Evelyne Roueff, Izaskun Jimenez-Serra, Paola Caselli, Jose Cernicharo, Maryvonne Gerin, Nuria Marcelino, Marcelino Agundez, Valerio Lattanzi, Jacob Laas, J. Malinen, Javier R. Goicoechea, Alvaro Hacar, Mario Tafalla, Rafael Bachiller, Jerome Pety, Bertrand Lefloch, Barbara Michela Giuliano
012-16	Measuring isotopic ratios in Galactic massive star forming regions with HC3N lines	Junzhi Wang, Bo Zhang, Juan Li, Yong Shi, Jiangshui Zhang, Zhiyu Zhang, Siyi Feng, Min Fang
013-16	Galactic Isotopic Ratio of $^{18}O/^{17}O$	Zhiwei Liu, Jiangshui Zhang, Yaoting Yan
014-16	The CO^+ chemistry in photon dominated environments	Sandra Trevino-Morales, Asuncion Fuente, Alvaro Sanchez-Monge, Javier R. Goicoechea, Paolo Pilleri, Volker Ossenkopf-Okada, Jose Cernicharo, Sara Cuadrado, Carsten Kramer
016-16	Complex organic molecules in strongly UV-irradiated environments	Javier R. Goicoechea, Sara Cuadrado, Jose Cernicharo, Asuncion Fuente, Belen Tercero Martinez

Ident.	Title of Investigations	Investigators
017-16	Unveiling the remarkable PDR of M8 and its link to Diffuse Interstellar Bands	Maitraiyee Tiwari, Karl M. Menten, Friedrich Wyrowski
018-16	The Anatomy of the Orion B Giant Molecular Cloud	Jan Orkisz, Jerome Pety, Evelyne Roueff, Harvey Liszt, Maryvonne Gerin, Javier R. Goicoechea, Albrecht Sievers, Karin Oberg, Pierre Gratier, Viviana Guzman Veloso, Sebastien Bardeau, Franck Le Petit, Francois Levrier, Pascal Tremblin, Emeric Bron, Nicolas Peretto
020-16	Gas Components Along the Lines-of-Sight Towards the Arched-Filaments in the GC	Pablo Garcia, Nicholas Abel, Markus Roellig, Michael Burton, Martin Steinke, Rebecca Blackwell
021-16	Cloud-cloud collision at the edge of the Galactic center region	Denise Riquelme, Jens Kauffmann, Thushara Pillai, Karl M. Menten, Rebeca Aladro, Nanase Harada
022-16	Resolved molecular gas at the interface of the Draco nebula	Quentin Salome, Marc Antoine Miville Deschenes, Peter Martin, Felix Jay Lockman, Gilles Joncas
023-16	Are Star-Forming Cores Created By Low-Velocity Shocks?	Sarah Sadavoy, Dmitry Semenov, Paola Caselli, Andy Pon, Valentine Wakelam, Eric Keto, Sibylle Anderl, Thomas Henning, Thomas H. G. Vidal
024-16	Representative Views of Line Emission from Entire Clouds	Jens Kauffmann, Paul F. Goldsmith, Satoshi Yamamoto, Yoshimasa Watanabe, Yuri Nishimura, Karl M. Menten, Friedrich Wyrowski, Marion Wienen, Tobias Albertsson, Laszlo Szucs
025-16	Probing the velocity field of the Taurus L1506 filament	Philippe Andre, Doris Arzoumanian, Yoshito Shimajiri, Pedro Palmeirim, Arabindo Roy, Bilal Ladjelate, Andrea Bracco, Nicolas Peretto, Vera Konyves
027-16	A 3 mm line survey of L483	Marcelino Agundez, Nuria Marcelino, Mario Tafalla, Jose Cernicharo
029-16	Molecular deuteration as an evolutionary clock in massive "starless" regions	Alessio Traficante, Gary Fuller, Sergio Molinari, Nicolas Peretto, Nicolas Billot, Ken'ichi Tatematsu
030-16	Deuteration in the earliest phase of high-mass star formation	Siyi Feng, Paola Caselli, Dmitry Semenov, Sarah Ragan, Olli Sipila, Ke Wang, Jaime Pineda, Henrik Beuther
031-16	Distribution of deuterium fraction in starless cores	Anna Punanova, Andy Pon, Paola Caselli, Jaime Pineda, Jorma Harju
032-16	Connecting Chemical and Protostellar Evolution: N_2D^+/N_2H^+ in Orion Protostars	John Tobin, Amelia Stutz, S. Thomas Megeath, Zsofia Nagy, M. Dunham, Friedrich Wyrowski, Nicolas Billot, James di Francesco, Thomas Stanke
033-16	Molecular complexity in the Intermediate-Mass Protostar CepE-mm	Juan Ospina-Zamudio, Bertrand Lefloch, Cecilia Ceccarelli, Cecile Favre, Ana Lopez-Sepulcre, Claudio Codella, Paola Caselli, Jaime Pineda, Vianney Taquet, Edgar Mendoza
034-16	Early evolution of embedded proto-clusters in the Orion A cloud	Alvaro Hacar, Joao Alves, Andreas Burkert, James Dale
035-16	Understanding cluster formation within the filamentary enviorn-ment.	Manash Samal, Igor Zinchenko, Devendra Ojha, Peter Zemlyanukha
037-16	Sulfur chemistry in protostellar outflows	Bertrand Lefloch, Jonathan Holdship, Serena Viti, Izaskun Jimenez-Serra, Claudio Codella
038-16	How large is the IRAS 04166 outflow?	Mario Tafalla
039-16	Searching for Molecules in edge-on disks	Stephane Guilloteau, Thomas Henning, Dmitry Semenov, Anne Dutrey, Edwige Chapillon, Vincent Pietu, Richard Teague, Valentine Wakelam
041-16	Gas in the Needle	Attila Moor, Agnes Kospal, Jane Greaves
042-16	The Magnetic Field Strength in Perseus B1-E	Sarah Sadavoy, Dmitry Semenov, Martin Houde, Paola Caselli, Shantanu Basu, Eric Keto
043-16	A measurement of the magnetic field toward the First Hydrostatic Core B1b through the rotational lines of the 3Sigma molecule SO	Jose Cernicharo, Maryvonne Gerin, cristina puzzarini, Asuncion Fuente, Andres Asensio Ramos, Nuria Marcelino, Javier Trujillo Bueno, Gabriel Paubert, Maria Jesus Martinez Gonzalez
044-16	Mapping the magnetic field in IRC+10216	Alizee Duthu, Fabrice Herpin, Helmut Wiesemeyer, Gabriel Paubert, Agnes Lebre
045-16	Time variability monitoring of molecular emission in IRC+10216	Juan R. Pardo, Jose Cernicharo, Michel Guelin, David Teyssier, Marcelino Agundez, Guillermo Quintana-Lacaci, Claudia Marka, Luis Velilla Prieto, Pedro Garcia-Lario
046-16	A sensitive 2mm line survey of IRC+10216: searching for the building blocks of dust grains	Jose Cernicharo, Marcelino Agundez, Claudia Marka, Carsten Kramer, Michel Guelin, Luis Velilla Prieto, Claudine Kahane, Juan R. Pardo

Ident.	Title of Investigations	Investigators
047-16	The molecular richness of Minkonwsky's Footprint II	Javier Alcolea, Carmen Sanchez Contreras, Valentin Bujarrabal, Marcelino Agundez, Arancha Castro-Carrizo, Miguel Santander-Garcia
049-16	Determining the initial mass of Mira by means of the $^{17}O/^{18}O$ isotopic ratio	Rutger De Nutte, Leen Decin, Hans Olofsson, Sofia Ramstedt, Stefanie Milam, R. Stancliffe, Robin Lombaert, Marie Van de Sande, W. Homan
050-16	AGB spiral patterns in post-AGB sources	Hyosun Kim, Javier Alcolea, Carmen Sanchez Contreras, Raghvendra Sahai, Sheng-Yuan Liu, Naomi Hirano, Valentin Bujarrabal
051-16	The first targeted CO observation of the youngest Galactic SNR G1.9+0.3	Gao-Yuan Zhang, Yang Chen, Ping Zhou
052-16	A shocked molecular bubble connecting the Type Ia cosmic-ray accelerator Tycho and its progenitor	Ping Zhou, Yang Chen, Samar Safi-Harb, Xiao Zhang, Zhiyu Zhang
053-16	Shocked molecular clumps around Cassiopeia A - A key probe of CR acceleration and asymmetric SN explosion	Li Jiangtao, Ping Zhou, Zhiyu Zhang, Yang Chen, Joel N. Bregman
054-16	Completing the chemical study of the outflow of M82: CN and C_2H	Tomas Alonso-Albi, Asuncion Fuente, Santiago Garcia-Burillo, Antonio Usero, David Ginard
055-16	Hydrogen millimeter recombination lines as a SFR indicator - resubmission	Toma Badescu, Frank Bertoldi, Alexander Karim, Benjamin Magnelli
058-16	Multi-Line EMIR Maps of Starbursts: The Role of Gas Density from Disks to Starbursts	Antonio Usero, Adam Leroy, Frank Bigiel, Santiago Garcia-Burillo, Annie Hughes, Diederik Kruijssen, Jerome Pety, Erik Rosolowsky, Karin Sandstrom, Eva Schinnerer, Andreas Schruba
059-16	The bulk molecular gas distribution in the EMPIRE nearby galaxy sample	Maria Jesus Jimenez Donaire, Frank Bigiel, Diane Cormier, Adam Leroy, Antonio Usero, Annie Hughes, Erik Rosolowsky, Jerome Pety, Diederik Kruijssen, Eva Schinnerer
060-16	Extra-planar CO in NGC 4565: Completing the Multiphase Census	Laura Zschaechner, Jerome Pety, Eva Schinnerer, S. Meidt, Fabian Walter, Ute Lisenfeld, Adam Leroy, Richard Rand, George Heald, Gianfranco Gentile, Flor Allaert, Ilse De Looze, Santiago Garcia-Burillo, Kijeong Yim
062-16	Molecular gas in the most massive isolated spiral galaxies	Li Jiangtao, Zhiyu Zhang, Joel N. Bregman
064-16	Triggered star formation in the gravitationally perturbed galaxy NGC 4449 (continuation)	Oskar Karczewski, Suzanne Madden, Deidre Hunter, Frederic Galliano, Vianney Lebouteiller
065-16	Molecular gas in the Medusa's dusty tail - continued	Sabine Konig, Susanne Aalto, Sebastien Muller, John Gallagher, Rob Beswick, Eva Jutte
066-16	Probing Molecular Gas Content Along a Virgo Cluster Filament	Pascale Jablonka, Francoise Combes, R. Finn, Gregory Rudnick, Fabian Walter
068-16	Exploring scaling relations between gas and dust across cosmic time	Georgios Magdis, Dimitra Rigopoulou, Almudena Alonso-Herrero, Francoise Combes, Emanuele Daddi, David Elbaz, Jiasheng Huang, Matthieu Bethermin, Miguel Pereira Santaella, Evanthia Hatziminaoglou, Ismael Perez-Fournon, Pat Roche, Antonio Antonio Hernan-Caballero, Carsten Kramer
069-16	Studying host properties of Giant Radio Galaxies with IRAM	Philippe Salome, Pratik Dabhade, Francoise Combes, Joydeep Bagchi, Madhuri Gaikwad, Bruno Guiderdoni, Mamta Pommier
070-16	MAPI: Monitoring AGN with Polarimetry at the IRAM-30m	Ivan Agudo, Clemens Thum, Jae-Young Kim, Ioannis Myserlis, Thomas Krichbaum, Emmanouil Angelakis, Eduardo Ros, Helmut Wiesemeyer, Anton Zensus, Carolina Casadio, Sol N. Molina, Jose L. Gomez, Alan Marscher, Svetlana Jorstad
073-16	Search for molecular gas in distant low luminosity radio galaxies in dense Mpc-scale environment	Gianluca Castignani, Philippe Salome, Marco Chiaberge, Gianfranco De Zotti, Chiara Ferrari, Francoise Combes
074-16	A First Look at The Molecular Gas Reservoirs of Normal Galaxies At z~2.5	Simona Vegetti, Matt Auger, Francesco Belfiore, Matthew Bothwell, Bethan James, Roberto Maiolino, John Mckean, Matus Rybak, Elise Ritondale, Stefano Carniani
075-16	Redshift scan of new strongly-magnified submm galaxies.	Tomo Goto, Denis Burgarella, Kazushi Sakamoto, Rieko Momose, Firas Mazyed, Veronique Buat

Ident.	Title of Investigations	Investigators
076-16	Observing the neutral carbon lines in lensed high-z ULIRGs with bright H_2O emission	Chentao Yang, Alain Omont, Alexandre Beelen, Dominik A. Riechers, Zhiyu Zhang, Rob Ivison, Paul van der Werf, Yu Gao, Yinghe Zhao, R. Gavazzi, Roberto Neri, Pierre Cox, Melanie Krips, Ivan Oteo, Saskia van den Broek
077-16	Spectroscopic redshifts of high-z proto-cluster candidates discovered with Planck & Herschel	Clement Martinache, Melanie Krips, Alexandre Beelen, Martin Giard, Guilaine Lagache, Herve Dole, Sabine Konig, Emeric Le Floc'h, Ranga-Ram Chary, Matthieu Bethermin, Ruediger Kneissl, Etienne Pointecouteau, Bruno Altieri, Chentao Yang, Benjamin Clarenc, Maria del Carmen Polletta, Alessandro Rettura
078-16	Unveiling high-z dusty lensed galaxies in the Herschel Virgo Cluster Survey	Darko Donevski, Frederic Boone, Veronique Buat, Ciro Pappalardo
079-16	EMIR/IRAM redshift search of z > 4 sub-mm sources in NGP and GAMA	Tom Bakx, Steve Eales, Matthew Smith, Gianfranco De Zotti, Paul van der Werf, Elisabetta Valiante, Pasquale Temi, Ivan Oteo, Michal J. Michalowski, Rob Ivison, Helmut Dannerbauer, David Clements, David Hughes, Joaquin Gonzalez-Nuevo, Stephen Serjeant, Andrea Lapi
083-16	Tracing the Physics of the Molecular Cloud Lifecycle in IC 342	Andreas Schruba, Diederik Kruijssen, Alex Hygate, Erik Rosolowsky, Eva Schinnerer, Jérôme Pety, Karin Sandstrom, Antonio Usero, Adam Leroy, Eric Emsellem, Annie Hughes, Frank Bigiel
084-16	The Evolution of Galactic Winds: A Small Survey of Resolved Molecular Outflows	Laura Zschaechner, Kathryn Kreckel, Fabian Walter, Adam Leroy, Martin Zwaan, Alberto D. Bolatto, Tom Oosterloo
D03-16	Infall and outflow in the Mon R2 filamentary hub	Sandra Trevino-Morales, Asuncion Fuente, Carsten Kramer, Alvaro Sanchez-Monge, Javier R. Goicoechea
D07-16	Search for CO in Outbursting Centaur 174P/Echeclus	Kacper Wierzchos, Maria Womack
GMVA-16A-293	Zeroing in on Sgr A*: polarization characteristics and source symmetry at 3 mm	Cornelia Mueller, Christiaan Brinkerink, Heino Falcke, Thomas Krichbaum, Monika Moscibrodzka, Geoffrey Bower, Michael Kramer, Remo Tilanus, Raquel Fraga-Encinas, Ciriaco Goddi, Adam Deller, Anton Zensus, Laurent Loinard, David Hughes, David Sanchez-Arguelles, Alfredo Montana, Grant Wilson, Jonathan Leon-Tavares
GMVA-16A-290	Imaging the biconical jet of M87 on scales of 3-100 Schwarzschild radii	Rusen Lu, Thomas Krichbaum, S. Doeleman, Gopal Narayanan, R. Craig Walker, Jose L. Gomez, Keiichi Asada, Michael Bremer, Pablo de Vicente, Michael Lindqvist, Jonathan Leon-Tavares, Gisela Ortiz, Monika Moscibrodzka, Cornelia Mueller, Michael Johnson
GMVA-16A-027	Looking into the heart of the nearest radioloud gamma-ray emitting NLSy1 galaxy	Thomas Krichbaum, Stefanie Komossa, Ioannis Myserlis, Emmanouil Angelakis, Ivan Agudo, Michael Bremer, Pablo de Vicente, Jonathan Leon-Tavares, Gisela Ortiz, Gopal Narayanan
GMVA-16B-134	Detecting the ring-like and the double compact structure of S5 0615+820 at 3mm	Eduardo Ros, Ivan Marti-Vidal, Francisco J. Abellan, Antonio Alberdi Odriozola, Gabriele Bruni, Jose Carlos Guirado, Thomas Krichbaum, Andrei Lobanov, Juan-Maria Marcaide, Miguel Angel Perez-Torres, Tuomas Savolainen, Laura Vega-Garcia, Kaj Wiik, Olaf Wucknitz, Erik Zackrisson, Anton Zensus
GMVA-16B-149	Understanding the jet formation in 3C454.3 and CTA102	Jose L. Gomez, Thomas Krichbaum, Andrei Lobanov, Alan Marscher, Gabriele Bruni, Svetlana Jorstad, Yuri Kovalev, Carolina Casadio, Jae-Young Kim, Laura Vega-Garcia, Pablo Galindo, Ivan Agudo, Sol N. Molina, Christian Fromm, Uwe Bach, Yosuke Mizuno, Jose M. Marti, Manel Perucho, Eduardo Ros, Anton Zensus

NOEMA INTERFEROMETER

Ident.	Title of Investigations	Investigators
X053	PHIBSS2: molecular gas at the peak epoch of galaxy formation	Francoise Combes, Santiago Garcia-Burillo, Roberto Neri, Linda Tacconi, Reinhard Genzel, Thierry Contini, Alberto Bolatto, Simon Lilly, Frederic Boone, Nicolas Bouche, Frederic Bournaud, Andreas Burkert, Marcella Carollo, Luis Colina, Michael Cooper, Pierre Cox, Chiara Feruglio, Jonathan Freundlich, Natascha Forster-Schreiber, Juneau, Kovac, Lippa, Dieter Lutz, Naab, Alain Omont, Alvio Renzini, Amelie Saintonge, Philippe Salome, Amiel Sternberg, Fabian Walter, Ben Weiner, Axel Weiss, Stijn Wuyts
L14AB	Fragmentation and disk formation during high-mass star formation	Henrik Beuther, Thomas Henning, Hendrik Linz, Siyi Feng, Katharine Johnston, Rolf Kuiper, Sarah Ragan, Dmitry Semenov, Frederic Gueth, Jan Martin Winters, Karl M. Menten, James Urquhart, Timea Csengeri, Pamela Klaassen, Joseph C. Mottram, Peter Schilke, Melvin Hoare, Luke Maud, Stuart Lumsden, Maria Teresa Beltran, Riccardo Cesaroni, Malcolm Walmsley, Alvaro Sanchez-Monge, Qizhou Zhang, Cornelis Dullemond, Frederique Motte, Philippe Andre, Gary Fuller, Nicolas Peretto, Roberto Galvan-Madrid, S. Longmore, Sylvain Bontemps, Th. Peters, Aina Palau, R. Pudritz, Hans Zinnecker
D14AF	Complex Organic Molecules in the protocluster OMC2-FIR4	Cecilia Ceccarelli, Paola Caselli, Claudio Codella, Francesco Fontani, Bertrand Lefloch, Luca Bizzocchi
W14AP	Probing the birth of low mass stars : confirmation of the detection of a FHSC in Barnard 1b	Maryvonne Gerin, Asuncion Fuente, Jose Cernicharo, Jerome Pety, Evelyne Roueff, Benoit Commercon, Francois Levrier, Darek Lis, Nuria Marcelino
W14BU	The remarkable disk orbiting AC Her	Valentin Bujarrabal, Arancha Castro-Carrizo, Hans Van Winckel, Javier Alcolea
W14CB	Resolving the nuclear cold molecular gas in nearby Seyfert galaxies	Almudena Alonso-Herrero, Santiago Garcia-Burillo, Cristina Ramos Almeida, Luis Colina, Jose Miguel Rodriguez Espinosa, Eleonora Sani, Rachel Mason, Chris Packham, Nancy Levenson, Pat Roche, Dimitra Rigopoulou, Masatoshi Imanishi, Pilar Esquej
W14CG	Molecular Gas and Induced Star Formation in the Interacting Galaxy NGC 2276	Annie Hughes, Eva Schinnerer, Miguel Querejeta, Jerome Pety, Gaelle Dumas, Santiago Garcia-Burillo, Clare Dobbs, S. Meidt, Florent Renaud
W14CH	Resolving the molecular outflow in the buried QSO IRAS F08572+3915	Annemieke Janssen, Eckhard Sturm, Roberto Maiolino, Eduardo Gonzalez-Alfonso, Richard Davies, Sylvain Veilleux, Enrico Piconcelli, Fabrizio Fiore, Santiago Garcia-Burillo, Susanne Aalto, Claudia Cicone, David Rupke, Jacqueline Fischer, Javier Gracia-Carpio, Chiara Feruglio, Linda Tacconi, Dieter Lutz, Alessandra Contursi
W14DD	Do all ULIRGs have vibrationally excited HCN?	Susanne Aalto, Sergio Martin Ruiz, Kazushi Sakamoto, Eduardo Gonzalez-Alfonso, Sebastien Muller, Francesco Costagliola, Santiago Garcia-Burillo, Elisabeth Mills, Paul van der Werf, Christian Henkel
W14ES	Zooming in onto star formation in the brightest gravitationally lensed galaxies from the Planck all-sky survey	Nicole Nesvadba, R. Canameras, Herve Dole, Douglas Scott, Guilaine Lagache, Alexandre Beelen, I. Flores-Cacho, Ranga-Ram Chary, Emeric Le Floc'h, T. MacKenzie, Sabine Konig, Frederic Boone, Dan Dicken, Brenda Frye, Melanie Krips, Sangeeta Malhotra, G. Soucail, Lin Yan, Chentao Yang
W14FH	Dynamical Structure of the Star-Forming Interstellar Medium in a Newly-Discovered (Unlensed) Starburst at z=5.3	Dominik A. Riechers, Jacqueline Hodge, Fabian Walter, Emanuele Daddi, Roberto Neri, Chris L. Carilli
W14FK	Towards a Detailed Picture of Molecular Outflows at z>6	Dominik A. Riechers, Fabian Walter, Roberto Neri, Chris L. Carilli, Ran Wang, Pierre Cox, Axel Weiss

Ident.	Title of Investigations	Investigators
L15AA	Seeds Of Life in Space	Cecilia Ceccarelli, Paola Caselli, Francesco Fontani, Claudio Codella, Bertrand Lefloch, Charlotte Vastel, Jaime Pineda, Andy Pon, Pierre Hily-Blant, Roberto Neri, Luca Bizzocchi, Izaskun Jimenez-Serra, Felipe Alves, Rafael Bachiller, Sandrine Bottinelli, Emmanuel Caux, Gaelle Dumas, Robert Lucas, Linda Podio, Anna Punanova, Nami Sakai, Satoshi Yamamoto, Serena Viti, Anton Vasyunin, Francois Dulieu, Alexandre Faure, Silvia Spezzano, Laurent Wiesenfeld, Nadia Balucani, Ali Jaber, Albert Rimola, Ian Sims, Patrice Theule, Piero Ugliengo, Ana Chacon-Tanarro, Rumpa Choudhury, Vianney Taquet
S15AW	Dynamics in the dissipating HD 141569 disk	Jessica Pericaud, Emmanuel Di Folco, Anne Dutrey, Stephane Guilloteau, Vincent Pietu, Jean-Charles Augereau
S15BP	Gas in MASSIVE Galaxies: Dynamical IMF measurements with molecular gas	Timothy Davis, Jenny Greene, Chung-Pei Ma, John Blakeslee
S15BS	CO Outflows from Star Formation-Dominated ULIRGs	Fabian Walter, Adam Leroy, Axel Weiss, Roberto Decarli, Laura Zschaechner
S15CO	Molecular gas contents of galaxies in a forming massive cluster at z=2.503	Tao Wang, David Elbaz, Emanuele Daddi, Daizhong Liu, Sergio Martin Ruiz
S15CX	Fuel and consumption of a massive rotating disk galaxy 1.3Gyr after the Big Bang	Alexander Karim, Chris L. Carilli, Vernesa Smolcic, Dominik A. Riechers, Benjamin Magnelli, Eva Schinnerer, Kartik Sheth, Frank Bertoldi, Manuel Aravena, A. Koekemoer, E. van Kampen, Johannes Staguhn, Mark T. Sargent, Sune Toft, Ian Smail, Mark Swinbank, Elaine Grubmann
W15AA	Mapping the dynamics and thermal structure of Venus upper atmosphere	Arianna Piccialli, Raphael Moreno, Emmanuel Lellouch, Thierry Fouchet, Arielle Moullet, Thibault Cavalie
W15AD	Gravitational heating in a unique pre-stellar core	Jaime Pineda, Paola Caselli, Hector Arce, Gary Fuller, Tyler Bourke, Alyssa Goodman, Stella Offner
W15AE	Kinematics and a search for hierarchical structures within the B213-10 dense core	Anna Punanova, Jaime Pineda, Paola Caselli, Andy Pon
W15AH	Detecting the signature of nitrogen fractionation in ices	Victor de Souza Magalhaes, Alexandre Faure, Pierre Hily-Blant, Fabien Daniel
W15AO	HCO as a precursor of astrobiological molecules	Victor Rivilla, Maria Teresa Beltran, Claudio Codella, Francesco Fontani, Riccardo Cesaroni, Serena Viti, Paul M. Woods, Paola Caselli, Anton Vasyunin, Roberto Neri, Hannah Calcutt
W15AX	Imaging the water snowline in protostars with HCO^+	Ewine F. Van Dishoeck, Jes Jorgensen, Ruud Visser, Magnus Persson, Edwin A. Bergin, Daniel Harsono
W15AY	Are the gaps in the HL Tau protoplanetary disk due to ices lines?	Sebastien Maret, Sibylle Anderl, Edwin A. Bergin, Ke Zhang, Geoffroy Lesur, Myriam Benisty
W15BJ	Gaseous silicon and the formation of dust in AGB circumstellar envelopes	Valentin Bujarrabal, Arancha Castro-Carrizo, Javier Alcolea, Miguel Montarges
W15BL	The gaseous circumstellar environment of the red supergiant Mu Cep	Miguel Montarges, Arancha Castro-Carrizo, Valentin Bujarrabal, Jan Martin Winters, Pierre Kervella, Leen Decin, Andrea Chiavassa, Guy Perrin, Stephen Ridgway, Thibaut Le Bertre, Graham Harper, Iain McDonald, Xavier Haubois
W15BM	Search for radioactive aluminium in VY CMa	Guillermo Quintana-Lacaci, Jose Cernicharo, Marcelino Agundez, Luis Velilla Prieto, Arancha Castro-Carrizo, Michel Guelin
W15BQ	Characterizing Rapid Millimeter Frequency Variability in Black Hole X-ray Binaries	Alexandra Tetarenko, Gregory Sivakoff, Michael Bremer, Peter Curran, James Miller-Jones, Kunal Mooley, Thomas Russell
W15BR	Tracing Cloud Formation in a Spiral Arm	Erik Rosolowsky, Jonathan Braine, Eric Koch, Dario Colombo, Pierre Gratier, Frank Bertoldi, Sylvain Bontemps, Mederic Boquien, Christof Buchbender, D. Calzetti, Francoise Combes, Clare Dobbs, Santiago Garcia-Burillo, Carsten Kramer, Nicola Schneider, Paul van der Werf, Manolis Xilouris
W15BU	Tracing the impact of AGN feedback in the nucleus of M51a	Miguel Querejeta, Eva Schinnerer, Santiago Garcia-Burillo, Jerome Pety, David S. Meier, Frank Bigiel, Annie Hughes, S. Meidt, Guillermo Blanc, Kathryn Kreckel

Ident.	Title of Investigations	Investigators
W15BX	Jet-ISM interactions in NGC 4258	Quentin Salome, Philippe Salome, Francoise Combes
W15BZ	Peering through thick mist - probing compact obscured nuclei with vibrationally excited HCN	Richard Tunnard, Susanne Aalto, Timothy Davis, Thomas R. Greve, Kazushi Sakamoto, Aaron S. Evans
W15CK	Multi-phase outflows in ULIRGs: Mapping the massive cold component	Miguel Pereira Santaella, Luis Colina, Santiago Garcia-Burillo, Bjorn Emonts, Santiago Arribas, Javier Piqueras Lopez, Susanne Aalto, Francoise Combes, Paul van der Werf, Antonio Usero, Almudena Alonso-Herrero, Christian Henkel, Leslie Hunt, Roberto Neri, Sebastien Muller, Francesco Costagliola
W15CN	The Evolution of Galactic Winds: A Small Survey of Resolved Molecular Outflows	Laura Zschaechner, Kathryn Kreckel, Fabian Walter, Adam Leroy, Martin Zwaan, Alberto D. Bolatto, Tom Oosterloo
W15CS	An Observational Test of Quasar Feedback Models: Resolved Molecular Outflows in Nearby Type I Quasars	Kayhan Gultekin, David Rupke
W15CV	Molecular gas kinematics in H_2-bright quenched elliptical galaxies	Quentin Salome, Philippe Salome, Pierre Guillard, Matthew Lehnert
W15DA	Constraining the cold accretion onto the most massive Black Holes	Philippe Salome, Michael Hogan, Alastair Edge, Brian McNamara, Stephen Hamer, Francoise Combes, Helen Russell, A. C Fabian, Grant R. Tremblay
W15DB	NGC5044 - an extremely self-absorbed, low power AGN	Alastair Edge, Michael Hogan, Brian McNamara, Helen Russell, Philippe Salome, Francoise Combes, Keith Grainge
W15DF	NOEMA Observations of the Nearby Seyfert-1 Galaxy NGC 4051	Jon Miller, Edwin A. Bergin
W15DG	High velocity molecular outflows in BAL QSOs	Anelise Audibert, Francoise Combes, Kalliopi Dasyra, Philippe Salome, Melanie Krips, Sabine Konig, Julia Scharwachter
W15DY	Probing Buried Nuclei Through Vibrationally-Excited HCN in Distant Dusty Starbursts	Dominik A. Riechers, Susanne Aalto, Roberto Neri, Eduardo Gonzalez-Alfonso
W15DZ	An exceptional intensively star forming proto-cluster candidate at z=2.36 selected from Planck	Herve Dole, Emanuele Daddi, Clement Martinache, Melanie Krips, Guilaine Lagache, Alexandre Beelen, Martin Giard, Douglas Scott, Sabine Konig, Brenda Frye, Emeric Le Floc'h, Ranga-Ram Chary, Ruediger Kneissl, Etienne Pointecouteau, Bruno Altieri, Alessandro Rettura, Matthieu Bethermin, George Helou, Jean-Loup Puget, Lin Yan, Juan Macias-Perez, David Guery, Chentao Yang
W15EG	A giant molecular outflow in a z=2.85 QSO host galaxy: driven by starburst or AGN?	Scott Chapman, Arif Babul, Frank Bertoldi, Ian Smail, James Geach
W15EP	Probing the Spatial Distribution of H_2O Emission in a High-z Lensed Herschel Galaxy	Alain Omont, Chentao Yang, Roberto Neri, Alexandre Beelen, Paul van der Werf, Eduardo Gonzalez-Alfonso, Melanie Krips, Rob Ivison, R. Shane Bussmann, R. Gavazzi, Pierre Cox, Yu Gao, Matthew Lehnert, Helmut Dannerbauer, Ivan Oteo, Karl M. Menten, Axel Weiss, Michel Guelin, Simon Dye
W15EW	Fine structure line emission in a z = 4.7 dusty star-forming galaxy	Fabian Walter, Axel Weiss, Andrew Baker, Roberto Decarli, Tobias Marriage, Jesus Rivera
W15FG	Locating the IRAM/GISMO galaxies	Alexander Karim, Oskari Miettinen, Johannes Staguhn, Eva Schinnerer, Vernesa Smolcic, Frank Bertoldi, Manuel Aravena, Ian Smail, Mark Swinbank, Ting Su, Mark T. Sargent, Dominik A. Riechers, Axel Weiss, Benjamin Magnelli
W15FI	Radiation Processes in Gamma-Ray Burst Afterglows	Antonio de Ugarte Postigo, Steve Schulze, Christina Thone, Andrea Mehner, Sergio Martin Ruiz, Michael Bremer, Franz Bauer, Pall Jakobsson, Dieter Hartmann, Paolo D'Avanzo, Itziar de Gregorio-Monsalvo, Jens Hjorth, Daniele Malesani, Michal J. Michalowski, Bo Milvang-Jensen, Martin Sparre, Rhaana Starling, Nial Tanvir, Darach J. Watson, Sam Kim, Carlos De Breuck, Zach Cano, Ruben Sanchez-Ramirez, Jesus Corral-Santana, Thomas Kruhler, Daniel Perley
E15AE	Imaging radioactive ^{26}AlF in the remnant of a stellar merger II	Tomasz Kaminski, Karl M. Menten, Romuald Tylenda, Nimesh Patel, Jan Martin Winters
E15AF	Assessing high velocity CO in APM 08279+5255 beyond any doubt	Chiara Feruglio, Roberto Neri, Dennis Downes, Fabrizio Fiore, Cecilia Ceccarelli, Andrea Ferrara, Simona Gallerani, Enrico Piconcelli, Roberto Maiolino

Ident.	Title of Investigations	Investigators
S16AA	Chemical structures in the diffuse interstellar medium	Maryvonne Gerin, Jerome Pety, Harvey Liszt, Patrick Boisse, Benjamin Godard
S16AC	Do Binaries Form in the Starless Core Phase?	Sarah Sadavoy, Yancy Shirley, Thomas Henning, Leslie W. Looney, Claire Chandler, Rachel Friesen, M. Dunham, John Tobin, Dominique Segura-Cox, Zhi-Yun Li, Kaitlin Kratter, Stella Offner
S16AD	Constraining the Nitrogen Abundance Towards a Class 0 Protostar	Kamber Schwarz, Edwin A. Bergin, Sebastien Maret, Sibylle Anderl, Philippe Andre, Arnaud Belloche, Claudio Codella
S16AE	Exploring the deuterium enhancement in HCO^+ and HCN	Audrey Coutens, Jes Jorgensen
S16AG	Velocity structure of a quiescent portion of the NGC 2024 filament	Philippe Andre, Yoshito Shimajiri, Vera Konyves, Doris Arzoumanian, Eva Ntormousi, Patrick Hennebelle, Arabindo Roy, Nicola Schneider, Bilal Ladjelate, Alexander Men'shchikov
S16AI	Massive Starless Cores: Deuteration and Dynamics	Jonathan Tan, Shuo Kong, Paola Caselli, Francesco Fontani, Michael Butler, Charlene Lefevre
S16AK	Are Hydrogen and Nitrogen fractionation related in massive star forming cores?	Francesco Fontani, Paola Caselli, Cecilia Ceccarelli, Luca Bizzocchi, Silvia Leurini
S16AM	Nature of ultra-low-mass Herschel cores in Ophiuchus	Bilal Ladjelate, Philippe Andre, Pedro Palmeirim, Vera Konyves, Alexander Men'shchikov
S16AQ	Classification and characterization of newly discovered young eruptive stars	Agnes Kospal, Peter Abraham, Orsolya Feher
S16AR	A deeper insight into the chemistry of the AB Auriga disk	Asuncion Fuente, Susana Pacheco Vazquez, Roberto Neri, Marcelino Agundez, Jose Cernicharo, Rafael Bachiller, Javier R. Goicoechea, Tomas Alonso-Albi
S16AS	Probing disk chemical changes driven by dust growth at the earliest stage	Ke Zhang, Edwin A. Bergin, Kamber Schwarz, Fujun Du
S16AT	Grain growth in a Class I protoplanetary disk	Carolina Agurto Gangas, Paola Caselli, Jaime Pineda, Leonardo Testi, M. Dunham
S16AU	The Colliding Winds of Cyg OB2 No. 8A	Ronny Blomme, Danielle Fenech, Raman Prinja, Julian Pittard, Jack Morford
S16AV	Structure and chemistry of a stellar-merger remnant	Tomasz Kaminski, Karl M. Menten, Nimesh Patel, Romuald Tylenda, Jan Martin Winters
S16AZ	Molecular gas kinematics in H_2-bright quenched elliptical galaxies	Quentin Salome, Philippe Salome, Pierre Guillard, Matthew Lehnert, Francoise Combes
S16BC	Stellar feedback and turbulence in metal-poor dwarf starbursts	Leslie Hunt, Francoise Combes, Santiago Garcia-Burillo, Viviana Casasola, Paola Caselli, Christian Henkel, Karl M. Menten, Axel Weiss, Leonardo Testi
S16BD	Imaging the molecular gas in a multi-phase ram pressure stripped gas tail	Pavel Jachym, Ming Sun, Francoise Combes, Jeffrey Kenney, Elke Roediger, Jan Palous
S16BE	Interaction with a dark galaxy?	Lihwai Lin, Michal J. Michalowski, Hai Fu, Matthew Bothwell, Francesco Belfiore, Wei-Hao Wang, Edmond Cheung, David Stark, Ting Xiao, Cheng Li
S16BF	Tracing the Physics of the Molecular Cloud Lifecycle in IC 342	Andreas Schruba, Diederik Kruijssen, Alex Hygate, Erik Rosolowsky, Eva Schinnerer, Jerome Pety, Karin Sandstrom, Antonio Usero, Adam Leroy, Eric Emsellem, Annie Hughes, Frank Bigiel
S16BG	The Evolution of Galactic Winds: A Small Survey of Resolved Molecular Outflows	Laura Zschaechner, Kathryn Kreckel, Fabian Walter, Adam Leroy, Martin Zwaan, Alberto D. Bolatto, Tom Oosterloo
S16BH	Identifying molecular outflows in our neighborhood	Dieter Lutz, Eckhard Sturm, Annemieke Janssen, Alessandra Contursi, Sylvain Veilleux, Richard Davies, Linda Tacconi, Reinhard Genzel
S16BK	What is really driving the properties in turbulent disks?	David Fisher, R. Abraham, Karl Glazebrook, Danail Obreschkow, Alberto D. Bolatto, Heidi White, Paola Oliva-Altamirano
S16BM	Jet-Feedback in Action: Resolved Molecular Outflow Driven by a Jet in PG 1700+518	Kayhan Gultekin, David Rupke
S16BQ	Triplets of Quasars: Exploring the Formation of a Cluster with NOEMA	Emanuele Paolo Farina, Fabian Walter, Roberto Decarli, Michele Fumagalli
S16BW	Probing Buried Nuclei Through Vibrationally-Excited HCN in Distant Dusty Starbursts	Dominik A. Riechers, Susanne Aalto, Roberto Neri

Ident.	Title of Investigations	Investigators
S16BX	Molecular outflow in a normal high-z galaxy	Dieter Lutz, Eva Wuyts, Andrew Baker, Chelsea Sharon, Amitpal Tagore, Reinhard Genzel, Linda Tacconi, Natascha Forster Schreiber, Eckhard Sturm
S16CC	CH^+(1-0) in high-redshift starburst galaxies: probes of massive turbulent reservoirs	Edith Falgarone, Chentao Yang, Roberto Neri, Ivan Oteo, Fabian Walter, Martin Zwaan, Rob Ivison, Paola Andreani, Benjamin Godard, Frederic Bournaud, David Elbaz, Alain Omont
S16CD	Infrared-selected Main-sequence Galaxies above Redshift 3: Tracing the Pace of Rapid Evolution	Emanuele Daddi, Daizhong Liu, Shuowen JIN, Mark Dickinson, Hanae Inami, Mark T. Sargent, Georgios Magdis, Yu Gao
S16CI	Fine structure line emission in a z = 4.7 dusty star-forming galaxy	Fabian Walter, Axel Weiss, Andrew Baker, Roberto Decarli, Tobias Marriage, Jesus Rivera
S16CO	The formation of the first QSOs	Roberto Decarli, Fabian Walter, Bram Venemans, Eduardo Banados, Emanuele Paolo Farina, Dominik A. Riechers
S16CQ	Exploring [CII] and Dust Emission in a Bright Star-forming Galaxy at z=11.09	Fabian Walter, Pascal Oesch, Roberto Decarli, Daniel Schaerer, Paul van der Werf, Dominik A. Riechers, Chris L. Carilli, Gabriel Brammer, Pieter van Dokkum, Garth Illingworth, Ivo Labbe, Rychard Bouwens, Miroslava Dessauges-Zavadsky, Stephane de Barros
S16CR	Radiation Processes in Gamma-Ray Burst Afterglows	Antonio de Ugarte Postigo, Steve Schulze, Sergio Martin Ruiz, Michael Bremer, Christina Thone, Franz Bauer, Pall Jakobsson, Andrea Mehner, Dieter Hartmann, Paolo D'Avanzo, Itziar de Gregorio-Monsalvo, Jens Hjorth, Daniele Malesani, Michal J. Michalowski, Bo Milvang-Jensen, Martin Sparre, Rhaana Starling, Nial Tanvir, Darach J. Watson, Zach Cano, Ruben Sanchez-Ramirez, Jesus Corral-Santana, Thomas Kruhler, Kuntal Misra, Resmi Lekshmi
W16AA	Are changes in Io's bulk atmosphere the cause for magnetospheric variability?	Lorenz Roth, Alvaro Sanchez-Monge, Joachim Saur, G. Randall Gladstone, Kurt D. Retherford, D. Strobel, Katherine de Kleer, Peter Schilke, Sven Thorwirth, Mizuki Yoneda, Nickolay Ivchenko
W16AD	Probing dynamics of a protostellar envelope	Marina Kounkel, Lee Hartmann, Cecile Favre
W16AE	The role of the carbon isotope ratio in 15_N-measurements of protostars	Susanne Wampfler, Jes Jorgensen, Martin Bizzarro
W16AN	Constraining the Spatial Abundance of HCN Towards Five Protostars	Thomas Rice, Edwin A. Bergin
W16AQ	The disk-jet-outflow system of the almost massive YSO AFGL490	Claudia Marka, Katharina Schreyer
W16BC	Probing the dust trap in AB Aur - a cradle of planets?	Asuncion Fuente, Clement Baruteau, Roberto Neri, Jose Cernicharo, Rafael Bachiller, Marcelino Agundez, Javier R. Goicoechea
W16BE	Mapping the central outflow kinematics of the AGB star RS Cnc	Jan Martin Winters, Hoai Do Thi, Nhung Pham, Pierre Darriulat, Thibaut Le Bertre
W16BL	In a Luminous Infrared Galaxy Far, Far Away: Observations of ^{13}CO and $C^{18}O$ in UGC 5101	Kazimierz Sliwa
W16BM	Markarian 71: A Green Pea Analog	Sally Oey, Megan Reiter, Genoveva Micheva, Cinthya Herrera Contreras, Sergiy Silich, Anne Jaskot, Bethan James
W16BP	Resolving the nuclear cold molecular gas in nearby Seyfert galaxies	Almudena Alonso-Herrero, Santiago Garcia-Burillo, Dimitra Rigopoulou, Antonio Usero, Eleonora Sani, Cristina Ramos Almeida, Jose Miguel Rodriguez Espinosa, Chris Packham, Nancy Levenson, Pat Roche, Masatoshi Imanishi, Antonio Antonio Hernan-Caballero
W16BQ	Resolving the Molecular Outflow of PG1440 to Test Quasar Feedback Models	Jessie Runnoe, Kayhan Gultekin, David Rupke
W16BS	In-Situ Disk Fragmentation VS. Accretion: What drives the massive Clump Formation?	Johannes Puschnig, Matthew Hayes, Goran Ostlin, John M. Cannon, Edmund Christian Herenz, Oscar Agertz, Veronica Menacho Menacho
W16BT	Why is the LINER galaxy NGC5195 extremely CN-luminous?	Rebeca Aladro, Katherine Alatalo, Francesco Costagliola, Susanne Aalto
W16CD	Quenching processes in HCG 57a and HCG 82b	Monica Rodriguez, Francoise Combes, Philippe Salome, Pierre Guillard

Ident.	Title of Investigations	Investigators
W16CE	Jet-ISM interactions in NGC 4258	Quentin Salome, Philippe Salome, Francoise Combes
W16CK	What is really driving the properties in turbulent disks?	David Fisher, Karl Glazebrook, Alberto D. Bolatto, R. Abraham, Danail Obreschkow, Heidi White
W16CN	Molecular gas in nearby analogs of cosmic reionization sources	Daniel Schaerer, Miroslava Dessauges-Zavadsky, Anne Verhamme, Yuri Izotov, Ivana Orlitova, John Chisholm
W16CT	Dust-obscured bulge growth in Milky Way and Andromeda progenitors	Erica Nelson, Reinhard Genzel, Natascha Forster Schreiber, Linda Tacconi, Ken-Ichi Tadaki, Emily Wisnioski, S. Wuyts, Dieter Lutz
W16CV	Observing the Rotation Curve and Baryon Content of a z~1.3 Twin of NGC891 and the Milky Way	Reinhard Genzel, Natascha Forster Schreiber, Dieter Lutz, Rodrigo Herrera-Camus, Linda Tacconi, Hannah Uebler, Sirio Belli, Erica Nelson, S. Wuyts, Richard Davies, Ken-Ichi Tadaki
W16DD	I. Continuum Observation of Gravitationally Lensed Submm Galaxies	Firas Mazyed, Denis Burgarella, Veronique Buat, Javier Alvarez Marquez, Hyung-Mok Lee, Stephen Serjeant
W16DS	The puzzle of the Garnet: [CI] and CO in the first extragalactic [CII] absorber at z=3.4	Nicole Nesvadba, Raoul Canameras, Edith Falgarone, Brenda Frye, Ruediger Kneissl, Sabine Konig, Douglas Scott
W16DV	1mm follow-up of Herschel-selected z>3 galaxies: resolving the multiplicity and securing the SEDs in the early Universe	Emanuele Daddi, Daizhong Liu, Georgios Magdis, Mark Dickinson, Hanae Inami, Qinghua Tan, Yu Gao, Mark T. Sargent, Matthieu Bethermin, Maurilio Pannella, Fabian Walter, Tao Wang, Xinwen Shu, Eva Schinnerer, Shuowen Jin
W16DX	CO delensing of six ACT-selected DSFGs	Axel Weiss, Fabian Walter, Roberto Decarli, Amitpal Tagore, Charles Keeton, Tobias Marriage, Jesus Rivera, Andrew Baker
W16EF	Detecting the [NII] 205 micron line at the highest redshifts.	Roberto Decarli, Carl Ferkinhoff, Fabian Walter, Eduardo Banados, Bram Venemans, Emanuele Paolo Farina
W16EH	Torn apart by its own monster: ultimate quasar feedback in a primeval galaxy	Roberto Maiolino, Claudia Cicone, Simona Gallerani, Roberto Neri, Andrea Ferrara, Fabrizio Fiore, Enrico Piconcelli, Chiara Feruglio, Frank Bertoldi, Stefano Carniani
W16EK	[CII] and Dust Emission in the Most Distant Galaxy with a Two-Line Redshift	Fabian Walter, Pascal Oesch, Roberto Decarli, Daniel Schaerer, Frederic Boone, Rychard Bouwens, Miroslava Dessauges-Zavadsky, Richard Ellis, Yoshinobu Fudamoto, Garth Illingworth, Ivo Labbe, Guido Roberts-Borsani, Renske Smit, Dan Stark
E16AA	Resolving the mm emission from the Components of T Tau	Karl-Friedrich Schuster, Vincent Pietu, Edwige Chapillon
GMVA-16A-293	Zeroing in on Sgr A*: polarization characteristics and source symmetry at 3 mm	Cornelia Mueller, Christiaan Brinkerink, Heino Falcke, Thomas Krichbaum, Monika Moscibrodzka, Geoffrey Bower, Michael Kramer, Remo Tilanus, Raquel Fraga-Encinas, Ciriaco Goddi, Adam Deller, Anton Zensus, Laurent Loinard, David Hughes, David Sanchez-Arguelles, Alfredo Montana, Grant Wilson, Jonathan Leon-Tavares
GMVA-16A-290	Imaging the biconical jet of M87 on scales of 3-100 Schwarzschild radii	Rusen Lu, Thomas Krichbaum, S. Doeleman, Gopal Narayanan, R. Craig Walker, Jose L. Gomez, Keiichi Asada, Michael Bremer, Pablo de Vicente, Michael Lindqvist, Jonathan Leon-Tavares, Gisela Ortiz, Monika Moscibrodzka, Cornelia Mueller, Michael Johnson
GMVA-16A-027	Looking into the heart of the nearest radioloud gamma-ray emitting NLSy1 galaxy	Thomas Krichbaum, Stefanie Komossa, Ioannis Myserlis, Emmanouil Angelakis, Ivan Agudo, Michael Bremer, Pablo de Vicente, Jonathan Leon-Tavares, Gisela Ortiz, Gopal Narayanan
GMVA-16B-134	Detecting the ring-like and the double compact structure of S5 0615+820 at 3mm	Eduardo Ros, Ivan Marti-Vidal, Francisco J. Abellan, Antonio Alberdi Odriozola, Gabriele Bruni, Jose Carlos Guirado, Thomas Krichbaum, Andrei Lobanov, Juan-Maria Marcaide, Miguel Angel Perez-Torres, Tuomas Savolainen, Laura Vega-Garcia, Kaj Wiik, Olaf Wucknitz, Erik Zackrisson, Anton Zensus
GMVA-16B-149	Understanding the jet formation in 3C454.3 and CTA102	Jose L. Gomez, Thomas Krichbaum, Andrei Lobanov, Alan Marscher, Gabriele Bruni, Svetlana Jorstad, Yuri Kovalev, Carolina Casadio, Jae-Young Kim, Laura Vega-Garcia, Pablo Galindo, Ivan Agudo, Sol N. Molina, Christian Fromm, Uwe Bach, Yosuke Mizuno, Jose M. Marti, Manel Perucho, Eduardo Ros, Anton Zensus

Publications

The list of publications, conferences and workshop papers as well as theses based upon data obtained by the IRAM user community and IRAM staff members are provided in the following two tables.

IRAM USERS' COMMUNITY

2124	Dense gas tracing the collisional past of Andromeda. An atypical inner region?	Melchior A.-L., Combes F.	2016, A&A 585, A44
2125	N131: A dust bubble born from the disruption of a gas filament	Zhang C.-P., Li G.-X., Wyrowski F., Wang J.-J., Yuan J.-H., Xu J.-L., Gong Y., Yeh C. C., Menten K. M.	2016, A&A 585, A117
2126	Infall through the evolution of high-mass star-forming clumps	Wyrowski F., Güsten R., Menten K. M., Wiesemeyer H., Csengeri T., Heyminck S., Klein B., König C., Urquhart J. S.	2016, A&A 585, A149
2127	A study of the C_3H_2 isomers and isotopologues: first interstellar detection of HDCCC	Spezzano S., Gupta H., Brünken S., Gottlieb C. A., Caselli P., Menten K. M., Müller H. S. P., Bizzocchi L., Schilke P., McCarthy M. C., Schlemmer S.	2016, A&A 586, A110
2128	Discovery of off-axis jet structure of TeV blazar Mrk 501 with mm-VLBI	Koyama S., Kino M., Giroletti M., Doi A., Giovannini G., Orienti M., Hada K., Ros E., Niinuma K., Nagai H., Savolainen T., Krichbaum T. P., Pérez-Torres M. Á.	2016, A&A 586, A113
2129	ATLASGAL-selected massive clumps in the inner Galaxy. II. Characterisation of different evolutionary stages and their SiO emission	Csengeri T., Leurini S., Wyrowski F., Urquhart J. S., Menten K. M., Walmsley M., Bontemps S., Wienen M., Beuther H., Motte F., Nguyen-Luong Q., Schilke P., Schuller F., Zavagno A., Sanna C.	2016, A&A 586, A149
2130	The NH_2D hyperfine structure revealed by astrophysical observations	Daniel F., Coudert L. H., Punanova A., Harju J., Faure A., Roueff E., Sipilä O., Caselli P., Güsten R., Pon A., Pineda J. E.	2016, A&A 586, L4
2131	Evidence for a chemically differentiated outflow in Mrk 231	Lindberg J. E., Aalto S., Muller S., Martí-Vidal I., Falstad N., Costagliola F., Henkel C., van der Werf P., García-Burillo S., González-Alfonso E.	2016, A&A 587, A15
2132	Mid-J CO shock tracing observations of infrared dark clouds. II. Low-J CO constraints on excitation, depletion, and kinematics	Pon A., Johnstone D., Caselli P., Fontani F., Palau A., Butler M. J., Kaufman M., Jiménez-Serra I., Tan J. C.	2016, A&A 587, A96
2133	Effects of environmental gas compression on the multiphase ISM and star formation . The Virgo spiral galaxies NGC 4501 and NGC 4567/68	Nehlig F., Vollmer B., Braine J.	2016, A&A 587, A108
2134	Deuterium fractionation in the Ophiuchus molecular cloud	Punanova A., Caselli P., Pon A., Belloche A., André P.	2016, A&A 587, A118
2135	The origin of gas-phase HCO and CH_3O radicals in prestellar cores	Bacmann A., Faure A.	2016, A&A 587, A130
2136	A rigorous detection of interstellar CH_3NCO: An important missing species in astrochemical networks	Cernicharo J., Kisiel Z., Tercero B., Kolesniková L., Medvedev I. R., López A., Fortman S., Winnewisser M., de Lucia F. C., Alonso J. L., Guillemin J.-C.	2016, A&A 587, L4
2137	Molecular gas in low-metallicity starburst galaxies:. Scaling relations and the CO-to-H_2 conversion factor	Amorín R., Muñoz-Tuñón C., Aguerri J. A. L., Planesas P.	2016, A&A 588, A23
2138	Dust emissivity in the star-forming filament OMC 2/3	Sadavoy S. I., Stutz A. M., Schnee S., Mason B. S., Di Francesco J., Friesen R. K.	2016, A&A 588, A30

2139	Probing spacetime around Sagittarius A* using modeled VLBI closure phases	Fraga-Encinas R., Mościbrodzka M., Brinkerink C., Falcke H.	2016, A&A 588, A57
2140	Detection of protonated formaldehyde in the prestellar core L1689B	Bacmann A., García-García E., Faure A.	2016, A&A 588, L8
2141	SiO: Not the perfect outflow tracer. Outflow studies of the massive star formation region IRAS 19410+2336	Widmann F., Beuther H., Schilke P., Stanke T.	2016, A&A 589, A29
2142	Star-forming dwarf galaxies in the Virgo cluster: the link between molecular gas, atomic gas, and dust	Grossi M., Corbelli E., Bizzocchi L., Giovanardi C., Bomans D., Coelho B., De Looze I., Gonçalves T. S., Hunt L. K., Leonardo E., Madden S., Menéndez-Delmestre K., Pappalardo C., Riguccini L.	2016, A&A 590, A27
2143	Constraining the physical structure of the inner few 100 AU scales of deeply embedded low-mass protostars	Persson M. V., Harsono D., Tobin J. J., van Dishoeck E. F., Jørgensen J. K., Murillo N., Lai S.-P.	2016, A&A 590, A33
2144	Molecular gas and star formation in the tidal dwarf galaxy VCC 2062	Lisenfeld U., Braine J., Duc P. A., Boquien M., Brinks E., Bournaud F., Lelli F., Charmandaris V.	2016, A&A 590, A92
2145	CN Zeeman and dust polarization in a high-mass cold clump	Pillai T., Kauffmann J., Wiesemeyer H., Menten K. M.	2016, A&A 591, A19
2146	The millimeter wave spectrum of methyl cyanate: a laboratory study and astronomical search in space	Kolesniková L., Alonso J. L., Bermúdez C., Alonso E. R., Tercero B., Cernicharo J., Guillemin J.-C.	2016, A&A 591, A75
2147	Laboratory measurements and astronomical search for the HSO radical	Cazzoli G., Lattanzi V., Kirsch T., Gauss J., Tercero B., Cernicharo J., Puzzarini C.	2016, A&A 591, A126
2148	Abundance of $HOCO^+$ and CO_2 in the outer layers of the L1544 prestellar core	Vastel C., Ceccarelli C., Lefloch B., Bachiller R.	2016, A&A 591, L2
2149	Are infrared dark clouds really quiescent?	Feng S., Beuther H., Zhang Q., Henning T., Linz H., Ragan S., Smith R.	2016, A&A 592, A21
2150	Millimeter wave spectra of carbonyl cyanide	Bteich S. B., Tercero B., Cernicharo J., Motiyenko R. A., Margulès L., Guillemin J.-C.	2016, A&A 592, A43
2151	N_2H^+ and $N^{15}NH^+$ toward the prestellar core 16293E in L1689N	Daniel F., Faure A., Pagani L., Lique F., Gérin M., Lis D., Hily-Blant P., Bacmann A., Roueff E.	2016, A&A 592, A45
2152	High-resolution HI and CO observations of high-latitude intermediate-velocity clouds	Röhser T., Kerp J., Ben Bekhti N., Winkel B.	2016, A&A 592, A142
2153	Chemical differentiation in a prestellar core traces non-uniform illumination	Spezzano S., Bizzocchi L., Caselli P., Harju J., Brünken S.	2016, A&A 592, L11
2154	Inferring the evolutionary stages of the internal structures of NGC 7538 S and IRS1 from chemistry	Feng S., Beuther H., Semenov D., Henning T., Linz H., Mills E. A. C., Teague R.	2016, A&A 593, A46
2155	The radio spectral energy distribution of infrared-faint radio sources	Herzog A., Norris R. P., Middelberg E., Seymour N., Spitler L. R., Emonts B. H. C., Franzen T. M. O., Hunstead R., Intema H. T., Marvil J., Parker Q. A., Sirothia S. K., Hurley-Walker N., Bell M., Bernardi G., Bowman J. D., Briggs F., Cappallo R. J., Callingham J. R., Deshpande A. A., Dwarakanath K. S., For B.-Q., Greenhill L. J., Hancock P., Hazelton B. J., Hindson L., Johnston-Hollitt M., Kapińska A. D., Kaplan D. L., Lenc E., Lonsdale C. J., McKinley B., McWhirter S. R., Mitchell D. A., Morales M. F., Morgan E., Morgan J., Oberoi D., Offringa A., Ord S. M., Prabu T., Procopio P., Udaya Shankar N., Srivani K. S., Staveley-Smith L., Subrahmanyan R., Tingay S. J., Wayth R. B., Webster R. L., Williams A., Williams C. L., Wu C., Zheng Q., Bannister K. W., Chippendale A. P., Harvey-Smith L., Heywood I., Indermuehle B., Popping A., Sault R. J., Whiting M. T.	2016, A&A 593, A130
2156	Planck's Dusty Gems. II. Extended [CII] emission and absorption in the Garnet at z=3.4 seen with ALMA	Nesvadba N.; Kneissl R.; Cañameras R.; Boone F.; Falgarone E.; Frye B.; Gerin M.; Koenig S.; Lagache G.; Le Floc'h E.; Malhotra S.; Scott D.	2016, A&A 593, L2

2157	Planck 2015 results. VIII. High Frequency Instrument data processing: Calibration and maps	Planck Collaboration, Adam R., Ade P. A. R., Aghanim N., Arnaud M., Ashdown M., Aumont J., Baccigalupi C., Banday A. J., Barreiro R. B., Bartolo N., Battaner E., Benabed K., Benoît A., Benoit-Lévy A., Bernard J.-P., Bersanelli M., Bertincourt B., Bielewicz P., Bock J. J., Bonavera L., Bond J. R., Borrill J., Bouchet F. R., Boulanger F., Bucher M., Burigana C., Calabrese E., Cardoso J.-F., Catalano A., Challinor A., Chamballu A., Chiang H. C., Christensen P. R., Clements D. L., Colombi S., Colombo L. P. L., Combet C., Couchot F., Coulais A., Crill B. P., Curto A., Cuttaia F., Danese L., Davies R. D., Davis A. Cuttaia F., Danese L., Davies R. D., Davis R. J., de Bernardis P., de Rosa A., de Zotti G., Delabrouille ., Delouis J.-M., Désert F.-X., Diego J. M., Dole H., Donzelli S., Doré O., Douspis M., Ducout A., Dupac X., Efstathiou G., Elsner F., Enßlin T. A., Eriksen H. K., Falgarone E., Fergusson J., Finelli F., Forni O., Frailis M., Fraisse A. A., Franceschi E., Frejsel A., Galeotta S., Galli S., Ganga K., Ghosh T., Giard M., Giraud-Héraud Y., Gjerløw E., González-Nuevo J., Górski K. M., Gratton S., Gruppuso A., Gudmundsson J. E., Hansen F. K., Hanson D., Harrison D. L., Henrot-Versillé S., Herranz D., Hildebrandt S. R., Hivon E., Hobson M., Holmes W. A., Hornstrup A., Hovest W., Huffenberger K. M., Hurier G., Jaffe A. H., Jaffe T. R., Jones W. C., Juvela M., Keihänen E., Keskitalo R., Kisner T. S., Kneissl R., Knoche J., Kunz M., Kurki-Suonio H., Lagache G., Lamarre J.-M., Lasenby A., Lattanzi M., Lawrence C. R., Le Jeune M., Leahy J. P., Lellouch E., Leonardi R., Lesgourgues J., Levrier F., Liguori M., Lilje P. B., Linden-Vørnle M., López-Caniego M., Lubin P. M., Macías-Pérez J. F., Maggio G., Maino D., Mandolesi N., Mangilli A., Maris M., Martin P. G., Martínez-González E., Masi S., Matarrese S., McGehee P., Melchiorri A., Mendes L., Mennella A., Migliaccio M., Mitra S., Miville-Deschênes M.-A., Moneti A., Montier L., Moreno R., Morgante G., Mortlock D., Moss A., Mottet S., Munshi D., Murphy J. A., Naselsky P., Nati F., Natoli P., Netterfield C. B., Nørgaard-Nielsen H. U., Noviello F., Novikov D., Novikov I., Oxborrow C. A., Paci F., Pagano L., Pajot F., Paoletti D., Pasian F., Patanchon G., Pearson T. J., Perdereau O., Perotto L., Perrotta F., Pettorino V., Piacentini F., Piat M., Pierpaoli E., Pietrobon D., Plaszczynski S., Pointecouteau E., Polenta G., Pratt G. W., Prézeau G., Prunet S., Puget J.-L., Rachen J. P., Reinecke M., Remazeilles M., Renault C., Renzi A., Ristorcelli I., Rocha G., Rosset C., Rossetti M., Roudier G., Rusholme B., Sandri M., Santos D., Sauvé A., Savelainen M., Savini G., Scott D., Seiffert M. D., Shellard E. P. S., Spencer L. D., Stolyarov V., Stompor R., Sudiwala R., Sutton D., Suur-Uski A.-S., Sygnet J.-F., Tauber J. A., Terenzi L., Toffolatti L., Tomasi M., Tristram M., Tucci M., Tuovinen J., Valenziano L., Valiviita J., Van Tent B., Vibert L., Vielva P., Villa F., Wade L. A., Wandelt B. D., Watson R., Wehus I. K., Yvon D., Zacchei A., Zonca A.	2016, A&A 594, A8
2158	The CO-H_2 van der Waals complex and complex organic molecules in cold molecular clouds: A TMC-1C survey	Potapov A., Sánchez-Monge Á., Schilke P., Graf U. U., Möller T., Schlemmer S.	2016, A&A 594, A117
2159	The structure and early evolution of massive star forming regions. Substructure in the infrared dark cloud SDC13	McGuire C., Fuller G. A., Peretto N., Zhang Q., Traficante A., Avison A., Jimenez-Serra I.	2016, A&A 594, A118
2160	Multiwavelength study of the low-luminosity outbursting young star HBC 722	Kóspál Á., Ábrahám P., Acosta-Pulido J. A., Dunham M. M., García-Álvarez D., Hogerheijde M. R., Kun M., Moór A., Farkas A., Hajdu G., Hodosán G., Kovács T., Kriskovics L., Marton G., Molnár L., Pál A., Sárneczky K., Sódor Á., Szakáts R., Szalai T., Szegedi-Elek E., Szing A., Tóth I., Vida K., Vinkó J.	2016, A&A 596, A52
2161	Trans-cis molecular photoswitching in interstellar space	Cuadrado S., Goicoechea J. R., Roncero O., Aguado A., Tercero B., Cernicharo J.	2016, A&A 596, L1
2162	Carbon Chains and Methanol toward Embedded Protostars	Graninger D. M., Wilkins O. H., Öberg K. I.	2016, ApJ 819, 140
2163	Molecular Distribution in the Spiral Arm of M51	Watanabe Y., Sakai N., Sorai K., Ueda J., Yamamoto S.	2016, ApJ 819, 144
2164	Subarcsecond Analysis of the Infalling-Rotating Envelope around the Class I Protostar IRAS 04365+2535	Sakai N., Oya Y., López-Sepulcre A., Watanabe Y., Sakai T., Hirota T., Aikawa Y., Ceccarelli C., Lefloch B., Caux E., Vastel C., Kahane C., Yamamoto S.	2016, ApJ 820, L34
2165	The Deuterium Fraction in Massive Starless Cores and Dynamical Implications	Kong S., Tan J. C., Caselli P., Fontani F., Pillai T., Butler M. J., Shimajiri Y., Nakamura F., Sakai T.	2016, ApJ 821, 94
2166	Phosphorus-bearing Molecules in Massive Dense Cores	Fontani F., Rivilla V. M., Caselli P., Vasyunin A., Palau A.	2016, ApJ 822, L30

2167	Candidate Gravitationally Lensed Dusty Star-forming Galaxies in the Herschel Wide Area Surveys	Nayyeri H., Keele M., Cooray A., Riechers D. A., Ivison R. J., Harris A. I., Frayer D. T., Baker A. J., Chapman S. C., Eales S., Farrah D., Fu H., Marchetti L., Marques-Chaves R., Martinez-Navajas P. I., Oliver S. J., Omont A., Perez-Fournon I., Scott D., Vaccari M., Vieira J., Viero M., Wang L., Wardlow J.	2016, ApJ 823, 17
2168	Protostar L1455 IRS1: A Rotating Disk Connecting to a Filamentary Network	Chou H.-G., Yen H.-W., Koch P. M., Guilloteau S.	2016, ApJ 823, 151
2169	Revealing a Detailed Mass Distribution of a High-density Core MC27/L1521F in Taurus with ALMA	Tokuda K., Onishi T., Matsumoto T., Saigo K., Kawamura A., Fukui Y., Inutsuka S.-i., Machida M. N., Tomida K., Tachihara K., André P.	2016, ApJ 826, 26
2170	Expanding Molecular Bubble Surrounding Tycho's Supernova Remnant (SN 1572) Observed with the IRAM 30 m Telescope: Evidence for a Single-degenerate Progenitor	Zhou P., Chen Y., Zhang Z.-Y., Li X.-D., Safi-Harb S., Zhou X., Zhang X.	2016, ApJ 826, 34
2171	IRAS 16253-2429: The First Proto-brown Dwarf Binary Candidate Identified through the Dynamics of Jets	Hsieh T.-H., Lai S.-P., Belloche A., Wyrowski F.	2016, ApJ 826, 68
2172	New Debris Disks in Nearby Young Moving Groups	Moór A., Kóspál Á., Ábrahám P., Balog Z., Csengeri T., Henning T., Juhász A., Kiss C.	2016, ApJ 826, 123
2173	Acceleration of Compact Radio Jets on Sub-parsec Scales	Lee S.-S., Lobanov A. P., Krichbaum T. P., Zensus J. A.	2016, ApJ 826, 135
2174	The First Detections of the Key Prebiotic Molecule PO in Star-forming Regions	Rivilla V. M., Fontani F., Beltrán M. T., Vasyunin A., Caselli P., Martín-Pintado J., Cesaroni R.	2016, ApJ 826, 161
2175	Shocked Poststarburst Galaxy Survey. II. The Molecular Gas Content and Properties of a Subset of SPOGs	Alatalo K., Lisenfeld U., Lanz L., Appleton P. N., Ardila F., Cales S. L., Kewley L. J., Lacy M., Medling A. M., Nyland K., Rich J. A., Urry C. M.	2016, ApJ 827, 106
2176	Cloud Structure of Galactic OB Cluster-forming Regions from Combining Ground- and Space-based Bolometric Observations	Lin Y., Liu H. B., Li D., Zhang Z.-Y., Ginsburg A., Pineda J. E., Qian L., Galván-Madrid R., McLeod A. F., Rosolowsky E., Dale J. E., Immer K., Koch E., Longmore S., Walker D., Testi L.	2016, ApJ 828, 32
2177	Outflow Detection in a 70 μm Dark High-Mass Core	Feng S., Beuther H., Zhang Q., Liu H. B., Zhang Z., Wang K., Qiu K.	2016, ApJ 828, 100
2178	Multi-wavelength Lens Reconstruction of a Planck and Herschel-detected Star-bursting Galaxy	Timmons N., Cooray A., Riechers D. A., Nayyeri H., Fu H., Jullo E., Gladders M. D., Baes M., Bussmann R. S., Calanog J., Clements D. L., da Cunha E., Dye S., Eales S. A., Furlanetto C., Gonzalez-Nuevo J., Greenslade J., Gurwell M., Messias H., MichaŃowski M. J., Oteo I., Pérez-Fournon I., Scott D., Valiante E.	2016, ApJ 829, 21
2179	Millimeter Wave Spectrum and Astronomical Search for Vinyl Formate	Alonso E. R., Kolesniková L., Tercero B., Cabezas C., Alonso J. L., Cernicharo J., Guillemin J.-C.	2016, ApJ 832, 42
2180	Infall/Expansion Velocities in the Low-mass Dense Cores L492, L694-2, and L1521F: Dependence on Position and Molecular Tracer	Keown J., Schnee S., Bourke T. L., Di Francesco J., Friesen R., Caselli P., Myers P., Williger G., Tafalla M.	2016, ApJ 833, 97
2181	The MASSIVE survey - III. Molecular gas and a broken Tully-Fisher relation in the most massive early-type galaxies	Davis T. A., Greene J., Ma C.-P., Pandya V., Blakeslee J. P., McConnell N., Thomas J.	2016, MNRAS 455, 214
2182	Galaxy gas flows inferred from a detailed, spatially resolved metal budget	Belfiore F., Maiolino R., Bothwell M.	2016, MNRAS 455, 1218
2183	Testing the molecular-hydrogen Kennicutt-Schmidt law in the low-density environments of extended ultraviolet disc galaxies	Watson L. C., Martini P., Lisenfeld U., Böker T., Schinnerer E.	2016, MNRAS 455, 1807
2184	Dense-gas properties in Arp 220 revealed by isotopologue lines	Wang J., Zhang Z.-Y., Zhang J., Shi Y., Fang M.	2016, MNRAS 455, 3986

2185	Collisional excitation of doubly and triply deuterated ammonia ND_2H and ND_3 by H_2	Daniel F., Rist C., Faure A., Roueff E., Gérin M., Lis D. C., Hily-Blant P., Bacmann A., Wiesenfeld L.	2016, MNRAS 457, 1535
2186	Forming isolated brown dwarfs by turbulent fragmentation	Lomax O., Whitworth A. P., Hubber D. A.	2016, MNRAS 458, 1242
2187	Thick discs, and an outflow, of dense gas in the nuclei of nearby Seyfert galaxies	Lin M.-Y., Davies R. I., Burtscher L., Contursi A., Genzel R., González-Alfonso E., Graciá-Carpio J., Janssen A., Lutz D., Orban de Xivry G., Rosario D., Schnorr-Müller A., Sternberg A., Sturm E., Tacconi L.	2016, MNRAS 458, 1375
2188	Detection of CH_3SH in protostar IRAS 16293-2422	Majumdar L., Gratier P., Vidal T., Wakelam V., Loison J.-C., Hickson K. M., Caux E.	2016, MNRAS 458, 1859
2189	Widespread deuteration across the IRDC G035.39-00.33	Barnes A. T., Kong S., Tan J. C., Henshaw J. D., Caselli P., Jiménez-Serra I., Fontani F.	2016, MNRAS 458, 1990
2190	Class I methanol megamasers: a potential probe of starburst activity and feedback in active galaxies	Chen X., Ellingsen S. P., Zhang J.-S., Wang J.-Z., Shen Z.-Q., Wu Q.-W., Wu Z.-Z.	2016, MNRAS 459, 357
2191	The spatially resolved dynamics of dusty starburst galaxies in a z ~ 0.4 cluster: beginning the transition from spirals to S0s	Johnson H. L., Harrison C. M., Swinbank A. M., Bower R. G., Smail I., Koyama Y., Geach J. E.	2016, MNRAS 460, 1059
2192	The Tully-Fisher relation of COLD GASS Galaxies	Tiley A. L., Bureau M., Saintonge A., Topal S., Davis T. A., Torii K.	2016, MNRAS 461, 3494
2193	Space reconstruction of the morphology and kinematics of axisymmetric radio sources	Diep P. N., Phuong N. T., Hoai D. T., Nhung P. T., Thao N. T., Tuan-Anh P., Darriulat P.	2016, MNRAS 461, 4276
2194	Hot and dense water in the inner 25 au of SVS13-A	Codella C., Ceccarelli C., Bianchi E., Podio L., Bachiller R., Lefloch B., Fontani F., Taquet V., Testi L.	2016, MNRAS 462, L75
2195	Phosphorus-bearing molecules in solar-type star-forming regions: first PO detection	Lefloch B., Vastel C., Viti S., Jimenez-Serra I., Codella C., Podio L., Ceccarelli C., Mendoza E., Lepine J. R. D., Bachiller R.	2016, MNRAS 462, 3937
2196	Investigating the structure and fragmentation of a highly filamentary IRDC	Henshaw J. D., Caselli P., Fontani F., Jiménez-Serra I., Tan J. C., Longmore S. N., Pineda J. E., Parker R. J., Barnes A. T.	2016, MNRAS 463, 146
2197	H_2S in the L1157-B1 bow shock	Holdship J., Viti S., Jimenez-Serra I., Lefloch B., Codella C., Podio L., Benedettini M., Fontani F., Bachiller R., Tafalla M., Ceccarelli C.	2016, MNRAS 463, 802
2198	Star formation and gas accretion in nearby galaxies	Yim K., van der Hulst J. M.	2016, MNRAS 463, 2092
2199	The First Proto-Brown Dwarf Binary Candidate Identified through Dynamics of Jets	Hsieh T.-H., Lai S.-P., Belloche A., Wyrowski F.	2016, IAU Symp. 315, E36
2200	The Intricate Role of Cold Gas and Dust in Galaxy Evolution at Early Cosmic Epochs	Riechers D. A., Capak P. L., Carilli C. L.	2016, IAU Symp. 319, 105
2201	z > 4 low luminosity dusty galaxy candidates in the Frontier Fields A2744, AS1063 and A370	Boone F., Schaerer D., Richard J., Clément B., Egami E., Rawle T., Lutz D., Weiss A., Staguhn J. G., Staguhn	2016, IAU Astron. in Focus 29, 818
2202	Kinematics of Selected Planck Galactic Cold Clumps	Varga-Verebélyi E., Tóth L. V., Marton G., Marshall D., Dobashi K., Shimoikura T.	2016, IAU Astron. in Focus 29, 64
2203	H I and CO Velocity Dispersions in Nearby Galaxies	Mogotsi K. M., de Blok W. J. G., Caldú-Primo A., Walter F., Ianjamasimanana R., Leroy A. K.	2016, The Astronom. Journal 151, 15
2204	Molecular Gas Velocity Dispersions in the Andromeda Galaxy	Caldú-Primo A., Schruba A.	2016, The Astronom. Journal 151, 34
2205	The Impact of Molecular Gas on Mass Models of Nearby Galaxies	Frank B. S., de Blok W. J. G., Walter F., Leroy A., Carignan C.	2016, The Astronom. Journal 151, 94
2206	HIghMass - High H I Mass, H I-rich Galaxies at z ~ 0: Combined H I and H_2 Observations	Hallenbeck G., Huang S., Spekkens K., Haynes M. P., Giovanelli R., Adams E. A. K., Brinchmann J., Carpenter J., Chengalur J., Hunt L. K., Masters K. L., Saintonge A.	2016, The Astronom. Journal 152, 225

2207	Fast outflows in broad absorption line quasars and their connection with CSS/GPS sources	Bruni G., Mack K.-H., Montenegro-Montes F. M., Brienza M., González-Serrano J. I.	2016, Astronomische Nachrichten 337, 180
2208	A study of the region of massive star formation L379IRS1 in radio lines of methanol and other molecules	Kalenskii S. V., Shchorov M. A.	2016, Astron. Reports 60, 438
2209	Carbon monoxide in an extremely metal-poor galaxy	Shi Y., Wang J., Zhang Z.-Y., Gao Y., Hao C.-N., Xia X.-Y., Gu Q.	2016, Nature Communications 7, 13789
2210	Oxygen isotopic ratios toward molecular clouds in the Galactic disk	Li H.-K., Zhang J.-S., Liu Z.-W., Lu D.-R., Wang M., Wang J.	2016, Research in Astr. and Astrophys. 16, 47
2211	Inner jet kinematics and the viewing angle towards the γ-ray narrow-line Seyfert 1 galaxy 1H 0323+342	Fuhrmann L., Karamanavis V., Komossa S., Angelakis E., Krichbaum T. P., Schulz R., Kreikenbohm A., Kadler M., Myserlis I., Ros E., Nestoras I., Zensus J. A.	2016, Research in Astr. And Astrophys. 16, 176
2212	Exploring the Magnetic Field Configuration in BL Lac Using GMVA	Rani B., Krichbaum T., Hodgson J., Koyama S., Zensus A., Fuhramnn L., Marscher A., Jorstad S.	2016, Galaxies 4, 32
2213	Modelling the millimetre/submillimeter emission of the gas envelope of evolved axially symmetric stars	Diep P. N., Thi Hoai D., Tuyet Nhung P., Thi Phuong N., Thi Thao N., Tuan-Anh P., Darriulat P.	2016, Journal of Physics: Conf. Series 728, 072001
2214	Transitory O-rich chemistry in heavily obscured C-rich post-AGB stars	García-Hernández D. A., García-Lario P., Cernicharo J., Engels D., Perea-Calderón J. V.	2016, Journal of Physics: Conf. Series 728, 052003
2215	Star formation in infrared dark clouds: Self-gravity and dynamics	Peretto N., Gaudel M., Louvet F., Fuller G. A., Traficante A., Duarte-Cabral A.	2016, EAS 75, 167
2216	Gravity as main driver of non-thermal motions in massive star forming regions	Traficante A., Fuller G. A., Smith R., Billot N., Duarte-Cabral A., Peretto N., Molinari S., Pineda J. E.	2016, EAS 75, 185
2217	IRAS16293E revisited: a new understanding of a prestellar core in interaction with an outflow	Pagani L., Lefèvre C., Belloche A., Menten K., Parise B., Güsten R.	2016, EAS 75, 201
2218	Excitation conditions and energetics of the dense gas in M17 SW	Pérez-Beaupuits J. P., Güsten R., Spaans M., Ossenkopf V., Menten K. M., Requena-Torres M. A., Stutzki J., Wiesemeyer H., Guevara C.	2016, EAS 75, 205
2219	Physical properties of Planck Cold Dust Clumps	Wu Y., Liu T., Meng F., Yuan J., Zhang T., Chen P., Hu R., Li D., Qin S., Ju B.	2016, EAS 75, 277
2220	Probing the methanol and CO snow lines in young protostars	Anderl S., Maret S.	2016, EAS 75, 321
2221	The Deuteration Clock for Massive Starless Cores	Kong S., Tan J. C., Caselli P., Fontani F.	2016, EAS 75, 337
2222	The Physics and Chemistry of Massive Starless Cores	Kong S., Tan J. C., Caselli P., Fontani F., Goodson M. D.	2016, AAS 227, 418.05
2223	Spatial Distribution of Small Organics in Prestellar and Protostellar Cores	Waalkes W., Guzman V., Oberg K. I.	2016, AAS 227, 347.07
2224	Star Formation and Dense Gas in Galaxy Mergers from the VIXENS Survey	Heiderman A. L., VIXENS Team	2016, AAS 227, 346.06
2225	A Systematic Investigation of Cold Gas and Dust in "Normal" Star-Forming Galaxies and Starbursts at Redshifts 5-6	Riechers D. A., Carilli C. L., Capak P. L., COSMOS H.	2016, AAS 227, 342.51
2226	The Pan-STARRS1 z>6 quasar survey: More than 100 quasars within the first Gyr of the universe	Walter F., Banados E., Venemans B., Decarli R., Farina E., Mazzucchelli C., Fan X., Chambers K. C.	2016, AAS 227, 243.39
2227	Spatially resolved star-formation in nearby analogues of Lyman break galaxies	Appel S., Baker A. J., Hall K.	2016, AAS 227, 234.08

2228	The interplay between galaxy transition and molecular gas in the next generation of radio facilities	Alatalo K. A., SPOGS Team	2016, AAS 227, 217.01
2229	Evidence for Expulsion of the Star Formation Gas Reservoir by the AGN in Local Blue Ellipticals	Schwamb M. E., Lintott C., Smethurst R., Kruk S., Matsushita S., Wong I., Wang S.-Y.	2016, AAS 227, 209.03
2230	The CO-H_2 Conversion Factor in Star-Forming Galaxies at z<1.5	Carleton T., Cooper M., PHIBSS Team	2016, AAS 228, 118.03
2231	Zooming in on star formation in the brightest galaxies of the early Universe discovered with the Planck and Herschel satellites	Canameras R.	2016, PhD Thesis
2232	An infrared/submillimetre perspective on Active Galactic Nuclei	Janssen, A.	2016, PhD Thesis
2233	Characterising the Dense Molecular Gas in Exceptional Local Galaxies	Tunnard R. C. A.	2016, PhD Thesis

IRAM (CO) AUTHORS

2094	The close circumstellar environment of Betelgeuse. III. SPHERE/ZIMPOL imaging polarimetry in the visible	Kervella P., Lagadec E., Montargès M., Ridgway S. T., Chiavassa A., Haubois X., Schmid H.-M., Langlois M., Gallenne A., Perrin G.	2016, A&A 585, A28
2095	Velocity resolved [C II] spectroscopy of the center and the BCLMP 302 region of M 33 (HerM 33es)	Mookerjea B., Israel F., Kramer C., Nikola T., Braine J., Ossenkopf V., Röllig M., Henkel C., van der Werf P., van der Tak F., Wiedner M. C.	2016, A&A 586, A37
2096	PKS 1502+106: A high-redshift Fermi blazar at extreme angular resolution. Structural dynamics with VLBI imaging up to 86 GHz	Karamanavis V., Fuhrmann L., Krichbaum T. P., Angelakis E., Hodgson J., Nestoras I., Myserlis I., Zensus J. A., Sievers A., Ciprini S.	2016, A&A 586, A60
2097	High angular resolution Sunyaev-Zel'dovich observations of MACS J1423.8+2404 with NIKA: Multiwavelength analysis	Adam R., Comis B., Bartalucci I., Adane A., Ade P., André P., Arnaud M., Beelen A., Belier B., Benoît A., Bideaud A., Billot N., Bourrion O., Calvo M., Catalano A., Coiffard G., D'Addabbo A., Désert F.-X., Doyle S., Goupy J., Hasnoun B., Hermelo I., Kramer C., Lagache G., Leclercq S., Macías-Pérez J.-F., Martino J., Mauskopf P., Mayet F., Monfardini A., Pajot F., Pascale E., Perotto L., Pointecouteau E., Ponthieu N., Pratt G. W., Revéret V., Ritacco A., Rodriguez L., Savini G., Schuster K., Sievers A., Triqueneaux S., Tucker C., Zylka R.	2016, A&A 586, A122
2098	The shadow of the Flying Saucer: A very low temperature for large dust grains	Guilloteau S., Piétu V., Chapillon E., Di Folco E., Dutrey A., Henning T., Semenov D., Birnstiel T., Grosso N.	2016, A&A 586, L1
2099	Water and acetaldehyde in HH212: The first hot corino in Orion	Codella C., Ceccarelli C., Cabrit S., Gueth F., Podio L., Bachiller R., Fontani F., Gusdorf A., Lefloch B., Leurini S., Tafalla M.	2016, A&A 586, L3
2100	Ongoing star formation in the protocluster IRAS 22134+5834	Wang Y., Audard M., Fontani F., Sánchez-Monge Á., Busquet G., Palau A., Beuther H., Tan J. C., Estalella R., Isella A., Gueth F., Jiménez-Serra I.	2016, A&A 587, A69
2101	A low-luminosity type-1 QSO sample . IV. Molecular gas contents and conditions of star formation in three nearby Seyfert galaxies	Moser L., Krips M., Busch G., Scharwächter J., König S., Eckart A., Smajić S., García-Marin M., Valencia-S. M., Fischer S., Dierkes J.	2016, A&A 587, A137
2102	Gravitational torques imply molecular gas inflow towards the nucleus of M 51	Querejeta M., Meidt S. E., Schinnerer E., García-Burillo S., Dobbs C. L., Colombo D., Dumas G., Hughes A., Kramer C., Leroy A. K., Pety J., Schuster K. F., Thompson T. A.	2016, A&A 588, A33

2103	The close circumstellar environment of Betelgeuse. IV. VLTI/PIONIER interferometric monitoring of the photosphere	Montargès M., Kervella P., Perrin G., Chiavassa A., Le Bouquin J.-B., Aurière M., López Ariste A., Mathias P., Ridgway S. T., Lacour S., Haubois X., Berger J.-P.	2016, A&A 588, A130
2104	Origin of the Lyman excess in early-type stars	Cesaroni R., Sánchez-Monge Á., Beltrán M. T., Molinari S., Olmi L., Treviño-Morales S. P.	2016, A&A 588, L5
2105	First 3 mm-VLBI imaging of the two-sided jet in Cygnus A. Zooming into the launching region	Boccardi B., Krichbaum T. P., Bach U., Bremer M., Zensus J. A.	2016, A&A 588, L9
2106	High spatial resolution imaging of SO and H_2CO in AB Auriga: The first SO image in a transitional disk	Pacheco-Vázquez S., Fuente A., Baruteau C., Berné O., Agúndez M., Neri R., Goicoechea J. R., Cernicharo J., Bachiller R.	2016, A&A 589, A60
2107	Isotopic ratios of H, C, N, O, and S in comets C/2012 F6 (Lemmon) and C/2014 Q2 (Lovejoy)	Biver N., Moreno R., Bockelée-Morvan D., Sandqvist A., Colom P., Crovisier J., Lis D. C., Boissier J., Debout V., Paubert G., Milam S., Hjalmarson A., Lundin S., Karlsson T., Battelino M., Frisk U., Murtagh D., Odin Team	2016, A&A 589, A78
2108	The unbearable opaqueness of Arp220	Martín S., Aalto S., Sakamoto K., González-Alfonso E., Muller S., Henkel C., García-Burillo S., Aladro R., Costagliola F., Harada N., Krips M., Martín-Pintado J., Mühle S., van der Werf P., Viti S.	2016, A&A 590, A25
2109	What can the 2008/10 broadband flare of PKS 1502+106 tell us? Nuclear opacity, magnetic fields, and the location of γ rays	Karamanavis V., Fuhrmann L., Angelakis E., Nestoras I., Myserlis I., Krichbaum T. P., Zensus J. A., Ungerechts H., Sievers A., Gurwell M. A.	2016, A&A 590, A48
2110	Millimeter and submillimeter excess emission in M 33 revealed by Planck and LABOCA	Hermelo I., Relaño M., Lisenfeld U., Verley S., Kramer C., Ruiz-Lara T., Boquien M., Xilouris E. M., Albrecht M.	2016, A&A 590, A56
2111	Exploring the nature of the broadband variability in the flat spectrum radio quasar 3C 273	Chidiac C., Rani B., Krichbaum T. P., Angelakis E., Fuhrmann L., Nestoras I., Zensus J. A., Sievers A., Ungerechts H., Itoh R., Fukazawa Y., Uemura M., Sasada M., Gurwell M., Fedorova E.	2016, A&A 590, A61
2112	A precessing molecular jet signaling an obscured, growing supermassive black hole in NGC 1377?	Aalto S., Costagliola F., Muller S., Sakamoto K., Gallagher J. S., Dasyra K., Wada K., Combes F., García-Burillo S., Kristensen L. E., Martín S., van der Werf P., Evans A. S., Kotilainen J.	2016, A&A 590, A73
2113	Probing the CO and methanol snow lines in young protostars. Results from the CALYPSO IRAM-PdBI survey	Anderl S., Maret S., Cabrit S., Belloche A., Maury A. J., André P., Codella C., Bacmann A., Bontemps S., Podio L., Gueth F., Bergin E.	2016, A&A 591, A3
2114	Fast outflows and star formation quenching in quasar host galaxies	Carniani S., Marconi A., Maiolino R., Balmaverde B., Brusa M., Cano-Díaz M., Cicone C., Comastri A., Cresci G., Fiore F., Feruglio C., La Franca F., Mainieri V., Mannucci F., Nagao T., Netzer H., Piconcelli E., Risaliti G. , Schneider R., Shemmer O.	2016, A&A 591, A28
2115	Discovery of a complex linearly polarized spectrum of Betelgeuse dominated by depolarization of the continuum	Aurière M., López Ariste A., Mathias P., Lèbre A., Josselin E., Montargès M., Petit P., Chiavassa A., Paletou F., Fabas N., Konstantinova-Antova R., Donati J.-F., Grunhut J. H., Wade G. A., Herpin F., Kervella P., Perrin G., Tessore B.	2016, A&A 591, A119
2116	Hi-GAL, the Herschel infrared Galactic Plane Survey: photometric maps and compact source catalogues. First data release for the inner Milky Way: +68° ≥ l ≥ -70°	Molinari S., Schisano E., Elia D., Pestalozzi M., Traficante A., Pezzuto S., Swinyard B. M., Noriega-Crespo A., Bally J., Moore T. J. T., Plume R., Zavagno A., di Giorgio A. M., Liu S. J., Pilbratt G. L., Mottram J. C., Russeil D., Piazzo L., Veneziani M., Benedettini M., Calzoletti L., Faustini F., Natoli P., Piacentini F., Merello M., Palmese A., Del Grande R., Polychroni D., Rygl K. L. J., Polenta G., Barlow M. J., Bernard J.-P., Martin P. G., Testi L., Ali B., André P., Beltrán M. T., Billot N., Carey S., Cesaroni R., Compiègne M., Eden D., Fukui Y., Garcia-Lario P., Hoare M. G., Huang M., Joncas G., Lim T. L., Lord S. D., Martinavarro-Armengol S., Motte F., Paladini R., Paradis D., Peretto N., Robitaille T., Schilke P., Schneider N., Schulz B., Sibthorpe B., Strafella F., Thompson M. A., Umana G., Ward-Thompson D., Wyrowski F.	2016, A&A 591, A149
2117	Maturity of lumped element kinetic inductance detectors for space-borne instruments in the range between 80 and 180 GHz	Catalano A., Benoit A., Bourrion O., Calvo M., Coiffard G., D'Addabbo A., Goupy J., Le Sueur H., Macías-Pérez J., Monfardini A.	2016, A&A 592, A26
2118	An observational study of dust nucleation in Mira (o Ceti). I. Variable features of AlO and other Al-bearing species	Kamiński T., Wong K. T., Schmidt M. R., Müller H. S. P., Gottlieb C. A., Cherchneff I., Menten K. M., Keller D., Brünken S., Winters J. M., Patel N. A.	2016, A&A 592, A42

2119	Measuring turbulence in TW Hydrae with ALMA: methods and limitations	Teague R., Guilloteau S., Semenov D., Henning T., Dutrey A., Piétu V., Birnstiel T., Chapillon E., Hollenbach D., Gorti U.	2016, A&A 592, A49
2120	A λ 3 mm and 1 mm line survey toward the yellow hypergiant IRC +10420. N-rich chemistry and IR flux variations	Quintana-Lacaci G., Agúndez M., Cernicharo J., Bujarrabal V., Sánchez Contreras C., Castro-Carrizo A., Alcolea J.	2016, A&A 592, A51
2121	ACA [CI] observations of the starburst galaxy NGC 253	Krips M., Martín S., Sakamoto K., Aalto S., Bisbas T. G., Bolatto A. D., Downes D., Eckart A., Feruglio C., García-Burillo S., Geach J., Greve T. R., König S., Matsushita S., Neri R., Offner S., Peck A. B., Viti S., Wagg J.	2016, A&A 592, L3
2122	Chemistry in disks. X. The molecular content of protoplanetary disks in Taurus	Guilloteau S., Reboussin L., Dutrey A., Chapillon E., Wakelam V., Piétu V., Di Folco E., Semenov D., Henning T.	2016, A&A 592, A124
2123	A highly magnetized twin-jet base pinpoints a supermassive black hole	Baczko A.-K., Schulz R., Kadler M., Ros E., Perucho M., Krichbaum T. P., Böck M., Bremer M., Grossberger C., Lindqvist M., Lobanov A. P., Mannheim K., Martí-Vidal I., Müller C., Wilms J., Zensus J. A.	2016, A&A 593, A47
2124	Further ALMA observations and detailed modeling of the Red Rectangle	Bujarrabal V., Castro-Carrizo A., Alcolea J., Santander-García M., van Winckel H., Sánchez Contreras C.	2016, A&A 593, A92
2125	Ionization fraction and the enhanced sulfur chemistry in Barnard 1	Fuente A., Cernicharo J., Roueff E., Gerin M., Pety J., Marcelino N., Bachiller R., Lefloch B., Roncero O., Aguado A.	2016, A&A 593, A94
2126	AGN feedback in the nucleus of M 51	Querejeta M., Schinnerer E., García-Burillo S., Bigiel F., Blanc G. A., Colombo D., Hughes A., Kreckel K., Leroy A. K., Meidt S. E., Meier D. S., Pety J., Sliwa K.	2016, A&A 593, A118
2127	First image of the L1157 molecular jet by the CALYPSO IRAM-PdBI survey	Podio L., Codella C., Gueth F., Cabrit S., Maury A., Tabone B., Lefèvre C., Anderl S., André P., Belloche A., Bontemps S., Hennebelle P., Lefloch B., Maret S., Testi L.	2016, A&A 593, L4
2128	The first CO^+ image. I. Probing the HI/H_2 layer around the ultracompact HII region Mon R2	Treviño-Morales S. P., Fuente A., Sánchez-Monge Á., Pilleri P., Goicoechea J. R., Ossenkopf-Okada V., Roueff E., Rizzo J. R., Gerin M., Berné O., Cernicharo J., Gónzalez-García M., Kramer C., García-Burillo S., Pety J.	2016, A&A 593, L12
2129	Dust properties in H II regions in M 33	Relaño M., Kennicutt R., Lisenfeld U., Verley S., Hermelo I., Boquien M., Albrecht M., Kramer C., Braine J., Pérez-Montero E., De Looze I., Xilouris M., Kovács A., Staguhn J.	2016, A&A 595, A43
2130	Submillimeter H_2O and H_2O^+ emission in lensed ultra- and hyper-luminous infrared galaxies at z ~ 2-4	Yang C., Omont A., Beelen A., González-Alfonso E., Neri R., Gao Y., van der Werf P., Weiß A., Gavazzi R., Falstad N., Baker A. J., Bussmann R. S., Cooray A., Cox P., Dannerbauer H., Dye S., Guélin M., Ivison R., Krips M., Lehnert M., MichaŃowski M. J., Riechers D. A., Spaans M., Valiante E.	2016, A&A 595, A80
2131	Isotopic ratios at z = 0.68 from molecular absorption lines toward B 0218+357	Wallström S. H. J., Muller S., Guélin M.	2016, A&A 595, A96
2132	Tracing extended low-velocity shocks through SiO emission. Case study of the W43-MM1 ridge	Louvet F., Motte F., Gusdorf A., Nguyên Luong Q., Lesaffre P., Duarte-Cabral A., Maury A., Schneider N., Hill T., Schilke P., Gueth F.	2016, A&A 595, A122
2133	OH^+ and H_2O^+ absorption toward PKS 1830-211	Muller S., Müller H. S. P., Black J. H., Beelen A., Combes F., Curran S., Gérin M., Guélin M., Henkel C., Martín S., Aalto S., Falgarone E., Menten K. M., Schilke P., Wiklind T., Zwaan M. A.	2016, A&A 595, A128
2134	Hot methanol from the inner region of the HH 212 protostellar system	Leurini S., Codella C., Cabrit S., Gueth F., Giannetti A., Bacciotti F., Bachiller R., Ceccarelli C., Gusdorf A., Lefloch B., Podio L., Tafalla M.	2016, A&A 595, L4
2135	The F-GAMMA programme: multi-frequency study of active galactic nuclei in the Fermi era. Programme description and the first 2.5 years of monitoring	Fuhrmann L., Angelakis E., Zensus J. A., Nestoras I., Marchili N., Pavlidou V., Karamanavis V., Ungerechts H., Krichbaum T. P., Larsson S., Lee S. S., Max-Moerbeck W., Myserlis I., Pearson T. J., Readhead A. C. S., Richards J. L., Sievers A., Sohn B. W.	2016, A&A 596, A45
2136	ALMA observations of the Th 28 protostellar disk. A new example of counter-rotation between disk and optical jet	Louvet F., Dougados C., Cabrit S., Hales A., Pinte C., Ménard F., Bacciotti F., Coffey D., Mardones D., Bronfman L., Gueth F.	2016, A&A 596, A88
2137	ALMA observations of the nearby AGB star L_2 Puppis. I. Mass of the central star and detection of a candidate planet	Kervella P., Homan W., Richards A. M. S., Decin L., McDonald I., Montargès M., Ohnaka K.	2016, A&A 596, A92
2138	Submillimeter-HCN Diagram for Energy Diagnostics in the Centers of Galaxies	Izumi T., Kohno K., Aalto S., Espada D., Fathi K., Harada N., Hatsukade B., Hsieh P.-Y., Imanishi M., Krips M., Martín S., Matsushita S., Meier D. S., Nakai N., Nakanishi K., Schinnerer E., Sheth K., Terashima Y., Turner J. L.	2016, ApJ 818, 42

2139	Hints of a Rotating Spiral Structure in the Innermost Regions around IRC+10216	Quintana-Lacaci G., Cernicharo J., Agúndez M., Velilla Prieto L., Castro-Carrizo A., Marcelino N., Cabezas C., Peña I., Alonso J. L., Zúñiga J., Requena A., Bastida A., Kalugina Y., Lique F., Guélin M.	2016, ApJ 818, 192
2140	Multiwavelength Study of Quiescent States of Mrk 421 with Unprecedented Hard X-Ray Coverage Provided by NuSTAR in 2013	Baloković M., Paneque D., Madejski G., Furniss A., Chiang J., Ajello M., Alexander D. M., Barret D., Blandford R. D., Boggs S. E., Christensen F. E., Craig W. W., Forster K., Giommi P., Grefenstette B., Hailey C., Harrison F. A., Hornstrup A., Kitaguchi T., Koglin J. E., Madsen K. K., Mao P. H., Miyasaka H., Mori K., Perri M., Pivovaroff M. J., Puccetti S., Rana V., Stern D., Tagliaferri G., Urry C. M., Westergaard N. J., Zhang W. W., Zoglauer A., NuSTAR Team, Archambault S., Archer A., Barnacka A., Benbow W., Bird R., Buckley J. H., Bugaev V., Cerruti M., Chen X., Ciupik L., Connolly M. P., Cui W., Dickinson H. J., Dumm J., Eisch J. D., Falcone A., Feng Q., Finley J. P., Fleischhack H., Fortson L., Griffin S., Griffiths S. T., Grube J., Gyuk G., Huetten M., Håkansson N., Holder J., Humensky T. B., Johnson C. A., Kaaret P., Kertzman M., Khassen Y., Kieda D., Krause M., Krennrich F., Lang M. J., Maier G., McArthur S., Meagher K., Moriarty P., Nelson T., Nieto D., Ong R. A., Park N., Pohl M., Popkow A., Pueschel E., Reynolds P. T., Richards G. T., Roache E., Santander M., Sembroski G. H., Shahinyan K., Smith A. W., Staszak D., Telezhinsky I., Todd N. W., Tucci J. V., Tyler J., Vincent S., Weinstein A., Wilhelm A., Williams D. A., Zitzer B., VERITAS Collaboration, Ahnen M. L., Ansoldi S., Antonelli L. A., Antoranz P., Babic A., Banerjee B., Bangale P., Barres de Almeida U., Barrio J. A., Becerra González J., Bednarek W., Bernardini E., Biasuzzi B., Biland A., Blanch O., Bonnefoy S., Bonnoli G., Borracci F., Bretz T., Carmona E., Carosi A., Chatterjee A., Clavero R., Colin P., Colombo E., Contreras J. L., Cortina J., Covino S., Da Vela P., Dazzi F., De Angelis A., De Lotto B., de Oña Wilhelmi E., Delgado Mendez C., Di Pierro F., Dominis Prester D., Dorner D., Doro M., Einecke S., Elsaesser D., Fernández-Barral A., Fidalgo D., Fonseca M. V.,Font L., Frantzen K., Fruck C., Galindo D., García López R. J., Garczarczyk M., Garrido Terrats D., Gaug M., Giammaria P., Glawion (Eisenacher D., Godinović N., González Muñoz A., Guberman D., Hahn A., Hanabata Y., Hayashida M., Herrera J., Hose J., Hrupec D., Hughes G., Idec W., Kodani K., Konno Y., Kubo H., Kushida J., La Barbera A., Lelas D., Lindfors E., Lombardi S., Longo F., López M., López-Coto R., López-Oramas A., Lorenz E., Majumdar P., Makariev M., Mallot K., Maneva G., Manganaro M., Mannheim K., Maraschi L., Marcote B., Mariotti M., Martínez M., Mazin D., Menzel U., Miranda J. M., Mirzoyan R., Moralejo A., Moretti E., Nakajima D., Neustroev V., Niedzwiecki A., Nievas Rosillo M., Nilsson K., Nishijima K., Noda K., Orito R., Overkemping A., Paiano S., Palacio J., Palatiello M., Paoletti R., Paredes J. M., Paredes-Fortuny X., Persic M., Poutanen J., Prada Moroni P. G., Prandini E., Puljak I., Rhode W., Ribó M., Rico J., Rodriguez Garcia J., Saito T., Satalecka K., Scapin V., Schultz C., Schweizer T., Shore S. N., Sillanpää A., Sitarek J., Snidaric I., Sobczynska D., Stamerra A., Steinbring T., Strzys M., Takalo L., Takami H., Tavecchio F., Temnikov P., Terzić T., Tescaro D., Teshima M., Thaele J., Torres D. F., Toyama T., Treves A., Verguilov V., Vovk I., Ward J. E., Will M., Wu M. H., Zanin R., MAGIC Collaboration, Perkins J., Verrecchia F., Leto C., Böttcher M., Villata M., Raiteri C. M., Acosta-Pulido J. A., Poutanen J., Prada Moroni P. G., Prandini E., Puljak I., Rhode W., Ribó M., Rico J., Rodriguez Garcia J., Saito T., Satalecka K., Scapin V., Schultz C., Schweizer T., Shore S. N., Sillanpää A., Sitarek J., Snidaric I., Sobczynska D., Stamerra A., Steinbring T., Strzys M., Takalo L., Takami H., Tavecchio F., Temnikov P., Terzić T., Tescaro D., Teshima M., Thaele J., Torres D. F., Toyama T., Treves A., Verguilov V., Vovk I., Ward J. E., Will M., Wu M. H., Zanin R., MAGIC Collaboration, Perkins J., Verrecchia F., Leto C., Böttcher M., Villata M., Raiteri C. M., Acosta-Pulido J. A., Bachev R., Berdyugin A., Blinov D. A., Carnerero M. I., Chen W. P., Chinchilla P., Damljanovic G., Eswaraiah C., Grishina T. S., Ibryamov S., Jordan B., Jorstad S. G., Joshi M., Kopatskaya E. N., Kurtanidze O. M., Kurtanidze S. O., Larionova E. G., Larionova L. V., Larionov V. M., Latev G., Lin H. C., Marscher A. P., Mokrushina A. A., Morozova D. A., Nikolashvili M. G., Semkov E., Smith P. S., Strigachev A., Troitskaya Y. V., Troitsky I. S., Vince O., Barnes J., Güver T., Moody J. W., Sadun A. C., Sun S., Hovatta T., Richards J. L., Max-Moerbeck W., Readhead A. C. R., Lähteenmäki A., Tornikoski M., Tammi J., Ramakrishnan V., Reinthal R., Angelakis E., Fuhrmann L., Myserlis I., Karamanavis V., Sievers A., Ungerechts H., Zensus J. A.	2016, ApJ 819, 156
2141	Mapping CO Gas in the GG Tauri A Triple System with 50 au Spatial Resolution	Tang Y.-W., Dutrey A., Guilloteau S., Chapillon E., Pietu V., Di Folco E., Bary J., Beck T., Beust H., Boehler Y., Gueth F., Huré J.-M., Pierens A., Simon M.	2016, ApJ 820, 19
2142	SMA Observations of the Extended ^{12}CO(J = 6-5) Emission in the Starburst Galaxy NGC 253	Krips M., Martín S., Peck A. B., Sakamoto K., Neri R., Gurwell M., Petitpas G., Zhao J.-H.	2016, ApJ 821, 112
2143	The EMPIRE Survey: Systematic Variations in the Dense Gas Fraction and Star Formation Efficiency from Full-disk Mapping of M51	Bigiel F., Leroy A. K., Jiménez-Donaire M. J., Pety J., Usero A., Cormier D., Bolatto A., Garcia-Burillo S., Colombo D., González-García M., Hughes A., Kepley A. A., Kramer C., Sandstrom K., Schinnerer E., Schruba A., Schuster K., Tomicic N., Zschaechner L.	2016, ApJ 822, L26
2144	The Detectability of Millimeter-wave Molecular Rotational Transitions	Liszt H. S., Pety J.	2016, ApJ 823, 124

2145	ALMA Resolves the Torus of NGC 1068: Continuum and Molecular Line Emission	García-Burillo S., Combes F., Ramos Almeida C., Usero A., Krips M., Alonso-Herrero A., Aalto S., Casasola V., Hunt L. K., Martín S., Viti S., Colina L., Costagliola F., Eckart A., Fuente A., Henkel C., Márquez I., Neri R., Schinnerer E., Tacconi L. J., van der Werf P. P.	2016, ApJ 823, L12
2146	High-resolution Rotational Spectrum, Dunham Coefficients, and Potential Energy Function of NaCl	Cabezas C., Cernicharo J., Quintana-Lacaci G., Peña I., Agundez M., Velilla Prieto L., Castro-Carrizo A., Zuñiga J., Bastida A., Alonso J. L., Requena A.	2016, ApJ 825, 150
2147	Discovery of a Galaxy Cluster with a Violently Starbursting Core at z = 2.506	Wang T., Elbaz D., Daddi E., Finoguenov A., Liu D., Schreiber C., Martín S., Strazzullo V., Valentino F., van der Burg R., Zanella A., Ciesla L., Gobat R., Le Brun A., Pannella M., Sargent M., Shu X., Tan Q., Cappelluti N., Li Y.	2016, ApJ 828, 56
2148	Probing the Interstellar Medium and Star Formation of the Most Luminous Quasar at z = 6.3	Wang R., Wu X.-B., Neri R., Fan X., Walter F., Carilli C. L., Momjian E., Bertoldi F., Strauss M. A., Li Q., Wang F., Riechers D. A., Jiang L., Omont A., Wagg J., Cox P.	2016, ApJ 830, 53
2149	The Spatial Distribution of Complex Organic Molecules in the L1544 Pre-stellar Core	Jiménez-Serra I., Vasyunin A. I., Caselli P., Marcelino N., Billot N., Viti S., Testi L., Vastel C., Lefloch B., Bachiller R.	2016, ApJ 830, L6
2150	Discovery of a Hot Corino in the Bok Globule B335	Imai M., Sakai N., Oya Y., López-Sepulcre A., Watanabe Y., Ceccarelli C., Lefloch B., Caux E., Vastel C., Kahane C., Sakai T., Hirota T., Aikawa Y., Yamamoto S.	2016, ApJ 830, L37
2151	A Portrait of Cold Gas in Galaxies at 60 pc Resolution and a Simple Method to Test Hypotheses That Link Small-scale ISM Structure to Galaxy-scale Processes	Leroy A. K., Hughes A., Schruba A., Rosolowsky E., Blanc G. A., Bolatto A. D., Colombo D., Escala A., Kramer C., Kruijssen J. M. D., Meidt S., Pety J., Querejeta M., Sandstrom K., Schinnerer E., Sliwa K., Usero A.	2016, ApJ 831, 16
2152	ALMA Spectroscopic Survey in the Hubble Ultra Deep Field: Survey Description	Walter F., Decarli R., Aravena M., Carilli C., Bouwens R., da Cunha E., Daddi E., Ivison R. J., Riechers D., Smail I., Swinbank M., Weiss A., Anguita T., Assef R., Bacon R., Bauer F., Bell E. F., Bertoldi F., Chapman S., Colina L., Cortes P. C., Cox P., Dickinson M., Elbaz D., Gónzalez-López J., Ibar E., Inami H., Infante L., Hodge J., Karim A., Le Fevre O., Magnelli B., Neri R., Oesch P., Ota K., Popping G., Rix H.-W., Sargent M., Sheth K., van der Wel A., van der Werf P., Wagg J.	2016, ApJ 833, 67
2153	ALMA Spectroscopic Survey in the Hubble Ultra Deep Field: CO Luminosity Functions and the Evolution of the Cosmic Density of Molecular Gas	Decarli R., Walter F., Aravena M., Carilli C., Bouwens R., da Cunha E., Daddi E., Ivison R. J., Popping G., Riechers D., Smail I. R., Swinbank M., Weiss A., Anguita T., Assef R. J., Bauer F. E., Bell E. F., Bertoldi F., Chapman S., Colina L., Cortes P. C., Cox P., Dickinson M., Elbaz D., Gónzalez-López J., Ibar E., Infante L., Hodge J., Karim A., Le Fevre O., Magnelli B., Neri R., Oesch P., Ota K., Rix H.-W., Sargent M., Sheth K., van der Wel A., van der Werf P., Wagg J.	2016, ApJ 833, 69
2154	The interstellar chemistry of H_2C_3O isomers	Loison J.-C., Agúndez M., Marcelino N., Wakelam V., Hickson K. M., Cernicharo J., Gerin M., Roueff E., Guélin M.	2016, MNRAS 456, 4101
2155	Dense circumnuclear molecular gas in starburst galaxies	Green C.-E., Cunningham M. R., Green J. A., Dawson J. R., Jones P. A., López-Sánchez Á. R., Verdes-Montenegro L., Henkel C., Baan W. A., Martín S.	2016, MNRAS 457, 2470
2156	The overmassive black hole in NGC 1277: new constraints from molecular gas kinematics	Scharwächter J., Combes F., Salomé P., Sun M., Krips M.	2016, MNRAS 457, 4272
2157	YETI observations of the young transiting planet candidate CVSO 30 b	Raetz S., Schmidt T. O. B., Czesla S., Klocová T., Holmes L., Errmann R., Kitze M., Fernández M., Sota A., Briceño C., Hernández J., Downes J. J., Dimitrov D. P., Kjurkchieva D., Radeva V., Wu Z.-Y., Zhou X., Takahashi H., Henych T., Seeliger M., Mugrauer M., Adam C., Marka C., Schmidt J. G., Hohle M. M., Ginski C., Pribulla T., Trepl L., Moualla M., Pawellek N., Gelszinnis J., Buder S., Masda S., Maciejewski G., Neuhäuser R.	2016, MNRAS 460, 2834
2158	Molecular and atomic gas along and across the main sequence of star-forming galaxies	Saintonge A., Catinella B., Cortese L., Genzel R., Giovanelli R., Haynes M. P., Janowiecki S., Kramer C., Lutz K. A., Schiminovich D., Tacconi L. J., Wuyts S., Accurso G.	2016, MNRAS 462, 1749
2159	Long-term photometry of IC 348 with the Young Exoplanet Transit Initiative network	Fritzewski D. J., Kitze M., Mugrauer M., Neuhäuser R., Adam C., Briceño C., Buder S., Butterley T., Chen W.-P., Dinçel B., Dhillon V. S., Errmann R., Garai Z., Gilbert H. F. W., Ginski C., Greif J., Hardy L. K., Hernández J., Huang P. C., Kellerer A., Kundra E., Littlefair S. P., Mallonn M., Marka C., Pannicke A., Pribulla T., Raetz S., Schmidt J. G., Schmidt T. O. B., Seeliger M., Wilson R. W., Wolf V.	2016, MNRAS 462, 2396
2160	The BLUEDISK Survey: molecular gas distribution and scaling relations in the context of galaxy evolution	Cormier D., Bigiel F., Wang J., Pety J., Usero A., Roychowdhury S., Carton D., van der Hulst J. M., Józsa G. I. G., González-García M., Saintonge A.	2016, MNRAS 463, 1724
2161	Molecular gas kinematics and line diagnostics in early-type galaxies: NGC 4710 and NGC 5866	Topal S., Bureau M., Davis T. A., Krips M., Young L. M., Crocker A. F.	2016, MNRAS 463, 4121

2162	Compression and ablation of the photo-irradiated molecular cloud the Orion Bar	Goicoechea J. R., Pety J., Cuadrado S., Cernicharo J., Chapillon E., Fuente A., Gerin M., Joblin C., Marcelino N., Pilleri P.	2016, Nature 537, 207
2163	Small-scale properties of Class 0 protostars from the CALYPSO IRAM-PdBI survey	Maury A., André P., Maret S., Belloche A., Codella C., Cabrit S., Gueth F., Aff001	2016, IAU Symp. 315, 114
2164	Resolved star formation relations at high redshift from the IRAM PHIBSS program	Freundlich J., Combes F., Tacconi L., Cooper M., Genzel R., Neri R., Neri	2016, IAU Symp. 315, E22
2165	Intensity ratios for XDR/ PDR identification	Green C.-E., Cunningham M. R., Green J. A., Dawson J. R., Jones P. A., López-Sánchez Á. R., Verdes-Montenegro L., Henkel C., Baan W. A., Martín S.	2016, IAU Symp. 315, E30
2166	HD141569A: Disk Dissipation Caught in Action	Péricaud J., di Folco E., Dutrey A., Augereau J.-C., Piétu V., Guilloteau S.	2016, IAU Symp. 314, 201
2167	Measuring the Distribution and Excitation of Cometary CH_3OH Using ALMA	Cordiner M. A., Charnley S. B., Mumma M. J., Bockelée-Morvan D., Biver N., Villanueva G., Paganini L., Milam S. N., Remijan A. J., Lis D. C., Crovisier J., Boissier J., Kuan Y.-J., Coulson I. M.	2016, IAU Astron. in Focus 29, 233
2168	CO And HI Emission from The Circumstellar Envelopes of Some Evolved Stars	Diep P. N., Hoai D. T., Nhung P., Tuan-Anh P., Le Bertre T., Winters J. M., Matthews L. D., Phuong N. T., Thao N. T., Darriulat P.	2016, Astron. Society of the Pacific Conf. Proc. 502, 61
2169	The axisymmetric envelopes of RS Cnc and EP Aqr	Le Bertre T., Hoai D. T., Nhung P. T., Winters J. M.	2016, Proceedings of the SF2A-2016, 433
2170	NIKA2, a dual-band millimetre camera on the IRAM 30 m telescope to map the cold universe	Désert F.-X., Adam R., Ade P., André P., Aussel H., Beelen A., Benoît A., Bideaud A., Billot N., Bourrion O., Calvo M., Catalano A., Coiffard G., Comis B., Doyle S., Goupy J., Kramer C., Lagache G., Leclercq S., Lestrade J.-F., Macías-Pérez J. F., Maury A., Mauskopf P., Mayet F., Monfardini A., Pajot F., Pascale E., Perotto L., Pisano G., Ponthieu N., Revéret V., Ritacco A., Rodriguez L., Romero C., Roussel H., Ruppin F., Soler J., Schuster K., Sievers A., Triqueneaux S., Tucker C., Zylka R.	2016, Proceedings of the SF2A-2016, 439
2171	AGN feedback and star formation in young and old radio galaxies	Labiano A., García-Burillo S., Combes F., Usero A., Soria-Ruiz R., Piqueras López J., Tremblay G., Hunt L., Fuente A., Neri R., Oosterloo T.	2016, Astronomische Nachrichten 337, 188
2172	The Connection between the Radio Jet and the γ-ray Emission in the Radio Galaxy 3C 120 and the Blazar CTA 102	Casadio C., Gómez J., Jorstad S., Marscher A., Grandi P., Larionov V., Lister M., Smith P., Gurwell M., Lähteenmäki A., Agudo I., Molina S., Bala V., Joshi M., Taylor B., Williamson K., Kovalev Y., Savolainen T., Pushkarev A., Arkharov A., Blinov D., Borman G., Di Paola A., Grishina T., Hagen-Thorn V., Itoh R., Kopatskaya E., Larionova E., Larionova L., Morozova D., Rastorgueva-Foi E., Sergeev S., Tornikoski M., Troitsky I., Thum C., Wiesemeyer H.	2016, Galaxies 4, 34
2173	Resolving the Base of the Relativistic Jet in M87 at 6Rsch Resolution with Global mm-VLBI	Kim J.-Y., Lu R.-S., Krichbaum T., Bremer M., Zensus J., Walker R.	2016, Galaxies 4, 39
2174	Turbulence In Tw Hya: Methods And Limitations	Teague R., Birnstiel T., Chapillon E.	2016, ESO/NRAO Workshop on Resolving Planet formation in the era of ALMA and extreme AO
2175	A rotating spiral structure in the innermost regions around IRC+10216	Quintana-Lacaci G., Cernicharo J., Agúndez M., Velilla Prieto L., Castro-Carrizo A., Marcelino N., Cabezas C., Peña I., Alonso J. L., Zuñiga J., Requena A., Bastida A., Kalugina Y., Lique F., Guélin M.	2016, Journal of Physics: Conf. Series 728, 022005
2176	Crosstalk in a KID Array Caused by the Thickness Variation of Superconducting Metal	Adane A., Boucher C., Coiffard G., Leclercq S., Schuster K. F., Goupy J., Calvo M., Hoarau C., Monfardini A.	2016, Journal of Low Temperature Physics 184, 137
2177	Microfabrication Technology for Large Lekid Arrays: From Nika2 to Future Applications	Goupy J., Adane A., Benoit A., Bourrion O., Calvo M., Catalano A., Coiffard G., Hoarau C., Leclercq S., Le Sueur H., Macias-Perez J., Monfardini A., Peck I., Schuster K.	2016, Journal of Low Temperature Physics 184, 661
2178	Uniform Non-stoichiometric Titanium Nitride Thin Films for Improved Kinetic Inductance Detector Arrays	Coiffard G., Schuster K.-F., Driessen E. F. C., Pignard S., Calvo M., Catalano A., Goupy J., Monfardini A.	2016, Journal of Low Temperature Physics 184, 654
2179	First Polarised Light with the NIKA Camera	Ritacco A., Adam R., Adane A., Ade P., André P., Beelen A., Belier B., Benoît A., Bideaud A., Billot N., Bourrion O., Calvo M., Catalano A., Coiffard G., Comis B., D'Addabbo A., Désert F.-X., Doyle S., Goupy J., Kramer C., Leclercq S., Macías-Pérez J. F., Martino J., Mauskopf P., Maury A., Mayet F., Monfardini A., Pajot F., Pascale E., Perotto L., Pisano G., Ponthieu N., Rebolo-Iglesias M., Revéret V., Rodriguez L., Savini G., Schuster K., Sievers A., Thum C., Triqueneaux S., Tucker C., Zylka R.	2016, Journal of Low Temperature Physics 184, 724

2180	The NIKA2 Instrument, A Dual-Band Kilopixel KID Array for Millimetric Astronomy	Calvo M., Benoît A., Catalano A., Goupy J., Monfardini A., Ponthieu N., Barria E., Bres G., Grollier M., Garde G., Leggeri J.-P., Pont G., Triqueneaux S., Adam R., Bourrion O., Macías-Pérez J.-F., Rebolo M., Ritacco A., Scordilis J.-P., Tourres D., Adane A., Coiffard G., Leclercq S., Désert F.-X., Doyle S., Mauskopf P., Tucker C., Ade P., André P., Beelen A., Belier B., Bideaud A., Billot N., Comis B., D'Addabbo A., Kramer C., Martino J., Mayet F., Pajot F., Pascale E., Perotto L., Revéret V., Ritacco A., Rodriguez L., Savini G., Schuster K., Sievers A., Zylka R.	2016, Journal of Low Temperature Physics 184, 816
2181	The Far Infrared Spectroscopic Explorer (FIRSPEX): probing the lifecycle of the ISM in the universe	Rigopoulou D., Caldwell M., Ellison B., Pearson C., Caux E., Cooray A., Gallego J. D., Gerin M., Goicoechea J. R., Goldsmith P., Kramer C., Lis D. C., Molinari S., Ossenkopf-Okada V., Savini G., Tan B. K., Tielens X., Viti S., Wiedner M., Yassin G.	2016, SPIE 9904, 99042K
2182	Behavior driven testing in ALMA telescope calibration software	Gil J. P., Garces M., Broguiere D., Shen T.-C.	2016, SPIE 9913, 99130C
2183	Analysis of antenna position measurements and weather station network data during the ALMA long baseline campaign of 2015	Hunter T. R., Lucas R., Broguière D., Fomalont E. B., Dent W. R. F., Phillips N., Rabanus D., Vlahakis C.	2016, SPIE 9914, 99142L
2184	Electronically Tuned Local Oscillators for the NOEMA Interferometer	Mattiocco F., Garnier O., Maier D., Navarrini A., Serres P.	2016, IEEE Trans. On THz Science and Technology 6, 212
2185	The Front-End of the NOEMA Interferometer	Chenu J.-Y., Navarrini A., Bortolotti Y., Butin G., Fontana A. L., Mahieu S., Maier D., Mattiocco F., Serres P., Berton M., Garnier O., Moutote Q., Parioleau M., Pissard B., Reverdy J.	2016, IEEE Trans. On THz Science and Technology 6, 223
2186	Exploring the molecular chemistry and excitation in obscured LIRGs: An ALMA mm-wave spectral scan of NGC 4418	Costagliola F., Sakamoto K., Muller S., Martín S., Aalto S.	2016, EAS 75, 67
2187	Physical Conditions in the Molecular Gas of the Local Group Dwarf Starburst, IC 10	Bittle L. E., Johnson K. E., Leroy A., Indebetouw R., Sandstrom K., Kepley A. A., Schruba A., Bolatto A. D., Walter F., Donovan Meyer J., Hughes A., Zschaechner L., Kramer C., Gratier P., Krips M., Lee C.	2016, AAS 227, 347.05
2188	GRB161017A: NOEMA detection of the millimetre afterglow.	Schulze S., de Ugarte Postigo A., Bremer M., Chapillon E., Winters J. M., Martin S.	2016, GCN 20081, 1
2189	GRB160131A: NOEMA detection of the millimetre afterglow.	de Ugarte Postigo A., Schulze S., Bremer M., Martin S.	2016, GCN 18976, 1

Committees

STEERING COMMITTEE

A. Barcia, CAY Spain
R. Bachiller, OAN Madrid, Spain
G. Chardin, CNRS Paris, France
R. Genzel, MPE Garching, Germany
J. Gomez-Gonzalez, IGN Madrid, Spain
S. Guilloteau, CNRS Bordeaux, France
K. Menten, MPIfR Bonn, Germany
D. Mourard, CNRS-INSU Paris, France
G. Perrin, Obs. de Paris, France
J.L. Puget, IAS Paris, France
M. Schleier, MPG Munich, Germany

SCIENTIFIC ADVISORY COMMITTEE

F. Boulanger, IAS Orsay, France
M. Gerin, LRA Paris, France
R. Moreno, LESIA Paris, France
P. Planesas, OAN Madrid, Spain
G.J. Stacey, Cornell Univ. New York, USA
L. Tacconi, MPE Garching, Germany
M. Tafalla, OAN Madrid, Spain
F. Walter, MPIA, Heidelberg, Germany
F. Wyrowski, MPIfR Bonn, Germany

PROGRAM COMMITTEE

J. Alcolea, OAN Madrid, Spain
A. Beelen, IAS Paris, France
A. Bolatto, Univ. Maryland, USA
N. Brouillet, OASU Bordeaux, France
C. Codella, Arcetri Obs Firenze, Italy
R. Davies, MPE Garching, Germany
J. Goicoechea, CSIC Madrid, Spain
L. Hartmann, Univ. Michigan, USA
K. Kohno, Univ. Tokyo, Japan
F. Levrier, LERMA Paris, France
H. Linz, MPIA Heidelberg, Germany
A. Usero, OAN Madrid, Spain
A. Weiss, MPIfR Bonn, Germany

AUDIT COMMISSION

J. Jeannenot, CNRS, France
G. Maar, MPG, Germany